Selected Experimental Studies on Machinability of Ti54M, Ti10.2.3, Ti5553 and Ti6Al4V Titanium Alloys

THESIS

Submitted in partial fulfilment
of the requirements for the degree of

DOCTOR OF PHILOSOPHY

by

NAVNEET KHANNA

Under the Supervision of
Prof. KULDIP SINGH SANGWAN

BITS Pilani
Pilani | Dubai | Goa | Hyderabad

BIRLA INSTITUTE OF TECHNOLOGY AND SCIENCE
PILANI (RAJASTHAN) INDIA
2013

DEDICATED

TO

My Parents, Wife
& Daughter

BIRLA INSTITUTE OF TECHNOLOGY AND SCIENCE

PILANI (RAJASTHAN) INDIA

CERTIFICATE

This is to certify that the thesis entitled **"Selected Experimental Studies on Machinability of Ti54M, Ti10.2.3, Ti5553 and Ti6Al4V Titanium Alloys"** submitted by **Navneet Khanna,** ID No. **2009PHXF027P** for the award of PhD Degree of the Institute, embodies the original work done by him under my supervision.

Signature in full of the Supervisor _____

Name in capital block letters **Dr KULDIP SINGH SANGWAN**

Designation Associate Professor, Head of the Department
Mechanical Engineering Department
BITS Pilani, India

Date: March 28, 2013

Acknowledgements

It gives me a deep sense of gratitude and immense pleasure to sincerely thank my supervisor **Dr Kuldip Singh Sangwan**, Associate Professor, Mechanical Engineering Department for his constant encouragement, constructive and valuable suggestions, invaluable insight, wisdom and moral support throughout the period of this research work. It has been a privilege and honour for me to work under his valuable guidance as his doctoral student. Working with Prof. Sangwan has transformed my life on several fronts.

Since the inception, it was my dream to work under the guidance of Prof. P.J. Arrazola, head of high performance cutting laboratory, Mondragon University, Spain and I express my sincere thanks to him for having given me the opportunity to work under him. It is indeed enormous learning, coupled with hands on experience, in the area of machining. This opportunity has given me the exposure to the experimental orthogonal metal cutting research in the areas of machining different heat treated titanium alloys. I would like to express my deepest appreciation and thanks to Dr Ainhara Garay and Dr Daniel Soler for their valuable advice and help which made the work more interesting and challenging at Mondragon University. I would also take this opportunity to thank Mr Luis M. Iriarte for his extended help in carrying out the experimental work and cooperation at High Performance Cutting Laboratory, Mondragon University, Spain.

I thank the members of Doctoral Advisory Committee, Dr Rajesh Prasad Mishra, Assistant Professor, Mechanical Engineering Department, and Dr Tufan C Bera, Assistant Professor, Mechanical Engineering Department for their support and suggestions to carry out this work effectively.

My sincere thank goes to Prof B N Jain, Vice-Chancellor, BITS Pilani for giving me the opportunity to carry out the PhD work in BITS. I am thankful to Prof G Raghurama, Director (Pilani Campus); Prof R K Mittal, Director, (Dubai Campus); Prof R N Saha, Deputy Director (Administration, Pilani Campus); Prof S K Verma, Dean, Academic Research Division for providing the necessary facility to carry out this work. I am indebted

to Dr Devika Sangwan, Assistant Professor, Languages Department, for her words of constant motivation and help.

It is my honour and pride to express thanks to my teachers Dr Vimmy Singh, Dr. Aparna Biswas, Dr Akhilendra Singh, Dr G Anand, Dr Sharad Srivastava, Dr S.P. Regalla, Dr. M.S. Dasgupta, Dr. A.K. Digalwar, Mr Sachin Belgamwar, Dr Rajbir Bhatti, Dr T.S. Sidhu, Dr N.M. Suri, Dr M. Khushwah to empower the knowledge in me and make me what I am today.

I extend my special thanks to Dr B.K. Rout, Dr Monica Sharma, Dr Dinesh Kumar, Dr Amit Singh, Dr Gunjan Soni, Dr S. Routroy, Dr Arun Kumar Jalan, Mr Jitendra Singh Rathore, Mr Maheshwar Dwivedy, Mr Girish Kant Garg, Mr Varinder Mittal, Mr Anil Jindal, Mr. Satish Dubey, Mr Arshad Javed, Mr Dileep Gupta, and Mr Kalluri Vinayak of Mechanical Engineering Department for their valuable advice and moral support throughout the work.

My special thanks and appreciation are due to my friends Mr Varinder Pal, Mr Manish Verma, Mr Pankaj Sharma, Mr Dipaloy Dutta, Mr Ankit Choudhary, Dr P.J. Singh, Mr J.P Bhamu, Mr Vikrant Bhakar and Mr Basheer Ahmed for their moral support and making me relaxed and motivated by exchanging words of encouragement.

This work could not have been completed without the moral support I got from my loving parents - Late Shri Ramesh Khanna and Smt Meena Khanna, in-laws - Shri Harish Chawla, Smt Usha Chawla, and Himanshu Chawla, and my loving wife - Kamini. Their unconditional love, constant encouragement, moral support and immense confidence in me made this work possible. I would like to express my appreciation and love to my younger brother- Vineet Khanna for his consistent motivation and daughter - Soham for her cute ways of bringing smiles on my face.

Last but not the least, I pray and thank to ALMIGHTY GOD for showering HIS blessings and giving me the inner strength and patience.

NAVNEET KHANNA

Table of Contents

List of Figures

List of Tables

List of Abbreviations

V_c	Cutting speed
F_c	Cutting force
f	Feed rate
F_f	Feed force
a_p	Depth of cut
r_ε	Corner radius
r_β	Cutting edge roundness
K_c	Specific cutting force
K_k	Specific feed force
%	Percentage
wt.	Weight
t	Time (sec)
T	Temperature (^oC)
T_β	Beta transus temperature (^oC)
α	Alpha
α'	Primary alpha
β	Beta
μ	Coefficient of friction
γ_0	Rake angle
κ_r	Cutting edge angle
λ_s	Cutting edge inclination angle
STA	Solution treated and aged
STOA	Solution treated and over aged
ANOVA	Analysis of variance
HRC	Rockwell C hardness
HV	Vickers hardness
UTS	Ultimate tensile strength
TYS	Tensile yield strength
MPa	Megapascal
EL	Elongation
RA	Reduction in area
LAM	Laser assisted machining
HPC	High pressure cooling
SEM	Scanning electron microscope

Abstract

Recently, titanium alloys have received considerable attention due to their excellent corrosion resistance, high strength-to-weight ratio, high strength at elevated temperatures, and biological compatibility. Hence, these alloys are used in a wide range of applications in aerospace, automotive, chemical, and medical industries. The demand of titanium has been steady increasing in aerospace industry because of its excellent strength-to-weight ratio and electrochemically compatibility with the increasingly applied composite materials in aerospace industry. Titanium alloys have outstanding physical-mechanical properties, but they are difficult-to-machine materials because of their high chemical reactivity, poor heat conductivity, low modulus of elasticity, which lead to lower production rates and increased tool wear.

To improve the productivity of titanium alloy components, efforts are made in the diverse areas affecting machinability. Titanium alloys like Ti54M, Ti10.2.3 and Ti5553 are increasingly being used in the aerospace industry. In the near future, Ti54M is likely to replace the Ti6Al4V in the aerospace applications. Among all titanium materials the group of β titanium alloys (Ti10.2.3 and Ti5553) offer the highest strength-to-weight ratio and deeper hardenability.

This study aims at understanding the reasons of good or poor machinability of titanium alloys, through the experimental investigations on Ti54M, Ti10.2.3, Ti5553, and Ti6Al4V alloys. The study also explores the effects of PVD coated tools with varying tool geometries and cutting parameters during interrupted machining of titanium alloys. Experimental studies have been carried out on the selected titanium alloys for understanding the

machinability in terms of cutting and feed forces; cutting tool temperature, and chip morphology.

There are clear indications that the machinability of Ti54M alloy in annealed condition is better than that of β annealed and STA conditions. The experimental studies carried out on Ti10.2.3 alloy in annealed, STA and STOA conditions show that this alloy has the poorest machinability in the STA heat treated condition. The comparison of titanium alloys in different heat treated conditions shows that Ti10.2.3 has poor machinability than Ti54M and Ti6Al4V alloys. The interrupted machining analysis for Ti6Al4V and Ti5553 titanium alloys using PVD coated carbide inserts show the poor machinability of Ti5553 alloy as compared to the Ti6Al4V alloy The ANOVA results have shown that most of the experimental findings are statistically significant.

The experimental studies have presented a lot of understanding and relationship between the mechanical properties and machinability. This gain in knowledge can be leveraged to develop varieties of these alloys by changing their chemical composition and/or heat treatment for different applications. The experimental studies performed for the industry requirement have also added machinability data to the existing scarce database on machinability of these alloys. This novel contribution to the database will help the researchers/practitioners in this area to develop numerical models in future for cost effective research. The industry is expected to gain from this research in terms of improved productivity and reduced cost.

Chapter 1
Introduction

1.1. Overview

Recently, titanium alloys have received considerable attention due to their excellent corrosion resistance, high strength-to-weight ratio, high strength at elevated temperatures, and biological compatibility. Hence, these alloys are used in a wide range of applications in aerospace, automotive, chemical, and medical industries (Armendia et al., 2010).

The high consumption of titanium alloys has increased its demand in the past few years in the aerospace sector. The excellent strength-to-weight ratio of titanium alloys decreases aircraft weight, leading to reduction in fuel consumption and emissions. The other typical aerospace material, aluminium, is electrochemically incompatible with the increasingly applied composite materials, forming a galvanic couple. Titanium does not pose this problem and, thus, is replacing aluminium in many applications (Lütjering and Williams, 2007). Titanium has emerged as a "wonder" metal that justifies its choice for a wide variety of applications including jewellery, bicycle frames, missiles, airplanes, helicopters, submarines, automobile, bone implants, and surgical instruments (Imam, 2011). Aerospace is still a major driver for research and development and it is anticipated that new programs at Airbus (A350 and A400M) will boost the titanium industry (Imam, 2011). To increase aircraft efficiency and reduce its lifecycle costs, aircraft manufacturers are using more titanium. Thus, with the anticipated demand, it is estimated that in the next decade there will be a huge demand of titanium machining worldwide.

Titanium alloys have outstanding physical-mechanical properties but they are difficult-to-machine materials, leading to lower production rates and increased tool wear. Some of the reasons for the poor machinability of titanium alloys are given below.

- The high chemical reactivity of titanium with almost all tool materials makes diffusion as the most influencing wear mechanism in the machining of titanium alloys (Truks, 1987; Yang and Liu, 1999).
- Titanium is a very poor heat conductor. During the machining of steel, more than 75% of the heat generated gets transferred to the chip, whereas during the machining of titanium-based parts, only 25% of the heat gets transferred to the chip, thus creating a greater heat concentration on the cutting edge of the tool. This leads to rapid tool failure. To avoid this, generally, machining is carried out at a lower speed leading to lowered productivity. So, thermal properties of cutting tools gain importance while machining titanium alloys (Colwell and Truckenmiller, 1953; Ezugwu et al., 2003).
- Good mechanical properties of titanium alloys at high temperatures lead to the formation of a thin chip, thereby decreasing the contact area with the tool (Machado and Wallbank, 1990). This reduction of the contact area leads to increased temperature and pressure distribution on the cutting tool (Ezugwu and Wallbank, 1997).
- The low modulus of elasticity of titanium (110 GPa) causes severe chatter during their machining (Yang and Liu, 1999).
- The phenomenon of the adiabatic shear banding is common during the machining of titanium alloys. This leads to cyclic temperature and mechanical loads, affecting tool behaviour (mechanical and thermal fatigue) (Molinari et al., 2002).

1.2. Research Motivation

Indian aerospace industry is witnessing an unprecedented growth. There is a huge potential and great opportunity for collaborative ventures in the aerospace sector in India for establishing Maintenance Repair Overhaul (MRO) facilities for civil and military aircraft, overhaul and maintenance of aero-engines, and production of avionics, components and accessories for both in the civil and military aviation sectors. Major global aviation industries are already eyeing the local market in India and scouting for outsourcing aerospace and defence products, as India is fast emerging as a centre for engineering and design services.

New aircraft designs that make extensive use of composite materials make extensive use of titanium at the same time. Compared to aluminium, titanium is more compatible with composites in aircraft assemblies. Still unaddressed, however, is the question of machinability improvement of titanium alloys. In recent times, the machinability of titanium alloys has become an important area of research (Arrazola et al., 2009). As discussed earlier, titanium poses several machining challenges. It requires low cutting parameters to avoid heat build-up. As a result, machining of titanium can cost 10 times more than machining aluminium (Quinto, 2007). To improve the productivity of titanium alloy components, efforts are made in the diverse areas affecting machinability — development of newer titanium alloys, heat treatment, tool material and geometry, cutting conditions, etc. Titanium alloys like Ti54M, Ti10.2.3 and Ti5553 are increasingly being used in the aerospace industry. Ti54M alloy is an $\alpha+\beta$ titanium alloy that was developed to improve the production

costs compared to Ti6Al4V while providing similar properties to that of Ti6Al4V but with better machinability (roughly 10 to 20% better than Ti6Al4V) (Kosaka and Fox, 2004; Venkatesh et al., 2007). In the near future, Ti54M is likely to replace the Ti6Al4V in the aerospace applications. Ti10.2.3 is a β titanium alloy developed in the 1970's; it has improved forgeability (Boyer, 2005). The concept of the β titanium alloy (Ti5553) was publicly introduced in 1997 as an enhanced version of the Russian alloys VT22 and VT22-1. Since then, TIMET has been manufacturing and evaluating TIMETAL® 555 (Ti5553) for a range of aerospace applications (Fanning, 2005). Among all titanium materials, the group of β (Ti10.2.3 and Ti5553) titanium alloys offers the highest strength-to-weight ratio. Materials like Ti10.2.3 and Ti5553 are being increasingly used due to their deeper hardenability in comparison to α+β titanium alloys (Ti6Al4V and Ti54M). These are mainly being used in the landing gear parts of the aircrafts. Unfortunately, these alloys are even more difficult to machine than traditional titanium alloy Ti6Al4V. This leads to higher manufacturing costs (Machai and Biermann, 2011; Arrazola et al. 2009).

It seems unlikely that there is currently enough titanium machining capacity to meet all the needs of the various high-titanium-content planes being introduced in the market. The aircraft-industry supply chain has started realizing the necessity of this increasing capacity. Companies will be asked to machine more titanium than ever before, and also to machine it faster. Limited understanding about the machinability of these increasingly used titanium alloys prevents industry from using these alloys in new structural components. This provides the motivation for the machinability studies on selected titanium alloys.

1.3. Objectives and Scope of the Study

Ongoing development work on newer titanium alloys with varying heat treatment conditions is driven by the need to continuously improve machining efficiency and productivity. Donachei (2004) and Kosaka et al. (2004) have found that the machinability depends on the chemistry as well as heat treatment conditions, i.e. on strength and microstructure. It is important to understand the reasons of the better or poor machinability of the increasingly used titanium alloys. According to Bouzakis et al. (2012), material and manufacturing engineers have shared their expertise, aiming at developing tool coatings to meet the needs of machining the most difficult-to-cut materials. A few research papers have been published dealing with the machining of Ti54M, Ti10.2.3 and Ti5553 alloys (Armendia et al., 2010; Machai and Biermann, 2011; Arrazola et al. 2009).

Thus, the objective of the present research is to perform selected experimental studies on the machinability of Ti54M, Ti10.2.3 and Ti5553 titanium alloys in order to establish and provide fundamental knowledge in machining of these titanium alloys. The study will be carried out on the turning process with tailor-made cutting tools at different cutting parameters. The objectives of this study are:

- to understand the reasons of good or poor machinability of titanium alloys through the experimental investigations on Ti54M, Ti10.2.3, Ti5553 and Ti6Al4V alloys,
- to understand the effects of chemical composition and heat treatment on the machinability of titanium alloys,
- to explore the effects of physical vapour deposition (PVD) coated tools with varying tool geometries and cutting parameters during interrupted machining of titanium alloys, and

- to carry out the experimental studies on selected titanium alloys for understanding the machinability in terms of the following indicators:

    i. Cutting and feed forces,
    ii. Cutting tool temperature, and
    iii. Chip morphology.

These experimental studies have been carried out as per the requirements of the sponsoring industries (TIMET, SANDVIK and SECO) at the cutting parameters discussed and suggested by them.

1.4. Methodology

To achieve the objectives of the proposed research, the following activities are to be carried out:

- A review of literature of titanium alloys, their machinability and machinability improvement techniques.
- Development of experimental setup and plan for carrying out the machinability studies on the selected titanium alloys.
- Machinability studies on Ti54M titanium alloy in different heat treatment conditions.
- Machinability studies on Ti10.2.3 titanium alloy in different heat treatment conditions.
- Machinability studies on Ti6Al4V titanium alloy in annealed conditions.
- Comparative machinability analysis of Ti6Al4V, Ti54M and Ti10.2.3 alloys.
- Interrupted machining studies on Ti6Al4V and Ti5553 titanium alloys using PVD coated carbide tools.

1.5. Significance of the Study

The experimental studies on the selected titanium alloys have presented a lot of understanding and relationship between the mechanical properties and machinability. This gain in knowledge can be leveraged to develop varieties of these alloys by changing their chemical composition and/or heat treatment for different applications. The experimental studies performed for the industry requirement have also added machinability data to the existing scarce database on machinability of these alloys. This novel contribution to the database will help the researchers/practitioners in this area to develop numerical models in future for cost effective research. The results have been transferred to the respective industries (TIMET, SANDVIK and SECO) and the society through publications in journals and conferences. The industry is expected to gain from this research in terms of improved productivity and reduced cost.

1.6. Organization of the Thesis

Chapter 1 presents the introduction to the thesis. A literature review of metallurgy, heat treatment, machinability, and machinability improvement techniques of titanium alloys is given in chapter 2. The experimental setup and plan are elaborated in chapter 3. Machinability studies on Ti54M and Ti10.2.3 titanium alloys at various heat treatment conditions are presented in chapter 4 and 5 respectively. Machinability analysis of Ti6Al4V is presented in chapter 6. Chapter 6 also presents the comparative machinability analysis of Ti10.2.3, Ti54M and Ti6Al4V alloys. Chapter 7 provides the results and analysis of interrupted machining of Ti6Al4V and Ti5553 titanium alloys by using PVD coated inserts. The important conclusions, major research contributions, and future scope of the research are highlighted in chapter 8.

Chapter 2

Literature Review

2.1. Introduction

Among the structural materials developed in the 20th century, titanium and its alloys played a leading role. Initially, the main focus was on titanium's high specific strength, including that at elevated temperature. This led to its widespread use in the aircraft and space industries. Later, attention was paid not only to high specific strength but also to excellent fatigue resistance, strong spring-back characteristics, high-temperature performance, corrosion resistance, and biocompatibility. Titanium emerged as a "wonder" metal that makes sense as the material of choice for a wide variety of applications, including jewellery, bicycle frames, missiles, airplanes, helicopters, submarines, automobile, bone implants, and surgical instruments (Imam, 2011). Aerospace is still a major driver for research and development and it is anticipated that new programs at Airbus (A350 and A400M) will boost the titanium industry (Imam, 2011). To increase aircraft efficiency and reduce lifecycle costs, aircraft manufacturers are using more titanium (Figure 2.1). Some of the basic characteristics of titanium as compared to other structural metallic materials like Iron (Fe), Nickel (Ni), and Aluminium (Al) are listed in table 2.1. The primary justifications for using titanium in the aerospace industry are (Boyer, 1996 and 2010):

- Weight savings (primarily as a steel replacement)
- Space limitation (replace Al alloys)
- Operating temperature (replace Al, Ni, and steel alloys)

- Corrosion resistance (replace Al and low alloy steels)
- Composite compatibility (replace Al alloys)

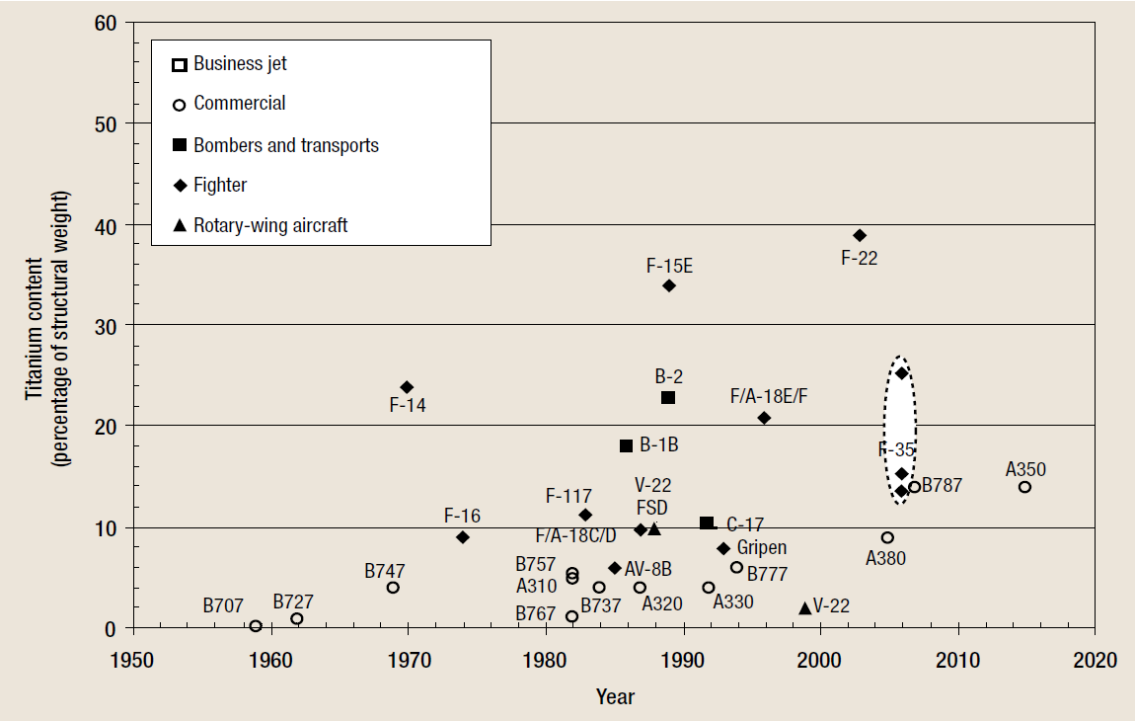

Figure 2.1. Change in titanium use in aircrafts over time (Lantrip, 2008)

Table 2.1. Properties of titanium and other structural metals (Lutjering, 2008)

	Ti	Fe	Ni	Al
Melting Temperature (°C)	1670	1538	1455	660
Allotropic Transformation (°C)	$\beta \xrightarrow{882} \alpha$	$\gamma \xrightarrow{912} \alpha$	-	-
Crystal Structure	bcc → hex	fcc → bcc	fcc	fcc
Room Temperature E (GPa)	115	215	200	72
Yield Stress Level (MPa)	1000	1000	1000	500
Density (g/cm^3)	4.5	7.9	8.9	2.7
Comparative Corrosion Resistance	Very High	Low	Medium	High
Comparative Reactivity with Oxygen	Very High	Low	Low	High
Comparative Price of Metal	Very High	Low	High	Medium

Weight savings are obvious with high strength-to-weight ratio of titanium. The lower density of titanium as compared with steel, permits weight savings by replacing steel with titanium. The strength of titanium alloys is significantly higher than aluminum alloys,

weight savings can be achieved by using titanium in spite of its 60% higher density, assuming that the component is not gage limited (Armendia et al., 2010). Titanium could also replace aluminium when the operating temperature exceeds about 130°C, which is normally the maximum operating temperature for conventional aluminium. Steel and nickel-based alloys are obvious alternatives, but they have a density about 1.7 times that of titanium (Boyer, 1996).

Excellent examples of utilization of titanium because of volume constraints are the landing gear beams on the Boeing 747 and 757 aircrafts. The beam for Boeing 747 is one of the largest titanium forgings produced. The preferable material for this application, in terms of cost, would have been an aluminum alloy, such as 7075. However, to carry the required loads, the machined aluminum component would not fit within the envelope of the wing. On the other hand if steel is used, it would have been heavier owing to the higher density (Boyer, 2010). Corrosion resistance is also a very important issue. The corrosion resistance of titanium is such that corrosion protective coatings or paints are not required. Much of the floor support structure under the galleys and lavatories is in a very corrosive environment which dictates the use of titanium to provide high structural durability in these applications (Boyer, 1996).

According to Boyer (1996 and 2010) Polymer Matrix Composite (PMC) compatibility is becoming a bigger issue with higher utilization of composite structures on aircraft. The titanium is galvanically compatible with the carbon fibers in the composites, whereas aluminium (and low alloy steels) generates a significant galvanic potential with carbon. The selection of titanium in these instances is related to the criticality of the structure. There are corrosion protection systems which are used to isolate aluminum from carbon composites to

preclude the corrosion problem, but the integrity of the coating over the life of the airframe must be taken into account. Titanium has also been used with PMC structure due to its relatively good match of coefficient of thermal expansion (CTE).

Titanium sponge production and mill products in the four major titanium producing countries are shown in figure 2.2. It is interesting to note that the production of titanium sponge and mill products among the four countries maintained a growth at different rates until 2008. In 2008, titanium sponge production established a new record of about 180,000 tons. However, in 2009, it decreased sharply because of the global economic crisis and the recession in the aerospace industry (Imam, 2011).

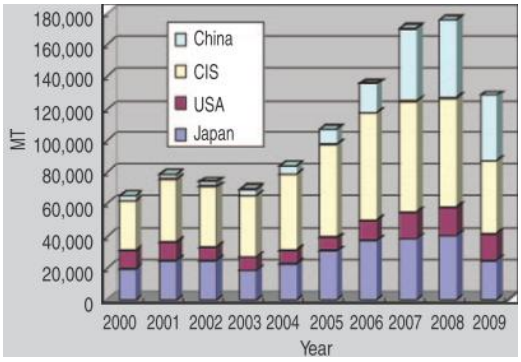

Figure 2.2. Amount of titanium sponge produced in metric tons (MT) in main sponge making countries (Adopted from Japan Titanium Society (Imam, 2011))

As mentioned previously, cost is always an important consideration in the competitive business environment. The titanium raw material may cost anywhere from three to ten times as much as steel or aluminum and the machining costs for titanium are generally significantly higher than for the other materials (at least ten times that to machine aluminium). Thus, the benefits of using titanium must outweigh the added cost for its successful application (Froes and Imam, 2010). The cost of titanium use may be minimized

by decreasing its machining cost. Material metallurgy is an important parameter to asses and evaluate the machinability.

2.2. Metallurgy

Titanium is an allotropic element, i.e. it exists in more than one crystallographic form. At room temperature, titanium has a hexagonal close-packed (hcp) crystal structure, which is referred to as α phase. This structure transforms to a body-centered cubic (bcc) crystal structure, called β phase, at 888°C (Donachei, 2004). Alloying elements in titanium alloys tend to stabilize either as α phase, or the allotrope β phase that alters the transformation temperature and changes the shape and extent of the α+β field (Eylon et al., 1984; Ezugwu and Wang, 1997). Elements that raise the transformation temperature are α stabilizers, these being aluminum (Al), oxygen (O), nitrogen (N), and carbon (C), of which Al is a very effective α strengthening element at ambient and elevated temperatures up to 550°C. The low density of Al is an important additional advantage. O, N and C are regarded as impurities in commercial alloys. However, O is used as a strengthening agent to provide several grades of commercially-pure titanium offering various combinations of strength and fabricability (IMI Titanium, 1978). The addition of tin (Sn) or zirconium (Zr) also strengthen the α phase. These elements have small influence on the transformation temperature and are known as 'neutral elements'.

Elements that lead to a decrease in the transformation temperature are β stabilizers. There are two types of β stabilizers - β isomorphous and β eutectoid (Machado and Wallbank, 1990). The most important β isomorphous alloying elements are molybdenum (Mo), vanadium (V) and niobium (Nb). These elements are mutually soluble with β titanium,

increasing addition of the solute element progressively depressing the β to α transformation up to ambient temperature. β eutectoid elements restrict solubility in β titanium and form intermetallic compounds by eutectoid decomposition of the β phase. The two most important examples of such elements used in commercial alloys are copper (Cu) and silicon (Si) (Ezugwu and Wang, 1997; Ezugwu et al., 2003). Titanium alloys may be divided into three main groups, according to their basic metallurgical characteristics: α and near α alloys, α+β alloys and β alloys (Ezugwu et al., 1997; Boyer, 1996).

2.2.1. α and near α alloys

α alloys contain α stabilizers, sometimes in combination with neutral elements, and hence have an α phase microstructure. These alloys have excellent tensile properties and creep stability at room and elevated temperatures up to 300°C. α alloys are primarily used for corrosion resistance and cryogenic applications. Near α alloys are highly α stabilized and contain only limited quantities of β stabilizing elements. They are characterized by a microstructure consisting of α phase containing only small quantities of β phase (Ezugwu et al., 2003). These are used for non-structural applications like floor support structure in the galley and lavatory areas, tubes or pipes in the lavatory system, clips and brackets, and ducting for environmental control systems (ECS). The ECS ducts operate at temperatures up to about 230 °C, which is too high for aluminum alloys. Stainless steels could be used for these applications but the titanium offers about a 40% weight savings (Ezugwu 1996).

2.2.2. α + β alloys

This group of alloys contains α and β stabilizers and possesses microstructures consisting of mixtures of α and β phases. Ti6Al4V is its most common alloy. These can be heat treated to

high strength levels and hence are used mainly for high-strength applications at elevated temperatures between 350°C and 400°C (Ezugwu et al., 1997). Ti6Al4V has been the workhorse of the titanium industry. Boyer (1996) reported that probably 80%-90% of the titanium used on aircraft structures is Ti6Al4V at that point of time. It is used in all sections of the aircraft: fuselage, landing gear and wing. Commonly used heat treatment conditions for this alloy are: Mill Annealed or Annealed (MA or A), Beta Annealed (BA) and Solution Treated and Aged (STA). In order to increase productivity and reduce the cost of the components, a new α+β alloy Ti-5Al-4V-0.6Mo-0.4Fe (TIMETAL® 54M, from now on will be written as Ti54M) with higher machinability has been developed (Kosaka and Fox, 2004).

2.2.3. β alloys

These alloys contain significant quantities of β stabilizers. These are one of the most promising groups of titanium alloys in term of processing, properties and potential applications; and represent the highest range of strength, fatigue resistance, and environmental resistance compared to other group of titanium alloys (Eylon et al., 1994). Among all titanium materials, the β titanium alloys offer the highest strength-to-weight ratio. Mo, V, Cr, Nb, Ta or Fe alloying elements lead to the stabilization of the β phase in the microstructure of the material at room temperature. Materials like Ti-10V-2Fe-3A1 (TIMETAL® 10.2.3, from now on will be written as Ti10.2.3) or Ti-5Al-5V-5Mo-3Cr (TIMETAL® 555, from now on will be written as Ti5553) are currently finding increasing share in the titanium market due to deeper hardenability and higher specific strengths in comparison to near α or α+β titanium alloys (Machai and Beirman, 2011).

In terms of tonnage, Ti10.2.3 is the most widely used of the β alloys. This easily forgeable alloy is used at three strength levels: 965 MPa, 1105 MPa and 1190 MPa (Kuhlman et al., 1991). Boeing uses the high strength level to achieve the maximum weight savings. Helicopter companies (Bell, Westland, Sikorsky and Eurocopter) are using Ti10.2.3 in their rotor systems. Westland cited advantages of using Ti10.2.3 in term of superior fatigue and tensile strength and lower stiffness over competing alloys (Boyer et al. 1993; Boyer et al. 1994). Machai and Biermann, (2011) also mentioned the possible applications of this alloy in engine and power transmission components of automobiles and helicopters.

The Boeing 787 used the next generation high-strength β alloy, Ti5553, which has slightly higher strength (Boyer, 2010). The concept for the alloy came into 1997 as an improved version of the Russian alloys VT22 and VT22-1. Since then, TIMET has been manufacturing and evaluating Ti5553 for a variety of aerospace applications. A classification of titanium alloys according to the presence of β stabilizers is presented in figure 2.3.

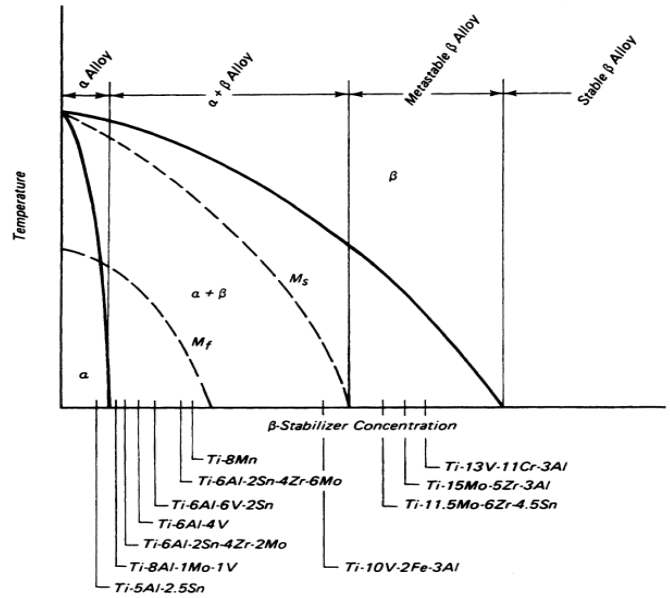

Figure 2.3. Titanium alloy compositions relative to a pseudobinary titanium phase diagram (Donachie, 2004)

2.3. Heat Treatment and Its Effects

It is apparent from the discussion in the previous section that once an alloy chemistry has been selected, microstructures in titanium alloys usually are developed by heat treatment or other processing (wrought/cast/powder metallurgy), which often use heat and/or is followed by heat treatment. The microstructure has a substantial influence on the properties of titanium alloys. The microstructure of conventional titanium alloys is primarily described by the size and arrangement of α and β phases. With the exception of commercially pure and α titanium alloys, microstructural changes are invariably produced through transformation of some or all of the α phase to β phase. The microstructure is a function of the way in which the subsequent changes in β phase or in residual (primary) α phase occur (Boyer, 1996; Donachei, 2004). There is limited phase transformation under normal heat treatment conditions (structure stays all α or almost all α), α alloys usually cannot be strengthened by heat treatment (Donachei, 2004).

α+β alloys contain one or more α stabilizers (e.g., aluminum) or α soluble elements plus one or more β stabilizers (e.g. vanadium or molybdenum) in larger amounts than in near α alloys. By moving alloy chemistry away from the α solvus phase boundary, these alloys form significant β phase when heated. When sufficient β formers are present, it is relatively easy to exceed the β transus by heating, and the alloy will be all β before subsequent cooling. The α+β alloys can retain significant untransformed β after solution treatment and cooling (Machado and Wallbank, 1982; Boyer, 1996; Donachei, 2004).

The transformation of lower-temperature α to higher-temperature β phase, which takes place upon heating α+β titanium alloys, is complete if the heating temperature goes above the β transus. The formation of a little β or a complete structure of β permits α+β alloys to be

strengthened by solution treating (exceeding the β transus, or at least producing significant β phase for subsequent transformation) and aging (heating to produce further change in the transformed β martensite, acicular α and the retained β). The specific amount of β available for transformation from a fixed temperature depends on the quantity of β stabilizers present and on processing conditions. A wide variety of microstructures can be generated in α+β alloys by adjusting the thermo-mechanical process parameters. It should be noted that β formed at high temperatures and transformed to α or martensitic variants when cooled, is often referred to as transformed β.

β alloys are characterized by high hardenability, with the metastable β phase being completely retained on air cooling of thin sections or water quenching of thick sections. Alloys of the metastable β systems are richer in β stabilizers and leaner in α stabilizers than α+β alloys (Figure 2.3). A major factor in the application of β alloys has been the excellent forgeability of alloys with cubic titanium lattice structures. In sheet form, β alloys can be cold formed more readily than high-strength α+β or α alloys. β alloys are actually metastable alloys; cold work at ambient temperature or heating to a slightly elevated temperature can cause partial transformation to α as the alloy reverts to the equilibrium condition. This metastability is exploited to produce exceptional structures from β alloys. The principal advantages of β alloys are that these have high hardenability, excellent forgeability, and good cold formability in the solution-treated condition, and can be hardened to fairly high strength levels. Because β phase is invariably metastable and has a long term tendency to transform to the equilibrium α+β structure, titanium producers use this tendency (to certain extent) by aging metastable β alloys after solution treatment and fabrication. Temperatures of 450°C to 650 °C are used to partially transform the metastable β phase to α. The α forms

as finely dispersed particles in the retained β, and room-temperature strength levels comparable or sometimes superior to those of aged α+β alloys can be attained (Donachei, 2004). In general, the class of β alloys serves a great need for titanium components that can be fabricated for moderate temperature applications. β titanium alloys show great promise in structurally demanding applications where their beneficial properties out-weigh their high cost. Microstructural control allows the tailoring of these mechanical properties. Indeed, these alloys present a range of microstructures resulting from variations of the processing parameters, leading to different levels of strength and ductility (Leyens and Peters, 2003).

2.4. Machinability of Titanium Alloys

Machinability of a material can be defined and measured as an indication of the ease or difficulty with which it can be machined. The machinability of material can be assessed by monitoring cutting tool (tool material, cutting parameters, tool geometry, cutting forces, and tool temperature, and by examining chip morphology (Barry et al., 2001; Rahman et al., 2003; Ezugwu, 2004). This section explains observed effects from literature on these issues.

2.4.1. Cutting tool

Ezugwu and Wang (1997) suggested that for improving the machinability of titanium alloys cutting tool should posses paramount qualities of: (i) high hot hardness to defy the high stresses involved; (ii) superior thermal conductivity to diminish thermal gradients; (iii) good chemical inertness to slow down the tendency to react with titanium; (iv) superior toughness to withstand the chip segmentation process (Byrant, 1998); and (v) high compressive, tensile and shear strengths.

The degree to which each of these properties is needed depends on the workpiece material. The difficulty is in finding all of these properties in the same material. Generally, there is a trade-off between hardness and toughness. As seen in figure 2.4, if wear resistance is more than toughness is less, e.g. Al_2O_3 and vice-versa, e.g. HSS. It is observed that practical cutting tools for titanium machining are carbide tools or PCD tools.

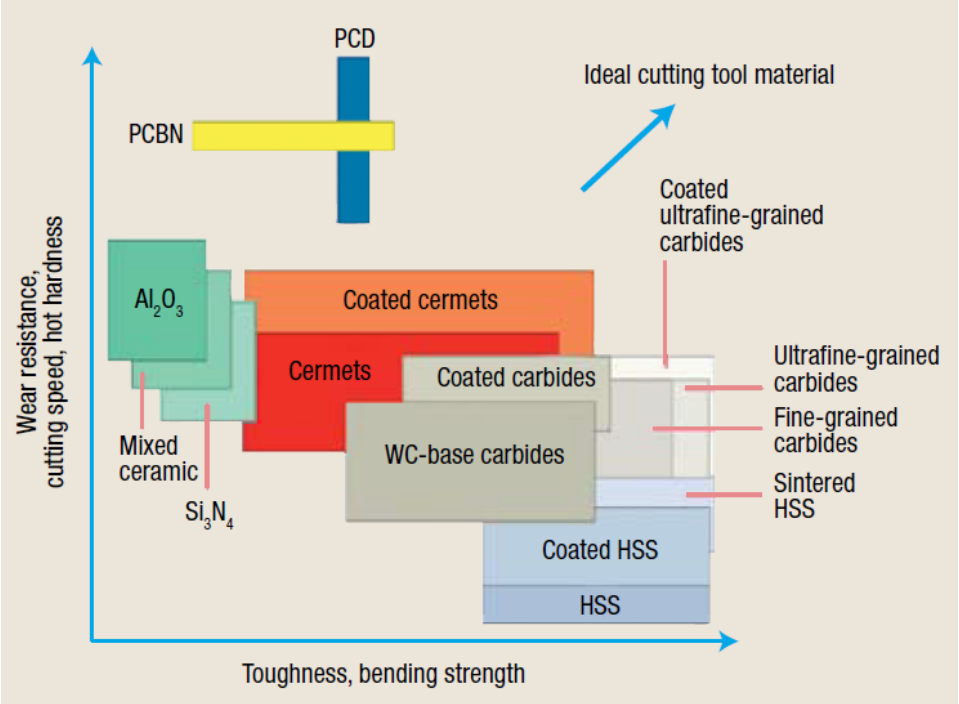

Figure 2.4. Hardness-toughness relationship for cutting tool materials (Lantrip, 2008)

2.4.1.1. Cutting tool materials for machining titanium alloys

Tool materials currently used for machining titanium alloys are shown in figure 2.5. Titanium alloys are usually machined with uncoated straight grade cemented carbide (WC–Co) tools at higher cutting speeds in excess of 45 m/min (Jawaid et al., 1999; Ezugwu and Wang, 1997). Machining at higher speeds tends to generate higher temperatures close to the tool nose resulting in excessive stresses at the tool nose causing plastic deformation and

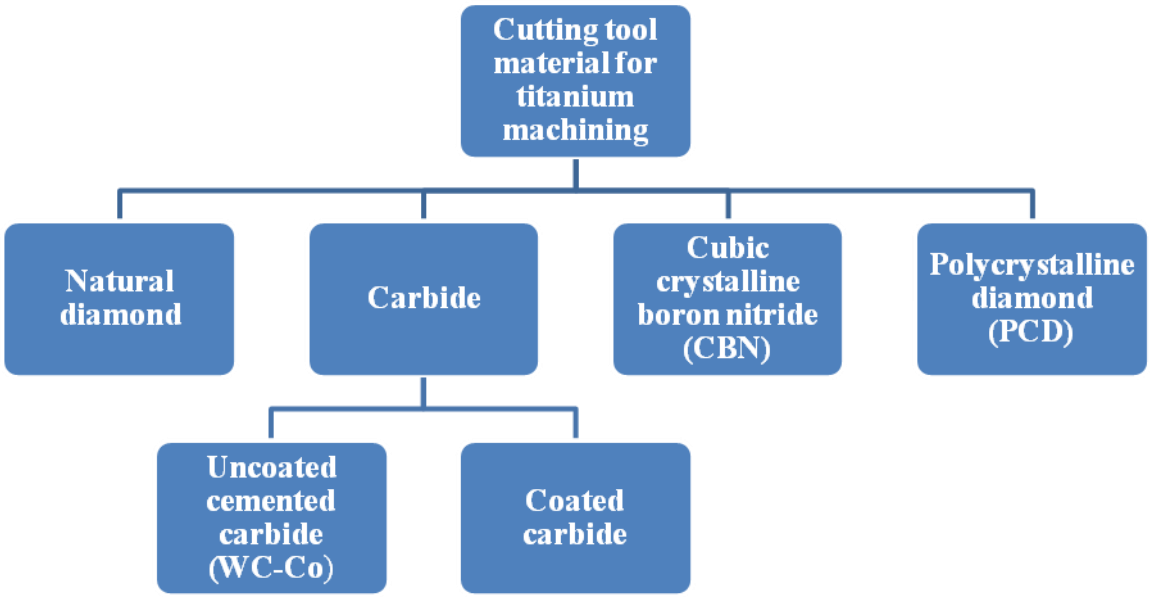

Figure 2.5. Cutting tool materials used for machining titanium alloys

subsequent tool failure (Che-Haron, 2001). At interfacial temperatures of 500°C and above, titanium and titanium alloys are very reactive with cutting tool materials (Bryant, 1998). At high temperatures the tungsten carbide-based compositions that are generally employed to machine titanium, react with the workpiece material to form titanium carbide (TiC), which is having high deformation resistance at high cutting temperatures. Titanium carbide layer adheres strongly to both the tool and the chip. The lone tool material which was found to be both more wear resistant and more deformation resistant than tungsten carbide (WC) is PCD (Hartung et al., 1982). Titanium alloys are machined with coated carbide tools in the speed range of 50 m/min and 100 m/min (Lopez de Lacalle et al., 2000). The coating provides a good thermal barrier for the tool and also lowers coefficient of friction thus lowering the cutting forces generated during machining of titanium alloys. Machining of titanium alloys with a WC–Co coated tool improves its crater wear resistance because WC–Co composite

coating suppresses diffusion of tool particles into the chip at high speed conditions by the formation of a protective layer saturated with tool particles. Cutting speeds of up to 150 m/min have been attained with this coating material (Dearnley and Grearson, 1986).

Narutaki et al. (1983) performed turning with different cutting tool materials and found that the natural diamond tool exhibits an outstanding cutting performance during machining of titanium alloys, the cutting speed could be increased up to 3.33 m/s if copious coolant is applied. Nabhani (2001) concluded PCD to be the most functionally satisfactory commercially available cutting tool material for machining titanium alloys. The PCD tools outperformed PCBN and CVD TiN/TiCN/TiC triple coated carbide tools in dry turning of Ti48 titanium alloy. This is mainly attributed to the chemical reaction between carbon substrates of the tool material and titanium forming a TiC layer. This TiC layer protects the cutting tool from abrasion and reduces the diffusion rate, thereby increasing the tool life. It could be concluded that chemical reactions between tool and workpiece materials could increase the tool life by the formation of a protective layer. Corduan et al. (2003) presented the interactions between polycrystalline diamond, cubic crystalline boron nitride, and TiB2 coated carbide with titanium based alloy. They suggested use of CBN inserts for finishing operations to get suitable tool life. Ezugwu et al. (2005) found that the performance of CBN tools, in terms of tool life, at the investigated cutting conditions is poor comparative to uncoated carbide tools. They also reported a diminution in tool life with an increase in the CBN content of the cutting tool.

Ginting and Nouari (2006) investigated the applicability of dry machining during end milling of titanium alloy Ti 6242S with uncoated alloyed carbide tools. They used an uncoated tungsten carbide with cobalt binders alloyed with 20.7 wt% of (Ti/Ta/Nb) C. The investigations were limited to the study of chip formations, tool wear, cutting temperature, and surface finish of the machined part. Observation of the worn-out tools after machining under the Scanning Electron Microscope (SEM) revealed that localized flank wear was the dominant tool failure mode. However, Dearnley and Grearson (1986) found excessive crater wear as dominant tool failure mode. This could be explained by the fact that in continuous machining such as turning, temperature at the cutting zone is much higher than that in intermittent machining. This high temperature facilitates the adhesion of the chip to the rake face of the cutting tool. The adhered material is then torn off by the flow of the chips. In addition, at high temperatures the cutting tool material diffuses into the chips at the tool–chip interface. Thus abrasion and diffusion due to high cutting temperature are responsible for crater wear on the rake face of the cutting tool in turning (Ginting and Nouari, 2006).

Ezugwu (2005) observed that there is an insignificant difference between coated and uncoated carbide tools in terms of recorded tool life; found no tangible benefit in machining with coated carbide tools with associated additional cost (typically 15%). It was further stated that the improvement in tool life can be achieved without compromising the surface finish of the machined surfaces. It is noticed that in most of the recent research findings (Table 2.2), uncoated tungsten carbides are mainly used for machining titanium alloys.

2.4.1.2. Cutting parameters and tool geometry

Data on cutting parameters have been developed experimentally on a wide variety of titanium alloys. Typical machining parameters recently used for machining titanium alloys are shown in table 2.2.

Cutting speed has the most considerable influence on tool life. It has been reported that economical machining of titanium alloys is limited to 30 m/min and 60 m/min for High Speed Steel (HSS) and tungsten carbide tools respectively, due to high tool wear (Ezugwu and Wang, 1997). Another important variable affecting the machining performance is the feed rate. Often the tool life is not changed dramatically with a change in feed, but machining of titanium alloys is very sensitive to change in feed (Khales et al., 1985). Machining at high feed rates is desirable to increase productivity. When machining titanium, the depth of cut is generally considered constant in most of the cases as indicated in table 2.2.

When machining titanium alloys, the tool geometry has a considerable influence on the tool life. The feed rates applied and chip thicknesses achieved are the key factors in extending tool life. Due to the highly localized forces close to the cutting edge, the feed rates are considerably lower than for other materials. For a CNMG 12 insert (finishing to semi roughing) the range is from 0.1 mm/rev to 0.3 mm/rev. The edge roundness on the insert is also a major factor and it must be correctly matched with the feed. Choosing the correct inserts for machining titanium is critical and the decision will largely determine the subsequent machining parameters as well as the final quality of the machined item (Sandvik, 2012).

Table 2.2. A review summary of recent tooling and cutting parameters used during machining of titanium alloys

Insert/Grade	Coolant	Cutting parameters			Author(s)
		Cutting speed (m/min)	Feed (mm/rev)	Depth of cut (mm)	
Kennametal K68 (uncoated WC-Co)	Laser assisted machining/cryogenic	107, 150, 200	0.075	0.76	Dandekar et al. (2010)
Kennametal KC5010 (TiAlN)		107, 150, 200			
Kennametal KC850 (TiC/TiN)		150			
SANDVIK CNMG 120408-23 H13A (uncoated WC–Co)	Conventional cooling (water based, 7% concentration, 6 bar, 12 l min−1)	50-90	0.1	2	Armendia et al. (2010)
		60-100			
Uncoated carbide/K10	Coolant containing alkaline salts of the fatty acid (Tri-(2-Hydroxyethyl)-Hexahydrotriazine)	100, 110, 120	0.10, 0.15, 0.20	0.5, 1.0, 1.5	Fadare et al. (2009)
CNMX1204A2-SMH13A	Cryogenic air	7-280	0.19, 0.28	1.0	Sun et al. (2010b)
Data not available	Laser assisted machining	20-230	0.214	1.0	Sun et al. (2010a)
Uncoated cemented carbide (grade K15 micrograin)	Conventional cooling method	40-90	0.1	2	Arrazola et al. (2009)
		40-60			
Uncoated straight tungsten carbide	High pressure coolant	75	0.25	2	Palanisamy et al. (2009)

Table 2.2 (Continued). A review summary of recent tooling and cutting parameters used during machining of titanium alloys

Insert/Grade	Coolant	Cutting parameters			Author(s)
		Cutting speed (m/min)	Feed (mm/rev)	Depth of cut (mm)	
(Kennametal Inc.)TPG 432/ Cemented carbide (KC 8050) with TiC/TiN/TiCN coating	Dry	58, 87, 116, 144, 174	0.075, 0.09, 0.105, 0.12	-	Fang et al. (2009)
K20 uncoated carbide	High pressure coolant	85	0.20	2.0	Nandy et al. (2008)
Sandvik type TPUN 1603 08 H10F (Uncoated fine grained WC)	Compressed air jet	Upto 140	0.05, 0.075, 0.1	-	Cotterell et al. (2008)
Uncoated microcrystalline grade carbide	Cryogenic	70, 100, 117	0.20	2.0	Venugopal et al. (2007)
PCD	High pressure coolant	175, 200, 230, 250	0.15	0.5	Ezugwu et al. (2007)
CNMG 120408-883-MR4 CNMG 120408-890-MR3	Dry	45-100	0.25, 0.35	2.0	Che-Haron and Jawaid (2005)
ISO grade K20, ISO grade K10, uncoated tungsten carbide	Data not available	50, 80, 120	0.15, 0.25	0.25	Hughes et al. (2004)
Kennametal insert CNMA432-K68 (WC-Co unalloyed grade)	Cryogenic	60-150	0.254	1.27	Hong et al. (2001a; 2001b)

2.4.1.3. Cutting forces

Determination of cutting forces has long been recognized as one of the major process parameter for: (a) monitoring cutting tool conditions (Altintas and Yellowley, 1989; Elbestawi et al., 1991) (b) characterizing machining processes (Toenshoff et al., 1995) and (c) designing and selecting cutting tools (Guo and Chou, 2004).

These days specific cutting force is also used in place of cutting force (Arrazola et al., 2009; Cotterell et al., 2010; Armendia et al., 2010) as a better indication of the power requirement. Specific force is the force needed to actually deform the material prior to any chip formation. It varies and is influenced by the undeformed chip thickness, feed rate and yield strength of the workpiece material. For example, a nickel-based alloy requires ten times more chip forming force as compared to a pure aluminium workpiece at the same cutting conditions (Smith, 2008).

Specific cutting force (K_c) and feed force (K_k) are computed as:

$$K_c = F_c / A \ (N/mm^2) \quad (2.1)$$

$$K_k = F_f / A \ (N/mm^2) \quad (2.2)$$

Where: F_c = cutting force (N), F_f = feed force (N) and A ($f * a_p$) = cutting area (mm^2)

Cutting tools used in industry have finite sharpness, and contact between tool flank and the machined surface induce ploughing force (parasitic force) (Albrecht, 1960). The ploughing force may be defined as the measured force just prior to the onset of chip formation, i.e. the force at no chip formation. The ploughing force is referred as zero-feed force by Stevenson (1998), and it explains the size effect (Boothroyd and Knight, 1989). The ploughing force is significantly important in tool wear monitoring, material flow, stress calculation, chip

formation mechanisms, and machined surface integrity. In addition, the ploughing force is also useful to evaluate the assumption of sharp cutting tools in a finite element modeling of metal cutting for predicting chips, forces, temperatures, and surface integrity (Guo and Chou, 2004). Guo and Chou (2004) obtained the ploughing forces in the cutting and feed (thrust) direction by linear extrapolation from the measured cutting and thrust forces versus uncut chip thickness at specific cutting speed. The similar approach was used by Wyen and Wegener (2010) for the determination of ploughing force components and is based on the assumption that (i) the total force in a cutting process increases linearly with increasing feed provided that the zone of the cutting edge, which is influenced by the ploughing force is fully engaged; (ii) the ploughing force does not change with increasing feed rate and (iii) the coefficient of friction μ on the tool/chip interface is independent of the uncut chip thickness. Force values can then be extrapolated to an uncut chip thickness of zero. The resulting force is the ploughing force, as shown in figure 2.6.

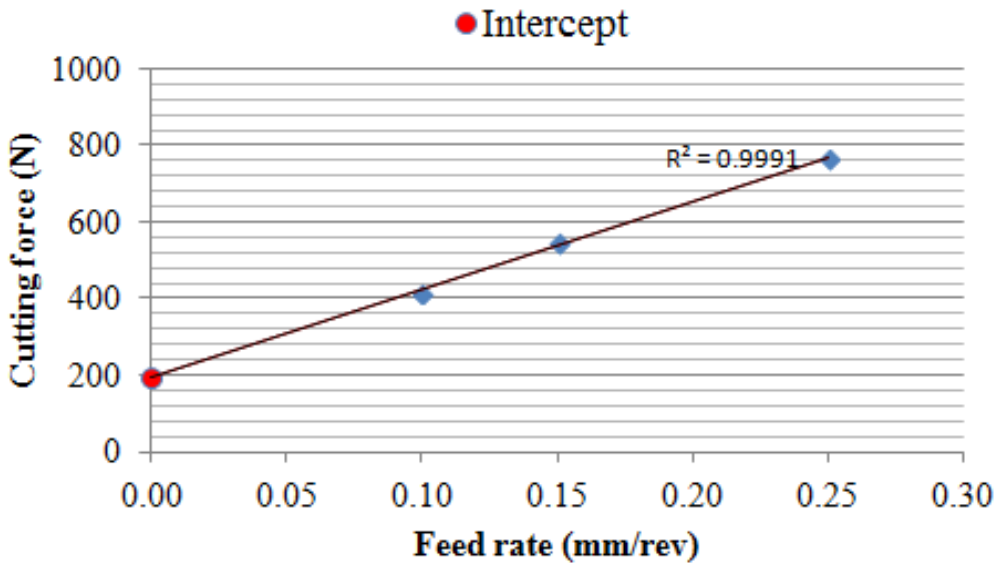

Figure 2.6. Ploughing force in cutting direction

Frictional Effects: Amontons (1699) stated in 'Law(s) of friction' that the 'friction is independent of the apparent area of contact and proportional to the normal load between two (mating) surfaces.' Coulomb (1785) confirmed these 'frictional laws' with the observation that 'the coefficient of friction is substantially independent of the speed of sliding'. Coefficient of friction is computed as:

$$\text{Coefficient of friction } (\mu) = F/N \qquad (2.3)$$

Where, F is the friction force between tool/chip interface and N is normal force perpendicular to it.

Thus, the friction force is proportional to the perpendicular force between contacting surfaces and is independent of the surface area, or its 'rubbing speed'. Friction processes in machining are characterized by the fact that new surfaces are constantly developing and these are coming into contact with the tool. The relative velocities, temperatures and contact pressures are very high and vary over wide ranges (Neugebauer et al., 2011). At very high velocities (V_c) and normal forces (N), the sliding surfaces are separated by a lubricating film of molten material reducing the friction coefficient (μ) to very low values. The findings presented by Philippon et al. (2004) underline these assumptions. These results are confirmed by the investigations of Sutter and Molinari (2005) and Zemzemi et al. (2009). The friction coefficient decreases significantly with increasing cutting speed and depth of cut (Neugebauer et al., 2011).

2.4.1.4. Cutting tool temperature

The importance of measuring temperatures during machining and evaluating their effects on both the cutting edge of the tool and the workpiece has long been appreciated (Taylor, 1906;

Barrow, 1973; Komanduri and Hou, 2001). The limiting factor to cutting speed variation for many workpiece materials is the tool wear and resulting tool failure. The temperature prediction is one of the most complex subjects in the metal cutting literature. The main reason for these complexities is that the temperature increases asymptotically with cutting speed and approaches the workpiece material melting temperature. Apart from the temperature prediction, temperature measurement is even more challenging in this area, because it is very difficult to make temperature measurement very close to the cutting edge of the tool (Dinc and Serpenguzel, 2008).

The main effect of temperature is on tool wear. It is generally known that the progressive tool wear is produced by temperature dependent mechanisms (Wanigarathne et al., 2005). Moreover, the tool life is determined by the maximum temperature on the tool rake face or the clearance face of a cutting tool. Apart from the tool, the maximum temperature and the temperature gradient influences subsurface deformation, metallurgical structural alterations in the machined surface, and residual stresses in the finished part (Komanduri and Hou, 2001).

The machining of low thermal conductivity materials such as titanium causes thermal stresses in the tool because of the lower conductivity, the heat generated during machining flow much more in the tool than the chip. As a result thermal stresses, tool fatigue, fracture failure, and tool wear occur more frequently. Sometimes the temperatures can also exceed the crystal binding limits of the tool, causing rapid wear of the tool because of the loss of bindings between the crystals in the tool material (Lazoglu and Altintas, 2002).

There are various techniques of tool temperature measurement. In addition to thermocouples, the infrared (IR) radiation techniques are probably the most used method for

the temperature measurement in machining (Robert, 2011). In the IR technique, the surface temperature of the body is measured based on its emitted thermal energy. The IR technique is applied for the temperature measurements using cameras with films or chips sensitive to IR radiation. The IR radiation technique has many advantages over the thermocouple technique (Dinc and Serpenguzel, 2008).

- The IR radiation technique is a non-intrusive technique, i.e. no physical contact with the heat source is maintained so there is no adverse effect on the temperatures and materials. In other words, the IR radiation technique does not interfere with the flow of heat like thermocouples do.
- The IR radiation technique has a very fast response, making it a very useful technique in temperature measurements because the high cutting speeds used in machining experiments today make the response of the experimental system a very important criterion.

Armendia et al. (2010c) claimed to be the first user of a micro-thermal imaging system (Figure 2.7) to determine the temperature distribution during interrupted cutting of Ti6Al4V titanium alloys. This system allowed them to measure the localized maximum temperature with 30 µm resolution on the tool rather than the spatially averaged maximum temperatures measured by the tool/chip thermocouple and two color pyrometer as reported in the literature. Ivester (2011) presented infrared-based measurements (Figure 2.8) and analysis of cutting tool temperatures for orthogonal machining of Ti6Al4V titanium alloys.

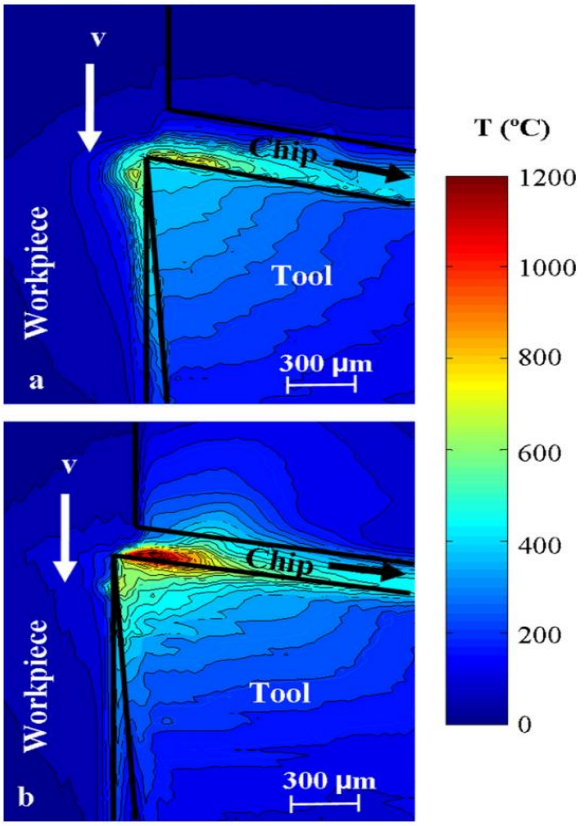

Figure 2.7. Thermal maps (V_c = 180 m/min) for machining: (a) AISI 4140 steel; (b) Ti6Al4V alloy in continuous cutting at 0.1 mm of uncut chip thickness, 1 mm of depth of cut and dry cutting conditions (Armendia et al., 2010c)

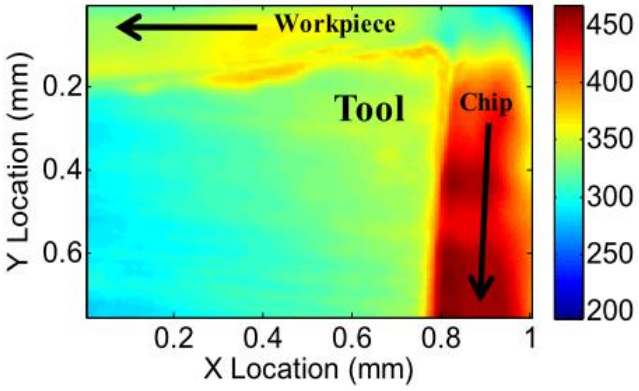

Figure 2.8. Infrared spectrum camera image – side view of orthogonal cutting (Ivester, 2011)

An increase in the peak tool temperature by approximately 70°C as the cutting speed increases from 55 m/min to 125 m/min is reported. O'Sullivan and Cotterell (2001) provided a summary of different temperature measurement techniques, based on conduction and radiation techniques used during machining (Figure 2.9). Table 2.3 presents a summary of tool temperature measurement techniques used by the researchers in the past.

Pioneering efforts by (Boothroyd, 1961) in infrared photography-based temperature measurement in metal cutting provided useful insight into the spatial distribution of cutting tool temperatures. The limited sensitivity of the infrared-sensitive film required substantial preheating of the workpiece and extremely long exposure times, thereby, reducing the quantitative utility of the measurements (Ivester, 2011). Recent advancements in digital infrared-sensitive detector arrays enable microsecond-level control of integration time and frame timing and provide dramatically improved sensitivity to infrared light (Aluwihare et al. 2000; Davies et al. 2003a; Davies et al. 2003b; Ivester et al. 2005; Whitenton et al. 2005; Arrazola et al. 2008; Cooke, 2008; Whitenton, 2010).

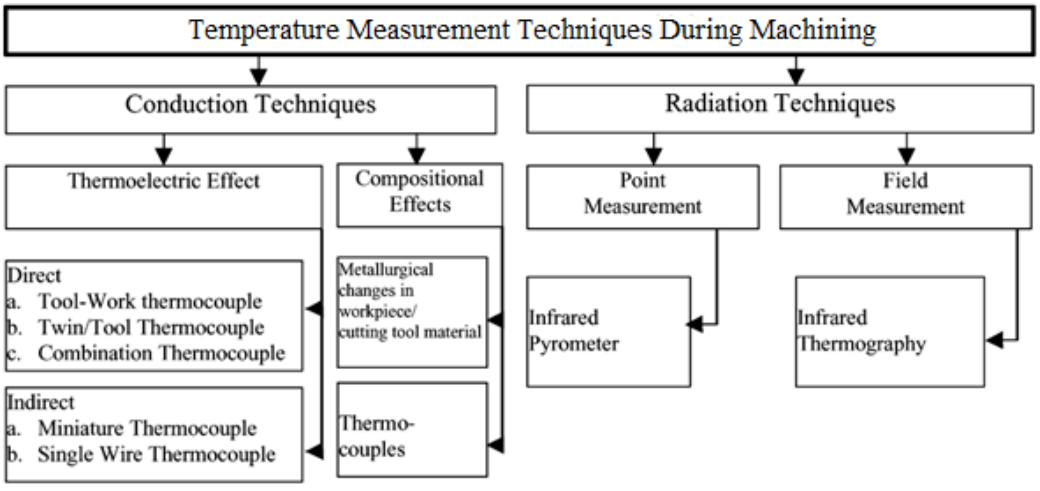

Figure 2.9. Temperature measurement techniques during machining (O'Sullivan and Cotterell, 2001)

Table 2.3. Summary of temperature measuring techniques

Material	Type	Technique	References
AISI 2024 aluminum and grey cast iron	Conduction	Tool/chip Thermocouple	Stephenson and Ali (1992)
Ti6Al6V2Sn alloy	Conduction	Micro thermocouple	Kitagawa et al. (1997)
6061 aluminum, copper, cast iron, and AISI 1045 steel alloy	Conduction, Radiation	K-type fine thermocouples, infrared thermovision	Ay et al. (1998)
Hardened steel alloy	Radiation, Conduction	IR camera system and a thermocouple system	Dewes et al. (1999)
Medium carbon steel and an austenitic stainless steel alloys	Conduction	K-type thermocouple	Grzesik (1999)
Aluminum 6082-T6 alloy	Conduction	Thermocouples	O'Sullivan and Cotterell (2001)
AISI 1045 steel alloy	Conduction	Fiber–optic two-color pyrometer	Ueda et al. (2001)
AISI 1045 alloy	Radiation	Fiber–optic two-color pyrometer	Muller and Renz (2003)
Aluminum alloy	Radiation	IR pyrometer	Ming et al. (2003)
Data not available	Radiation	Fiber–optic two-color pyrometer	Lazoglu et al. (2006)
AISI 1045 Steel alloy	Radiation	Thermal imaging system	Davies et al. (2005)
Al 7075 and AISI 1050 alloys	Radiation	IR camera	Dinc and Serpenguzel (2008)
AISI 4140 steel and Ti6Al4V alloys	Radiation	Micro-thermal imaging system	Armendia et al. (2010)
Ti6Al4V alloy	Radiation	Infrared-based	Ivester (2011)

The primary impediment to the understanding of thermal behavior in material removal is the inability to measure temperatures accurately, consistently, and with high resolution and high bandwidth. While technology has improved, the list of phenomena exploited to measure temperature has changed little (Davies, 2007).

2.4.2. Chip morphology

Chip morphology and segmentation play a predominant role in determining machinability and tool wear during the machining of titanium alloys. Due to its importance, the chip segmentation phenomenon has been extensively investigated and studied by researchers.

Attempts to describe the chip morphology in cutting titanium and its alloys date back to the work performed by Cook (1953). He investigated the chip morphology of titanium at different cutting speeds and proposed a thermodynamic theory for chip formation. Analyzing different titanium chips at cutting speed range of 1 inch/min to 300 ft/min, Cook (1953) attributed the difference in morphology between the chips at high speed and low speed to the temperature generated during the cutting process. The greater the cutting speed, the higher the temperature in primary deformation zone. When the temperature softening effect in the primary deformation zone is stronger than the strain hardening effect, the chip becomes serrated.

Numerous studies on the machining of titanium alloys in term of chip formation analysis and cutting forces have been carried out (Komanduri and von Turkovich (1981); Komanduri (1982); Narutaki and Murakoshi (1983); Hua and Shivpuri (2002); Sandstrom and Hodowany (1998); Trent (1991); Larbi (1990); Bayoumi and Xie (1995); Diack (1995); Hoffmiester et al. (1999) and Molinari et al. (1997)). These studies illustrated several unique features associated with the machining of these alloys (Komanduri, 1982; Syed, 2004):

- The role of poor thermal properties of titanium alloys, which interact with the physical properties in controlling the nature of plastic deformation (i.e. Strain localization) in the primary zone.

- Instability in the chip formation process results in the segmented or cyclic chip.
- Oscillations in the cutting and thrust components of force are caused due to chatter.
- High tool/chip interface temperatures and high chemical reactivity of titanium during machining with almost any tool material are responsible for the rapid tool wear.
- The low modulus of elasticity, which decreases rapidly even at moderate temperatures causes undue deflections of the workpiece especially when machining slender parts.
- Chip segmentation is observed to be related to adiabatic shear banding.
- Adiabatic shear bands are the manifestation of a thermo-mechanical instability resulting in the concentration of large shear deformations in narrow layers.
- Chip serration is related to the development of deformed shear bands for velocities lower than 1.2 m/s. However, at lower values of cutting speed, the instability process is weak and the localization is not as sharp as for higher speeds.

Barry et al. (2001) conducted orthogonal cutting tests to investigate the mechanism of chip formation and to assess the influence on acoustic emission (AE) for a Ti6Al4V alloy with an uncoated P10/P20 carbide tool. Figure 2.10 shows the influence of cutting speed and feed on chip morphology during the orthogonal cutting of Ti6Al4V. The chips obtained for different cutting conditions in the range 20 µm -100 µm feed and 0.25 m/s - 3 m/s cutting speed are classified as either aperiodic saw-tooth or periodic saw-tooth. Accordingly, it was observed that with low values of cutting speed and undeformed chip thickness (e.g., 20 µm), aperiodic saw-tooth chips were produced. Increase in either or both of these parameters resulted in a transition from aperiodic to periodic saw-tooth chip formation.

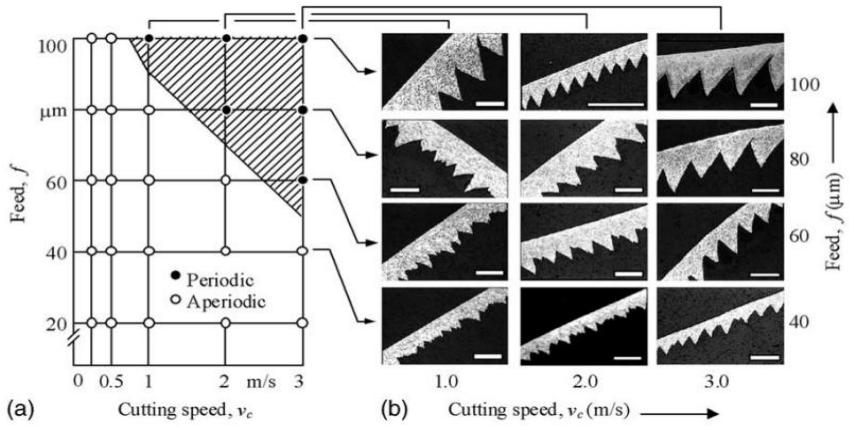

Figure 2.10. Chip morphology as a function of cutting speed and feed in orthogonal cutting of a Ti6Al4V alloy (Barry et al., 2001)

Bayoumi and Xie (1995) conducted orthogonal cutting tests on titanium alloys and concluded that the intensive shear takes place in a narrow zone rather than in a plane as is often assumed by some investigators in the analysis of orthogonal machining process. It was further reported that for each work material there exists a critical value (V_f) of chip load at which shear localized chips were observed. The cutting conditions also influence the shear banding in a way that the shear banding frequency increases with an increase in feed rate or a decrease in cutting speed.

Sun et al. (2009) conducted dry turning experiments on Ti6Al4V using a 3.5 hp Hafco Metal Master lathe (Model AL540). The investigations on the deformed chips for different cutting speeds under a microscope found that there is a mixture of segmented and continuous chips (Figure 2.11), which has not been reported previously. After examining these chips under higher magnification difference in deformation during the segmented and continuous chip formation was found as shown in figure 2.11 (b and c). Continuous and uniform shearing with smaller slipping angle (38^0) was found during the continuous chip period. In the sharp

‘‘saw-tooth’’ period, a narrow shear band with heavier deformation and larger slipping angle (55^0) was observed.

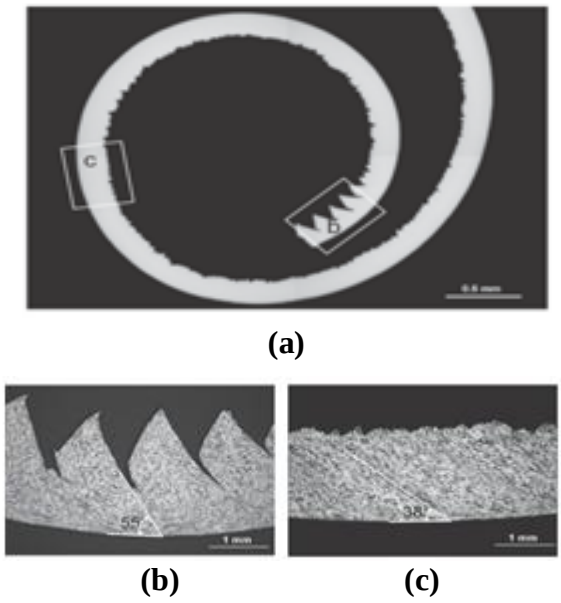

(a)

(b) **(c)**

Figure 2.11. Cross-sections of chip with mixed segmented and continuous chips at a cutting speed of 16 m/min, depth of cut of 1.50 mm and feed of 0.280 mm (Sun et al., 2009)

Armendia et al. (2010) concluded adiabatic shear-band formation in the chips of both Ti6Al4V and Ti54M alloys at all cutting speeds. The cross-section of chips obtained after machining both alloys at the cutting speeds of 50 m/min and 60 m/min for the Ti6Al4V and Ti54M alloys respectively are shown in figure 2.12.

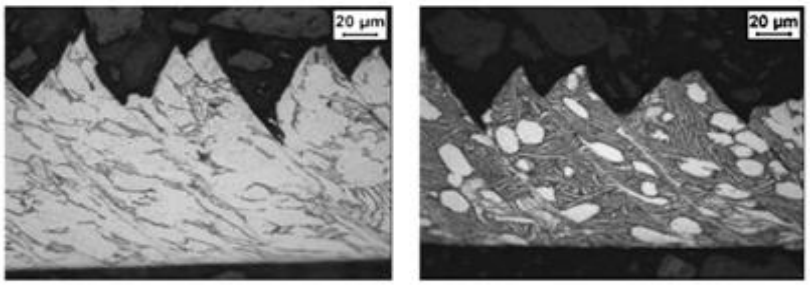

(a) **(b)**

Figure 2.12. Chip cross-section: (a) Ti6Al4V alloy at 50 m/min and (b) Ti54M alloy at 60 m/min (Armendia et al., 2010a)

2.5. Machinability Improvement Techniques

Researchers and industrial engineers have focused on improving the machining performance of titanium alloys through a number of methods. This has traditionally resulted in better heat management at the tool/chip interface using various technologies that incorporate new synthetic coolants, high pressure coolants, cryogenic coolants, minimum quantity lubrication (MQL), steam coolants, compressed gas coolants or hybrid combinations (Sutherland et al., 2000; Wang and Rajurkar, 2000; Sales et al., 2002; Ezugwu, 2004; Su et al., 2006; Sharma et al., 2009; Nandy et al., 2009; Palanisamy et al., 2009; Junyan et al., 2010; Yuan et al., 2011). Such technologies are reported to extract more heat from the cutting zone and offer better tool life than that achievable using flood cooling. Dry machining is considered as the best approach to eliminate the use of cutting fluids in machining and thus reduce the machining costs and ecological hazards (Klocke and Eisenbl¨atter, 1997; Rivero et al., 2006). Weinert et al. (2004) identified the benefits of dry machining as shown in figure 2.13. In dry machining, friction and cutting temperature could be more than that in wet machining (Shokrani et al., 2012). It could reduce the tool life, surface quality and cause thermally induced geometrical deviations in the machined part. However, this is not the case for all materials and machining operations. Dry cutting shows positive effects such as lower thermal shock and improved tool life in some cases (Sreejith and Ngoi, 2000; Klocke and Eisenbl¨atter, 1997).

To overcome machining difficulties and improving the productivity of titanium alloy machining, lot of research is directed in understanding how the machining performance can

be improved by modifying the workpiece material, specifically its microstructure by heat treatment process (Armendia et al., 2010a).

Figure 2.13. Benefits of adopting dry machining (Weinert et al., 2004)

2.5.1. Cryogenic cooling

Cryogenic cooling, which is an environmentally safe alternative to conventional emulsion cooling, is an efficient way of maintaining the temperature at the cutting interface well below the softening temperature of the cutting tool material (Akir et al., 2004). Liquid nitrogen is commonly used in cryogenic cooling applications because of its low cost and environment friendliness among other cryogenic fluids like helium, hydrogen, neon, air, or oxygen. Some potential benefits of cryogenic cooling mentioned in the literature are (Kopac, 2009; Ahmad-Yazid et al., 2010):

- sustainable manufacturing (cleaner, safer and environment friendly),

- increased material removal rate,
- increased tool life, and
- improved machined part surface quality/integrity.

Hong et al. (2001c) observed that the tool life increased up to 5 times using cryogenic cooling over the emulsion cooling. Venugopal et al. (2007) found that the maximum flank wear reduces 3.4 times as compared to dry turning and 2 times as compared to wet turning of Ti6Al4V titanium alloy under cryogenic cooling. Experiments showed that the cryogenic cooling by liquid nitrogen hampered the growth of tool wear very effectively at moderate cutting velocity of 70 m/min enhancing the tool life from 7 minutes under dry machining and 14 minutes under wet machining to 24 minutes. It was found that such advantages decrease under high cutting speed of 100 m/min and 117 m/min possibly due to improper penetration of liquid nitrogen in the chip/tool interface. Dhananchezian and Kumar (2011) concluded that cryogenic cooling showed a substantial improvement in the cutting force, surface roughness and tool wear through the control of the cutting zone temperature.

The main disadvantages of this technology, besides additional equipments, are relatively high price of liquid nitrogen and its non reusability unlike conventional cutting fluids. Therefore, it is very crucial to select the appropriate cryogenic cooling strategy to maximize the efficiency.

2.5.2. High pressure cooling

Another technique employed for reducing cutting zone temperature and improving overall productivity is high pressure cooling. In this method, a jet of pressurized cutting fluid is directed to penetrate the tool/chip interface so that maximum possible heat extraction from the cutting zone can be ensured. The aim is to reach the regime of hydrodynamic lubrication

whereby the seizure of the chip to the tool can be eliminated. The high pressure cooling technique has been successfully employed in machining of steel and titanium alloys (Nandy and Paul, 2008). Pigott and Colwell (1952), Sharma et al. (1971), Nagpal and Sharma (1973), Kaminski and Alvelid (2000), and Mazurkiewicz et al. (1989) reported improvements in tool life, surface finish, dimensional accuracy, and BUE elimination. This method results in not only reducing the wear of cutting tools but also brings about a drastic reduction in cutting forces, coefficient of friction at the tool/chip interface, improvement in surface quality, change in chip shape along with enhancement in productivity.

The high pressure cooling technique has also been attempted in machining of titanium alloys. Kovacevic et al. (1995) and Machado et al. (1998), reported reduction in cutting forces, coefficient of friction, cutting zone temperature along with improvement in tool life and productivity. Nandy et al. (2009) developed a high pressure cooling technique with water-soluble oil enhancing tool life at least by 250% compared to conventional wet environment. It was pointed out that high pressure cooling also provides desirable chip breaking, which is essential in automated machining environment. Authors also observed significant reductions in the cutting forces. Palanisamy et al. (2009) reported that the application of coolant at high pressure increases tool life by almost three times while turning Ti6Al4V alloy. Nandy et al. (2008) revealed that at a cutting speed of 85 m/min and feed rate of 0.2 mm/rev, high pressure cooling provided a tool life of 24 minutes in comparison with 12 minutes under cryogenic cooling.

2.5.3. Laser assisted machining (LAM)

Instead of enhanced cooling strategies which have been focused on improving the machinability of titanium alloys for years, laser assisted machining offers an alternative

strategy to improve the machinability by reducing the cutting pressure. Laser assisted machining (LAM) is a process in which an external laser source is employed to heat and soften the workpiece locally in front of the cutting tool. The process has attracted research interest for decades, because it offers a number of benefits when machining hard-to-cut materials. Cutting forces in all three directions have been reduced dramatically with the assistance of a laser beam and the reduction of cutting forces strongly depends on the cutting speed (laser energy input due to beam–workpiece interaction time), depth of cut, tool–beam distance, laser spot size, laser power and the beam incident angle (Rajagopal et al., 1982; Germain et al., 2007; Sun et al., 2008).

However, the heat source has to be carefully controlled to ensure that the thickness of the heat affected layer associated with Widmanstatten (needle-shaped) microstructure formation is within the cutting zone. The Widmanstatten microstructure that remains in the subsurface contributes to a reduction in its fatigue life (Germain et al., 2007). One advantage of a laser beam as an external heat source is its smaller and accurately controlled spot size (Lacalle et al., 2004), there is no Widmanstatten microstructure observed in the machined subsurface after laser assisted machining (Sun et al., 2008; Germain et al., 2007; Dandekar et al., 2010). The significant effect of laser power on the force reduction during laser assisted turning of commercially pure titanium (a ductile workpiece) is only found at the beam incident direction (Sun et al., 2008).

The machinability of titanium from low (60 m/min) to medium-high (107 m/min) cutting speeds; and from low to high (150–200 m/min) cutting speeds has been improved by laser assisted machining and hybrid machining (a combination of laser-assisted machining and cryogenic cooling of the tool) respectively (Dandekar et al., 2010). The optimum material

removal temperature was established as 250^{o}C. Two to three fold tool life improvements over conventional machining is attained for hybrid machining up to cutting speeds of 200 m/min with a TiAlN coated carbide cutting tool. Post-machining microstructure showed no change from pre-machining conditions. An overall cost savings of approximately 30% and 40%, can be yielded by LAM and the hybrid machining process respectively with a TiAlN coated tool (Dandekar et al., 2010).

2.5.4. Heat treatment

Recent work has shown an increasing trend towards exploring relationship between heat treatment and machinability. Kosaka and Fox (2004) concluded that the machining of Ti54M and Ti6Al4V titanium alloys depends substantially on the size and arrangement of the phases present in microstructure. During the development stage of Ti54M alloy, it was realized that the machinability also depends on the heat treatment conditions, i.e. on strength, microstructure, as well as chemistry of the material (Kosaka et al., 2004; Arrazola et al., 2009; Aermendia et al., 2010). Egorova et al. (2003) reported that the titanium alloys with fine lamellar or globular structures are cut better than alloys with a coarse lamellar structure. An improvement in the machinability of titanium alloys by decreasing the sizes of the β grains and the intragrain microstructural components was observed. The opinions of different authors on the effect of microstructural parameters on the machinability differ due to the great variety of combinations of structural components with various sizes and shapes.

Armendia et al. (2010) compared the machinability of Ti54M and Ti6Al4V alloys and found significant differences with reference to the morphology and volume fraction of the primary α phase for both alloys. The microstructure (Figure 2.14) of the studied alloys consists an

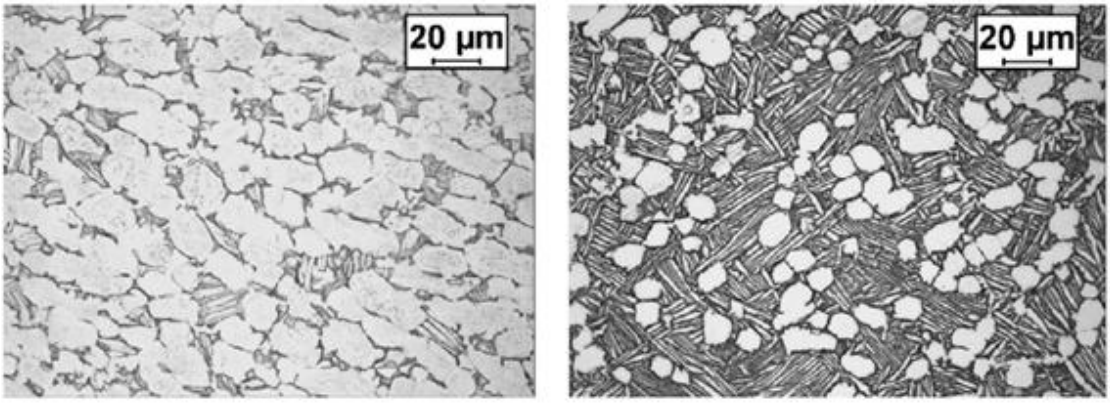

Figure 2.14. Microstructure of the: (a) Ti6Al4V and (b) Ti54M titanium alloys (Armendia et al., 2010a)

equiaxed α phase in a transformed β matrix. They compared the maximum cutting speed of the two alloys, and found that the machinability of the Ti54M could be approximately 10%–15% greater than the Ti6Al4V in the analyzed cutting conditions.

In order to compare the machinability of Ti6Al4V and Ti5553 alloys, Arrazola et al. (2009) measured and analyzed: (i) the specific cutting force and specific feed force, (ii) tool wear, (iii) chip morphology, and (iv) rake face and cutting edge after machining. They found significant difference in microstructures (Figure 2.15) of the Ti6Al4V and Ti5553 alloys with respect to the quantities and morphologies of the primary α and the transformed β phases as well as the grain size. They observed that the knowledge of the β transus temperature along with the thermal history of the respective treatments allow the generation of predictive information for each alloy. Titanium alloys can be classified based on the value of the Al and Mo equivalent parameters. The Al equivalent value indicates the capacity of the alloy to obtain a given hardness, whereas the Mo equivalent value indicates the capacity to obtain an ultimate tensile strength (UTS) and hardness in the aged condition (Arrazola et al., 2009).

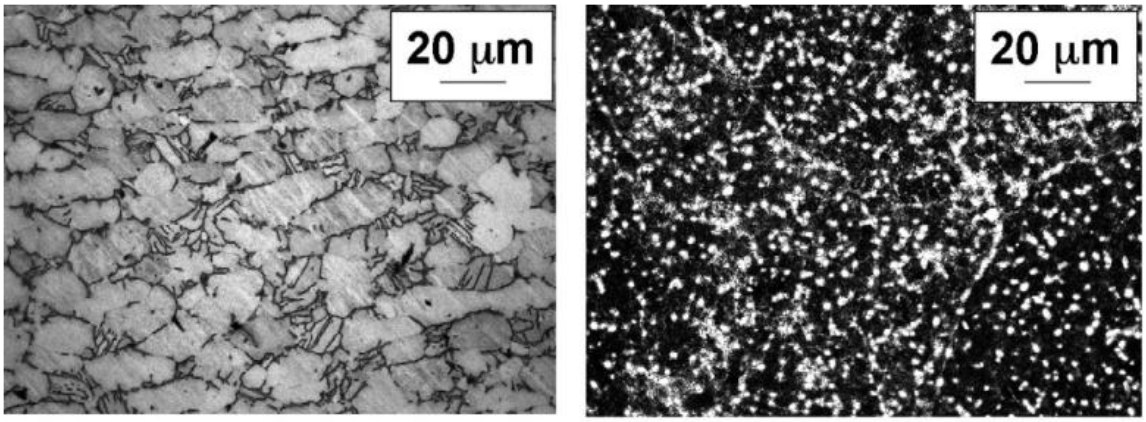

(a) **(b)**

Figure 2.15. Microstructure of the: (a) Ti6Al4V and (b) Ti5553 titanium alloys (Arrazola et al., 2009)

2.6 Gaps in the Existing Literature

Very less research has been done to explore the relationship between machinability and heat treatment for the titanium alloys. Several studies have been pointed out the difficulties in machining titanium alloys but most of them focused on the widely used Ti6Al4V alloy. A few numbers of research papers have been published dealing with machining of increasingly used Ti54M, Ti10.2.3 and Ti5553 alloys compared to the widely used Ti6Al4V alloy (Figure 2.16). Limited research on Ti10.2.3 and Ti5553 alloys demonstrate an even poorer machinability than Ti6Al4V leading to higher manufacturing costs. Therefore, there is a great need to explore the machinability improvement techniques, in this case heat treatment, for these increasingly used α+β and β alloys. There is also a need to generate more data on Ti54M alloy, a newly developed α+β titanium alloy having similar mechanical properties to Ti6Al4V alloy. Ti54M alloy has been developed to improve upon the overall production costs of Ti6Al4V and the replacement of Ti6Al4V alloy will provide huge benefits to aerospace industry.

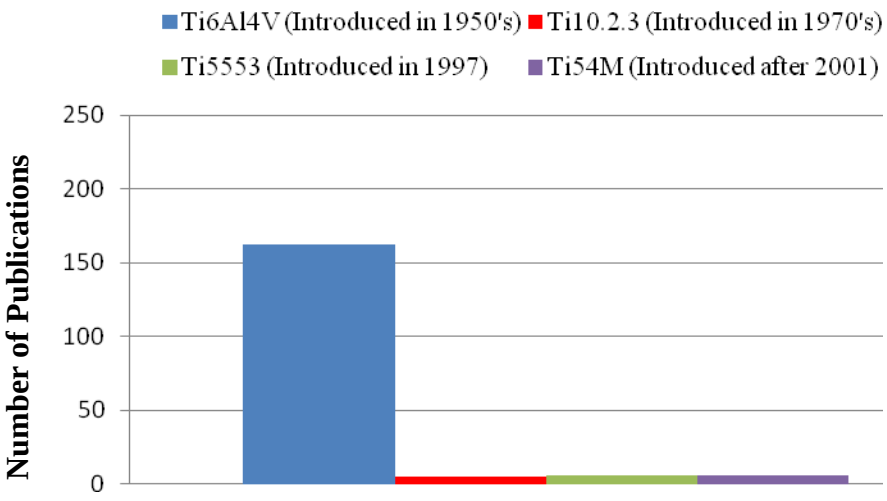

Figure 2.16. Publications referred on different titanium alloys

Chapter 3

Experimental Setup and Plan

3.1. Introduction

This chapter elucidates the experimental setup and the plan to obtain the cutting forces and temperature for the research. The specimen preparation for checking microstructure and chip morphology is also discussed. The experimental studies are performed to analyze the influence of chemical composition, heat treatment, machining process variables, and cutting tool geometry on machinability of the titanium alloys. The experimental setup was a combination of four elements: the machine tool, the workpieces, the thermal imaging system, and the dynamometer as shown in figure 3.1. The thermal imaging system, the dynamometer, and the workpieces were integrated on the machine tool. For this setup, the machining center was configured to act as a lathe with the tool oriented to produce an orthogonal cut by removing the end of the workpiece. The tool holder was placed on the dynamometer to record changes in the force measurement. The thermal imaging system was focused on the tool/chip interface, thus making thermal measurement acquisition possible.

3.2. Machine Tool

The LAGUN CNC machining centre (RPM: 18000, Power: 15kW, Torque: 80Nm) used for the experiments is shown in figure 3.1. This machine tool can be used with conventional and minimum quantity lubrication during machining operation. When the experiment is to begin, workpiece is placed in the off position but at a high altitude over the tool and will stand at a safe distance from the cutting tool.

Figure 3.1. Experimental setup (HPC Laboratory, 2011, Mondragon University, Spain)

At this point, it should be verified that everything is ready for recording.

3.3. Workpiece Materials

The four titanium alloys used for experimental purpose are Ti54M (α+β), Ti6Al4V (α+β), Ti5553 (β), and Ti10.2.3 (β). The experimental plan was divided into two areas. One, to study the effect of different heat treatment conditions on the machinability of Ti54M (α+β), Ti6Al4V (α+β), and Ti10.2.3 (β) titanium alloys. Two, to study the effect of cutting parameters and tool geometry on the machinability of Ti6Al4V (α+β) and Ti5553 (β) alloys Further, Ti54M (α+β) and Ti10.2.3 (β) titanium alloys were in three different heat treated conditions, while Ti6Al4V (α+β) titanium alloy was used in an annealed condition to study the effect of heat treatment on machinability of these alloys as shown in figure 3.2.

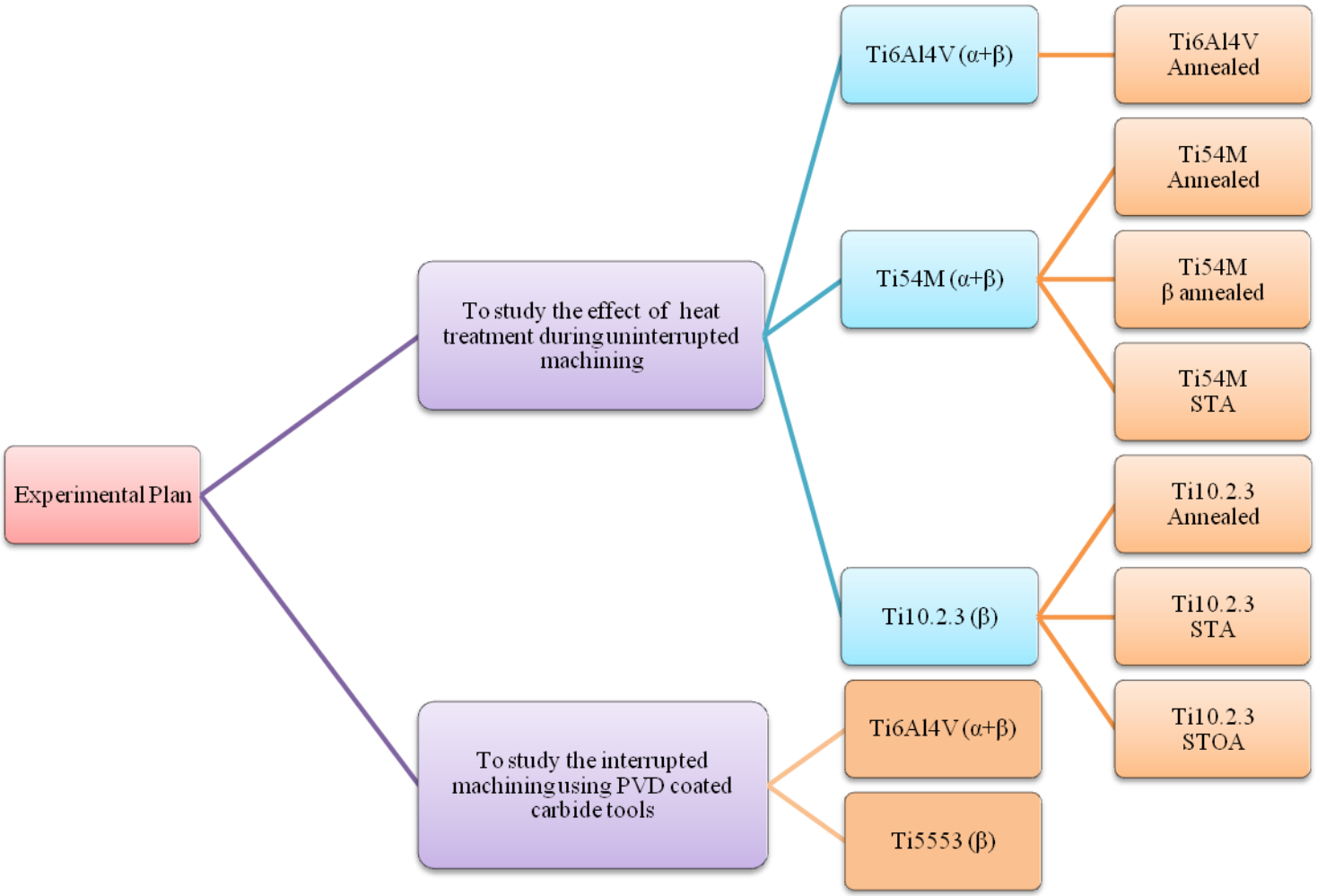

Figure 3.2. Details of experimental plan

The workpieces for heat treatment study were machined from the solid bars to a final dimension of 65 mm in length, 48 mm in outer diameter, and 2mm in thickness. A 30 mm long solid base was bolted to a tool holder that was then mounted in the vertical spindle of the machining centre. Similarly, the workpieces used for interrupted machining operations (Ti5553 and Ti6Al4V alloys) were machined from a solid bar to a final dimension of 45 mm in length, 40 mm in outer diameter, and 1mm in thickness as shown in figure 3.3. A 30 mm long solid base was bolted to a tool holder that was then mounted in the vertical spindle of the machining centre. All the workpieces were prepared from solid bars to maintain uniform properties. The workpieces were prepared to maintain concentricity between the workpiece surface and the spindle axis.

Figure 3.3. Workpiece for interrupted machining

In order to observe the microstructures, the test specimens were prepared for microscopic examination by grounding and polishing using a series of four silicon carbide disks and diamond paste at 240 - 300 rpm. The polished surface was then exposed to Kroll's reagent (6ml HNO_3 + 4ml HF + 20ml H_2O), allowing the microstructure of the material to be observed by means of optical microscopy.

3.4. Temperature Measurement and Calibration

The temperature at the rake of the cutting tool was measured, using infrared radiation technique, with the help of a FLIR thermal imaging system (FLIR 550M+) consisting of a 320 by 256 cooled indium antimonide focal plane array and a germanium lens (Figure 3.4). The control of the camera includes, but is not limited to, adjusting the integration time to increase or decrease sensitivity based on the temperature and characteristics of the measured surface. The frame size is adjusted to increase or decrease the number of frames captured per second. The integration time was fixed at 200 μs. The frame size was reduced to 80 by 64 pixels, allowing an acquisition frequency of 1250 Hz (40MPixles/s) at a spatial resolution of 10 μm per pixel. The temperature was measured for the last one second of machining and the total duration of cut was five seconds.

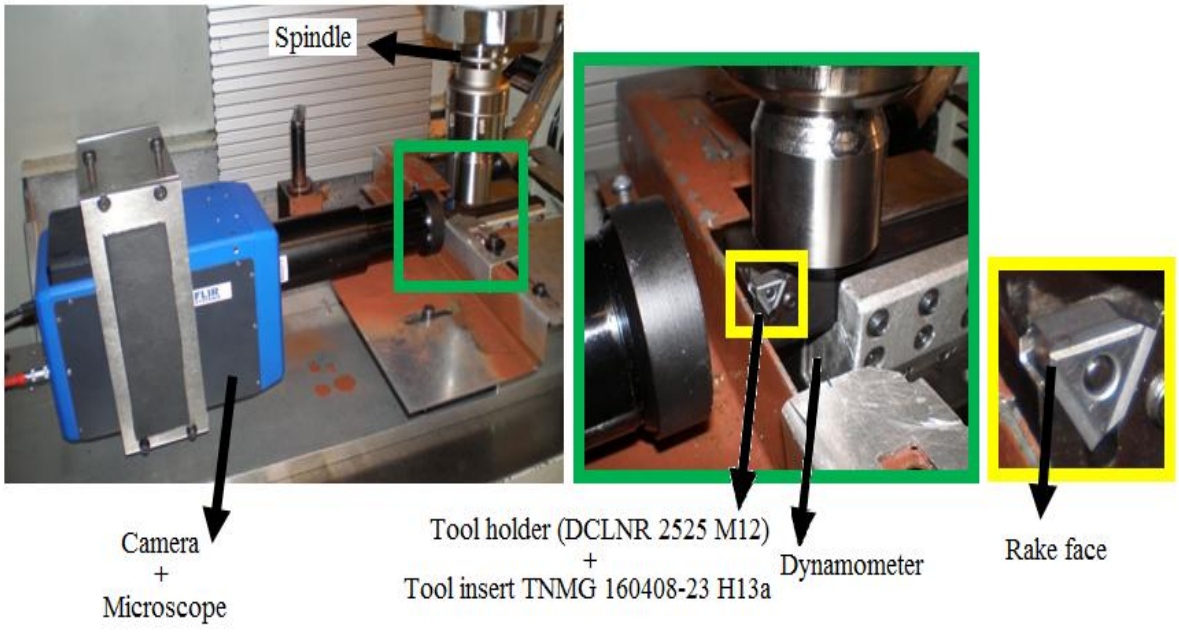

Figure 3.4. Temperature measuring system (HPC Laboratory, 2011, Mondragon University, Spain)

Temperature values were measured at 0.3 mm distance (d) from the grounded surface of the insert. Although the position of the workpiece/insert contact was also a controlled parameter before the experiment, high intensity during experimentation may involve some small variations thereof. The value of d is a critical parameter in determining the final temperature; therefore, inserts were inspected with a microscope to determine the value of d after each experiment. To analyze the influence of the parameter d on the final temperature, series of experiments were conducted on a titanium alloy at High Performance Cutting Laboratory, Mondragon University, Spain, for which the results are shown in figure 3.5. Therefore, on this basis temperature values have been added or subtracted to those measured temperature values, which were measured instead of 0.3 mm distance (d) from the grounded surface. This was done to make the results proportional.

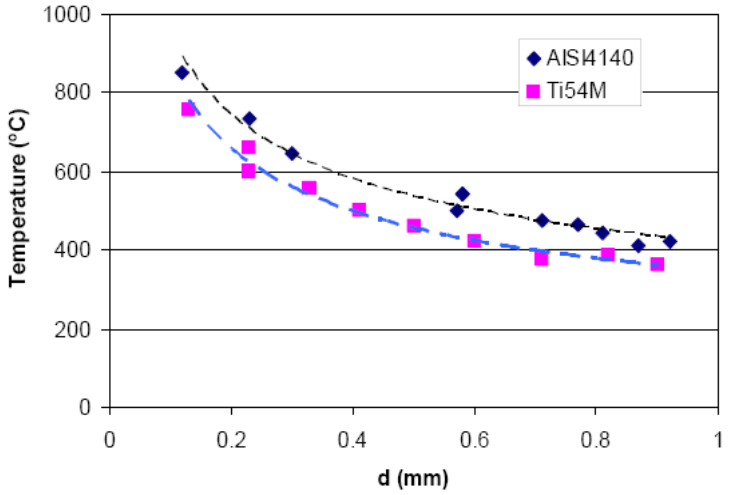

Figure 3.5. Influence of the parameter d on the final temperature (HPC Laboratory, 2011, Mondragon University, Spain)

The imaging system detector was calibrated against a black body with controlled temperature and an emissivity of 0.995 independent of the wavelength. The emissivity of the workpieces and tool materials were measured as a function of wavelength and temperature.

Thermal radiation was measured in the narrow band (3.97–4.01 μm) to obviate the wavelength variation so that only the influence of temperature is measured. A different value of emissivity was applied to each pixel depending on its blackbody temperature. The average values of emissivity were found to be 0.3 and 0.25 for the tailored carbide tools and Ti6Al4V workpiece material respectively.

To analyze the whole process, it is very important to use the tool spot to put a point on the cutting edge and get a 'Timing-graph' to see the evolution of that point throughout the trial (Figure 3.6). The step-wise details of temperature measurement are presented in figure 3.7.

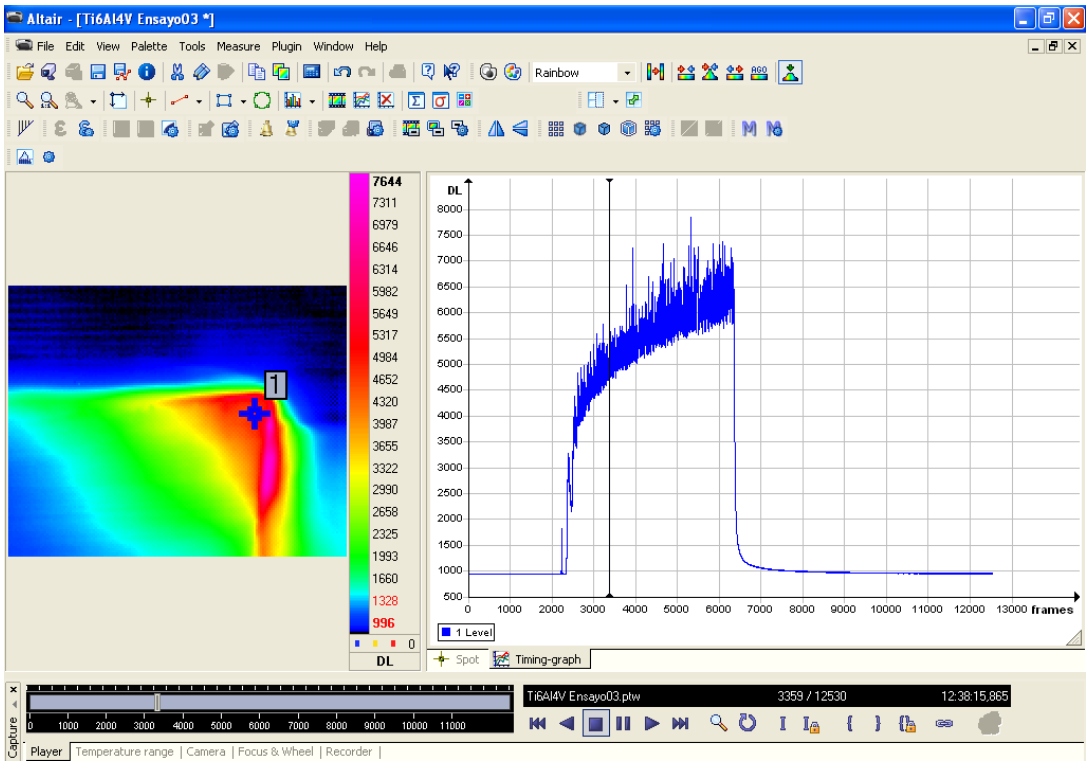

Figure 3.6. Altair software image showing a 'digital level timing graph' of point 1 marked on the cutting edge of the tool (HPC Laboratory, 2011, Mondragon University, Spain)

Figure 3.7. Schematic diagram showing temperature measurement

The average uncertainties for the cutting tests were approximately $\pm 50^0$C. These uncertainties were attributed to fluctuations around the mean emissivity, stray light from other sources, surface location fluctuations, and focus conditions due to the low Young's modulus of titanium alloys. A MATLAB program was used to find these uncertainties in the temperature profiles.

3.5. Dynamometer

A dynamometer was used to measure cutting forces on LAGUN CNC machine tool with tool turret. The tool was mounted on a stationary dynamometer (Kistler 9121) in order to measure the cutting force. The dynamometer (Figure 3.8) was firmly connected to the base plate of the machining centre. The cutting force produced by the turning process was resolved by the multi component dynamometer directly into the orthogonal components: main cutting force (F_c) and feed force (F_f). The dynamometer consists of four numbers of three-component force sensors fitted under high preload between a base plate and a top plate. Each sensor contains three pairs of quartz plates, one sensitive to pressure in the z direction and the other two responding to pressure in the x and y directions. The force components were measured practically without displacement. The dynamometer was connected to multichannel charge amplifier, which converts the dynamometer charge signals

into output voltages proportional to the forces. Technical details of the dynamometer are summed up in table 3.1.

Figure 3.8. Kistler 9121 dynamometer (Kistler)

Table 3.2. Technical data for Kistler 9121 dynamometer (Kistler)

Specifications	**Direction**	**Kistler dynamometer**
Type	Fx, Fy, Fz	9121
Calibration		Calibrated
Measuring Range	Fx, Fy, Fz	–3 ... 3 kN –6 ... 6 kN
Sensitivity	Fx, Fy, Fz	≈-7.9 pC/N ≈-3.8 pC/N
Natural Frequency	f_o (x, y, z)	≈1000 Hz
Operating temperature range		0.....70 ^{0}C
Application		Turning Process

The dynamometer was calibrated by the manufacturer in Switzerland. A simple test was conducted to see whether the output from dynamometer is still reliable or not. A metallic plate of 5kg weight was put on the tool holder of the dynamometer. A force of 49.5 N was measured reflecting an error of -0.25%. This small deviation may have happened because

the metallic plate could not be placed at the exact place for which dynamometer was calibrated.

A left hand 25mm by 25 mm tool holder of 150 mm length with a rigid clamping system was used to hold the tool insert as shown in figure 3.9.

Figure 3.9. Tool holder (HPC Laboratory, 2011, Mondragon University, Spain)

3.6. Data Acquisition Methodology

Data acquisition (DAQ) is a process of gathering information in an automated fashion. The information can be gathered from many measurement sources, in this specific application from the dynamometer and the thermal imaging system. The Medatek and Altair softwares are used to capture force and thermal sequences respectively. A DAQ system uses a combination of PC based hardware and software to provide a flexible and user friendly measurement system. The schematic of DAQ system is shown in figure 3.10.

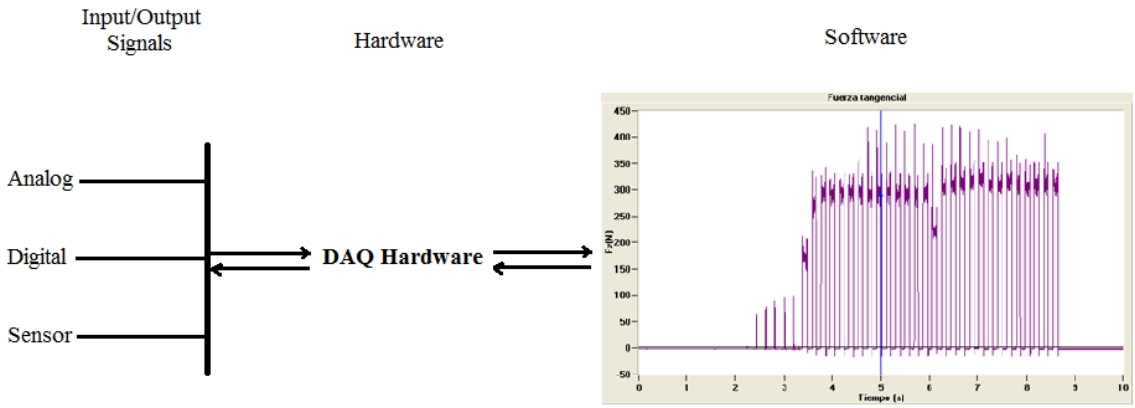

Figure 3.10. Schematic of DAQ system

The acquisition procedure was as follows:

i. Ready the Medatek and Altair softwares to capture force and thermal sequences.

ii. When the dynamometer and camera were ready, the vertical machining centre program was commenced and the dynamometer and camera were triggered simultaneously.

iii. When the data acquisition is completed, the sequences automatically loaded itself within the Medatek and Altair softwares and the files were saved. The frames were examined for pixel saturation and image quality. Integration time of 200 μs provided acceptable image quality. If the image quality was poor, the test was repeated following slight adjustments to the setup.

It is also required to synchronize the measurement of cutting forces, temperature measurement with the machining process (it will take more than one person to handle all equipment). The acquisition process was continued by repeating the above steps for all the desired feeds and speeds.

Chapter 4

Machinability Studies on Ti54M Titanium Alloys

4.1. Introduction

Titanium alloys are one of the most difficult materials to machine because of their low thermal conductivity and low elastic modulus, which lead to high cutting temperatures and tool vibrations respectively. The machining of titanium alloys is one of the principal challenges for their application (Machado and Wallbank, 1990; Amin and Khairusshima, 2007). However, in order to increase the machinability, new titanium alloys are being developed. One of those new alloys is TIMETAL® 54M (Ti54M), developed by TIMET (Largest sponge producer in the United States), an α+β alloy that provides cost benefits with superior machinability. The strength is comparable to similarly processed Ti6Al4V alloy (Armendia et al., 2010).

Kosaka et al. (2004) observed significant impact of the alloy chemistry on machinability and claimed Ti54M alloy exhibiting superior machinability compared to Ti6Al4V alloy. During the development work of Ti54M alloy, it was realized that the machinability also depends on the heat treatment conditions, i.e. with strength and microstructure, as well as chemistry (Kosaka and Fox, 2004). Materials with coarse microstructures are more difficult-to-cut than the ones with finer microstructures. Venkatesh et al. (2007) also found better machinability of Ti54M over Ti6Al4V at high cutting speeds. Armendia et al. (2010) analyzed the effect of heat treatment on the machinability of Ti54M (forged condition) and Ti6Al4V (mill annealed condition) alloys. For both the alloys, decrease in specific forces

were reported with increasing cutting speed up to around 80 m/min and then increase with the cutting speed as shown in figure 4.1. This effect was more pronounced in case of feed force. However, Rahim and Sharif (2006) concluded during drilling operation that Ti6Al4V exhibits superior machinability than Ti54M in term of tool life performance. It is noticed that in most of the research findings, Ti54M has finer microstructure than Ti6Al4V. Therefore, the rationale behind the better machinability of Ti54M alloy over Ti6Al4V alloy can be the finer microstructure of Ti54M alloy. The microstructure of an alloy can be changed by heat treatment without affecting other variables. Hence, in this chapter a machinability study of Ti54M alloy is carried out at different heat treated conditions – annealed, β annealed and solution treated plus aged (STA) conditions – in terms of specific forces, coefficient of friction, cutting tool temperature, and chip morphology.

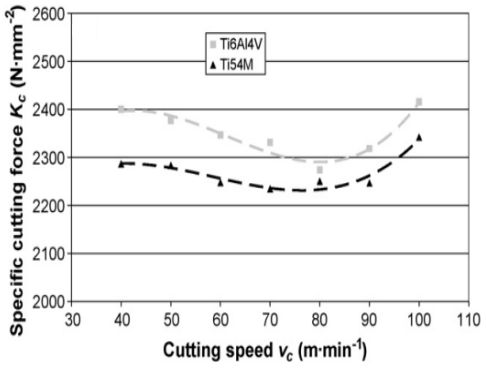

(a)

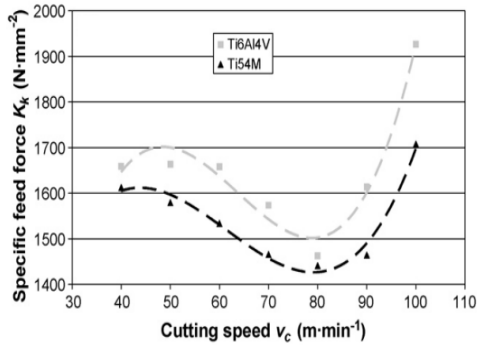

(b)

Figure 4.1. Cutting forces for both alloys: (a) specific cutting force and (b) specific feed force (Armendia et al., 2010a)

4.2. Workpiece Materials

Ti54M alloy belongs to the α+β titanium alloy family. Chemical composition and mechanical properties of Ti54M in different heat treated conditions are summarized in table 4.1. It can be observed from figure 4.2 that Ti54M alloys in different heat treated conditions show considerable differences with reference to the morphology and volume fraction of the primary α phase. Ti54M in annealed condition (Figure 4.2(a)) contains much finer primary α grains; whereas Ti54M in β annealed condition (Figure 4.2(b)) consists of large colonies that contain laths of α and β. Ti54M in STA condition (Figure 4.2(c)) consists of whiter particles of primary α in a transformed β matrix. Aging of this alloy resulted in α precipitation, which restricted the dislocation movement and subsequently increased the strength as seen in table 4.1. Due to the presence of high concentration of β stabilizers (Fe, V and Mo), the β transus temperature is 966^0C, which is almost 30^0C lower than that of the traditional Ti6Al4V titanium alloy.

Table 4.1. Chemical composition, and mechanical properties of different heat treated Ti54M titanium alloy

Titanium Alloy / Transus β (ºC)	Chemical Composition (Weight %)		Heat Treatment	Mechanical Properties				
				UTS (MPa)	TYS (MPa)	Elongation (%)	RA (%)	Hardness (HRC)
Ti54M / 966	Al	5	Annealed 705°C	935	860	23	49	31±3
	Mo	0.8						
	V	4	β annealed (990°C (1h) - air cool)	940	840	11	22	35±3
	Fe	0.5						
	O	0.18	STA (920°C (1h) - water quench, 500°C (4h) - air cool)	1070	960	19	52	37±3

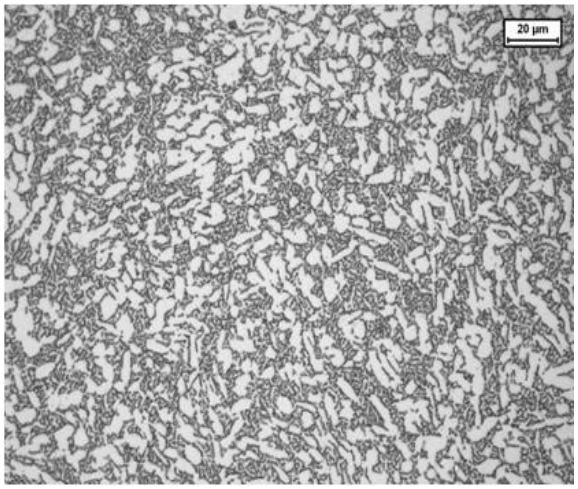

(a)

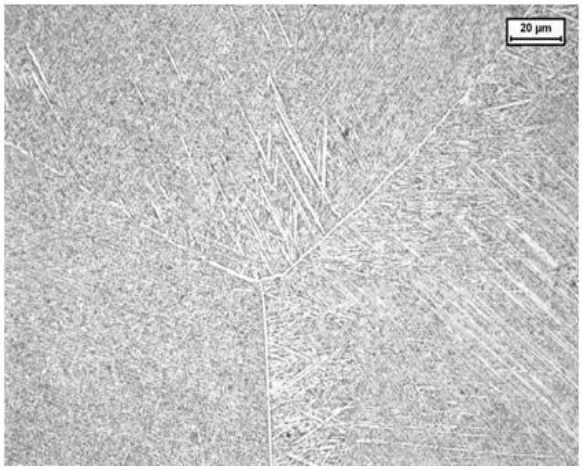

(b)

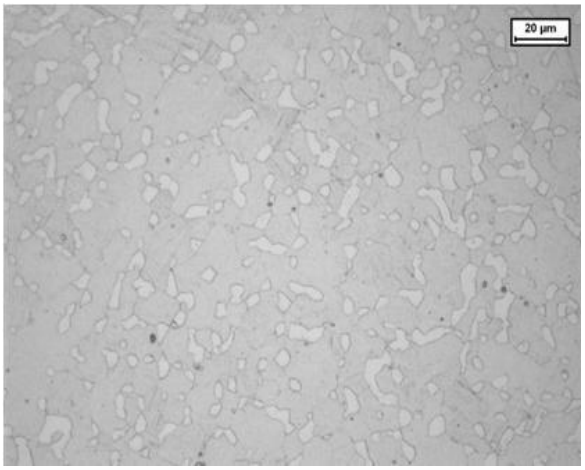

(c)

Figure 4.2. Ti54M in (a) annealed (b) β annealed, and (c) STA conditions

4.3. Experimental Methodology

Arrazola et al. (2009) reported a maximum cutting speed of 80 m/min for machining Ti6Al4V titanium alloy (0.1 mm/rev feed rate and 2 mm depth of cut) with uncoated carbide tools. Hughes et al. (2001) machined this material with round carbide inserts at 60 m/min (0.25 mm/rev feed rate and 2 mm depth of cut). Khales et al. (1985) concluded that the tool life during machining titanium is very sensitive to change in feed rates as compared to other materials. Authors predicted a very short tool life (5 minutes) at V_c = 61 m/min and f = 0.38 mm/rev as well as at V_c = 76 m/min and f = 0.22 mm/rev. Ch-Haron (2001) reported a better tool life at a feed rate of 0.25 mm/rev and cutting speed of 60 m/min than high cutting parameter values. Molinari et al. (2002) compared specific forces at similar cutting parameters for Ti6Al4V with those of Larbi (1990) and Hoffmeister et al. (1999). Reduction in specific cutting force with increasing speed showed the similar trends but the differences in the values of the specific forces are large for the different authors. Variations in the cutting conditions and thermo-mechanical history of the workpiece materials are considered to be the reasons for these differences (Molinari et al., 2002).

Armendia et al. (2010a) tested the machinability of Ti54M alloy at cutting speed ranges from 60 m/min to 100 m/min with constant feed rate and depth of cut. Armendia et al. (2010b) performed the machinability tests on Ti54M alloy in different heat treated conditions using conventional cooling at cutting speed of 40 m/min with four different feed rates (0.1 mm/rev, 0.15 mm/rev, 0.20 mm/rev and 0.25 mm/rev). Cutting temperature was measured only at fixed cutting parameters (V_C = 80 m/min and f = 0.1 mm/rev) without using any coolant. Venkatesh et al. (2007) performed dry turning tests on this alloy at

cutting speeds of 60 m/min, 80 m/min, and 100 m/min at fixed feed rate of 0.25 mm/rev. It has been observed that most of the studies on Ti54M alloy were carried out using cutting speed in a range of 40 m/min – 100 m/min and feed in range of 0.1 mm/rev – 0.25 mm/rev. Also, from figure 4.1 it can be observed that cutting speeds of 40 m/min and 80 m/min are critical speeds. Therefore, in the experimental investigations, these two cutting speeds are taken with the feed range of 0.1 mm/rev – 0.25 mm/rev. It is worthwhile to mention that the commercial availability of these alloys is also limited and titanium producer (TIMET) provided limited material to carry out research at these crucial parameters.

All the cutting conditions and tooling details are given in table 4.2.

Table 4.2. Cutting conditions with tooling summary

Cutting conditions	Cutting speed (V_c) = 40 m/min and 80 m/min Feed rate (f) = 0.1mm/rev, 0.15 mm/rev, 0.25 mm/rev Depth of cut (a_p) = 2mm
Cutting tool • Tool holder (SANDVIK DCLNR 2525 M12) • Tool insert (SANDVIK TNMG 160408-23 H13a)	Rake angle (γ_0) = 7º Cutting edge inclination angle (λ_s) = 0º Cutting edge angle (κ_r) = 0º Corner radius (r_ε) = 0. Cutting edge roundness (r_β) = 34±2 μm Chip breaker = -15 Grade = (H13a) K15 micrograin
Coolant	No coolant (Dry)
Workpiece dimensions	Outer diameter = 48mm Inner diameter = 44mm
Machine tool	LAGUN CNC vertical machining centre

Orthogonal dry machining of 5 second duration was conducted on a LAGUN vertical CNC machining centre as explained in chapter 3. To ensure edge sharpness, a new tool insert was used for each test. All the applied inserts were examined by a sensofar optical profiler in order to verify that the cutting edge radius is within 34±2 µm. Each test was carried out thrice to determine the result uncertainty. Chips were collected in order to study the chip morphology.

4.4. Results and Discussion

This section provides the results and discussion of the experimental values taken at different cutting speeds and feed rates in terms of specific forces, friction coefficient, cutting tool temperature, and chip morphology.

4.4.1. Specific forces

The specific force is better indication of the power requirement, as it is the force needed to actually deform the material prior to any chip formation (Smith, 2010). The specific forces are influenced by the feed rate, depth of cut and yield strength of the workpiece material (Smith, 2010). The specific forces are calculated from the measured forces by using equations 2.1 and 2.2. The specific cutting force (K_c) for all the analyzed titanium alloys at cutting speeds of 40 m/min and 80 m/min are shown in figure 4.3. The specific feed force (K_k) for all the Ti54M alloys at cutting speeds of 40 m/min and 80 m/min are shown in figure 4.4. Results plotted for the specific forces represent the mean values observed from the three experimental tests at each cutting condition.

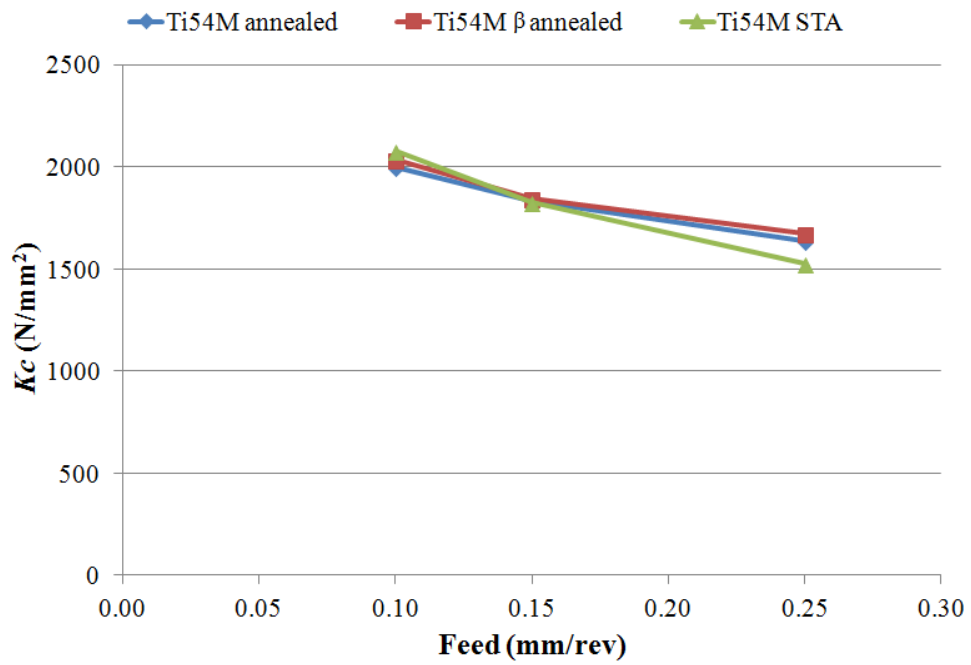

(a)

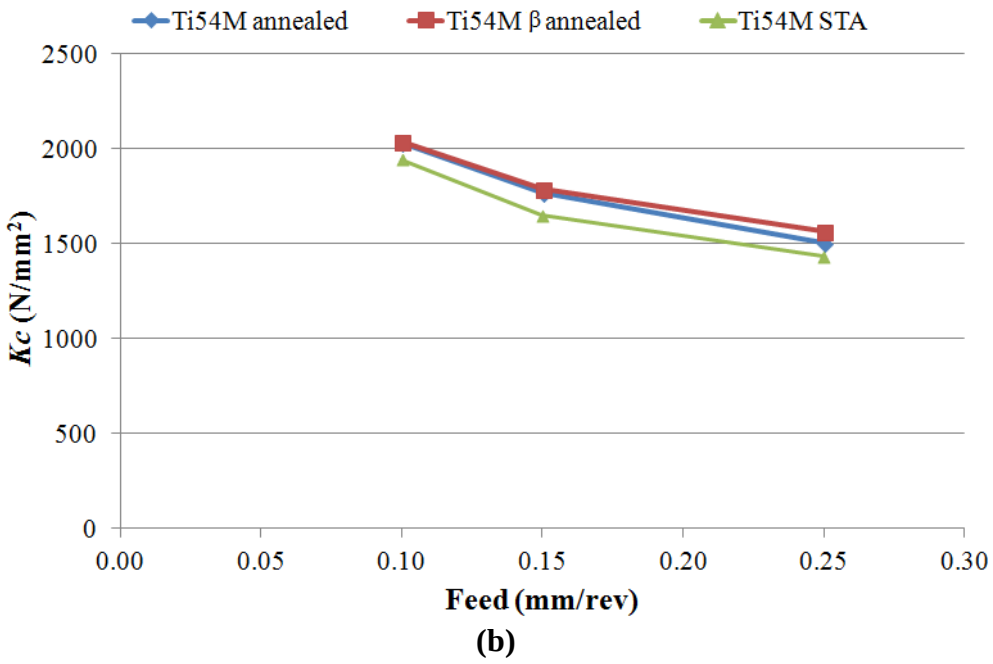

(b)

Figure 4.3. Specific cutting force (K_c) for all the Ti54M titanium alloys at cutting speed of (a) 40 m/min and (b) 80 m/min

The higher specific cutting forces were noticed for Ti54M β annealed at feed rate of 0.25 mm/rev. The irregular laminar microstructure (Figure 4.2(b)) seems to produce higher shear stresses resulting higher cutting forces (Kosaka and Fox, 2004). However, it can be noticed that the specific cutting force particularly at 80 m/min are lowest in case of Ti54M STA alloy at all feed rates. These results do not correlate with the mechanical properties obtained after STA process and the reasons are to be found out as a limited research data is available for Ti54M alloy in STA condition.

At cutting speed of 40 m/min, the highest specific feed force was observed for Ti54M in STA condition followed by Ti54M in β annealed condition. The trend is same for cutting speed of 80 m/min except at 0.25 mm/rev feed rate, where these two alloys showed similar value of specific feed force. The specific feed force (K_k) values correlated well with the mechanical properties of the alloys as higher values were obtained for the Ti54M alloy in STA condition followed by β annealed and annealed conditions. High strength and hardness of Ti54M STA are the reasons for its high specific feed force and its high hardness is due to the precipitation of α during the aging process carried out after solution treatment. The specific forces are decreasing with the increasing feed rate because of the size effect of the cutting edge. It is pertinent to write that the observed values of cutting and feed forces increase with the increase in feed rate. The specific feed forces are more sensitive to change in feed rate than specific cutting forces as observed in figures 4.3 and 4.4.

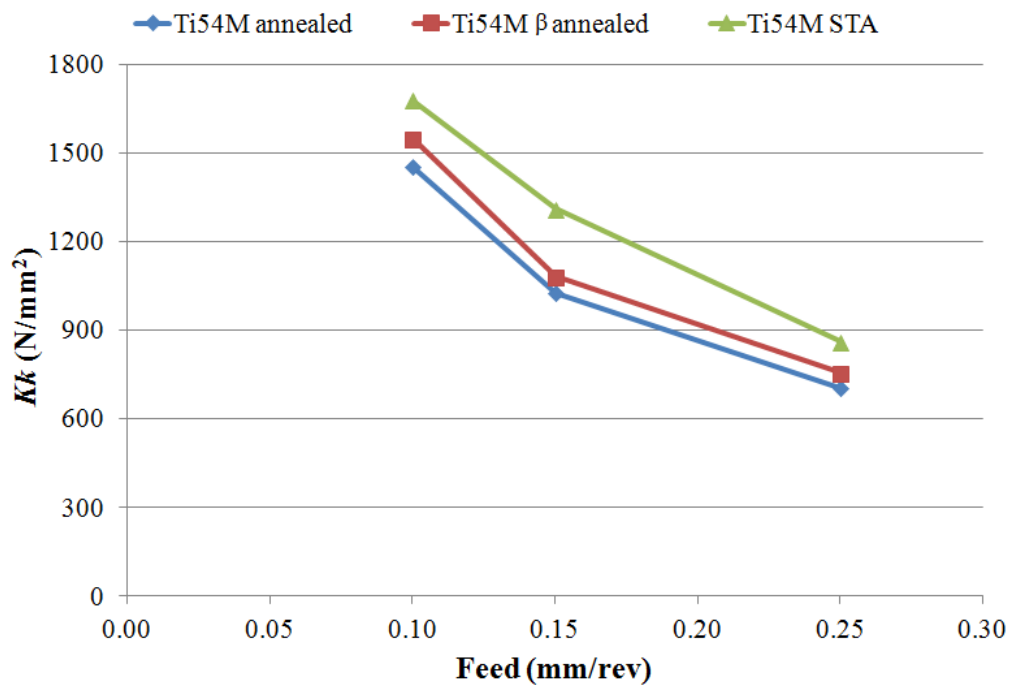

(a)

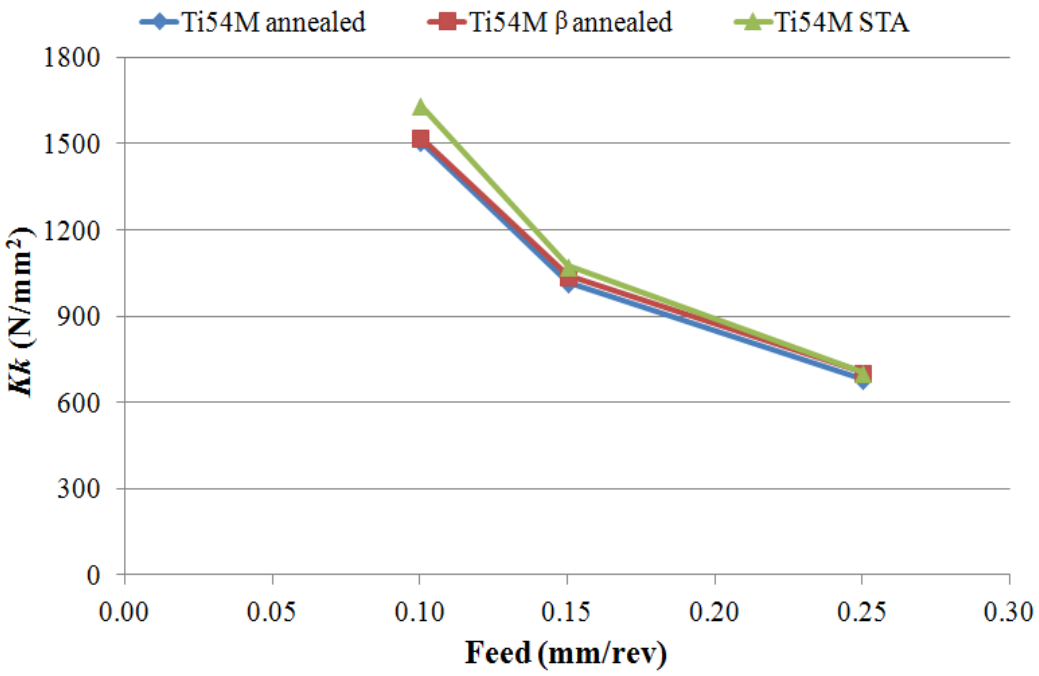

(b)

Figure 4.4. Specific feed force (K_k) for all the Ti54M titanium alloys at cutting speed of (a) 40 m/min and (b) 80 m/min

4.4.2. Friction coefficient

Wyen and Wegener (2010) studied the effect of cutting edge radius on coefficient of friction during the machining of Ti6Al4V alloy. The authors correlated the cutting edge radius with ploughing force which subsequently affects apparent coefficient of friction. A similar approach is taken here to find the coefficient of friction (μ) for Ti54M alloy using 4.1

$$\mu = \frac{F_{ch,c} \sin \gamma_0 + F_{ch,f} \cos \gamma_0}{F_{ch,c} \cos \gamma_0 - F_{ch,f} \sin \gamma_0} \quad (4.1)$$

Where, $F_{Ch,c}$ is chip forming force in cutting direction and $F_{Ch,f}$ is chip forming force in feed direction.

The chip forming forces in cutting and feed directions are calculated by using following equations (Guo and Chou, 2004):

$$F_{Ch,c} = F_c - F_{Pl,c} \quad (4.2)$$

$$F_{Ch,f} = F_f - F_{Pl,f} \quad (4.3)$$

Where, $F_{Pl,c}$ and $F_{Pl,f}$ are the extrapolated values of the measured forces in the cutting and feed directions respectively.

Ploughing forces are obtained by linear extrapolation of the measured cutting and feed forces versus feed rate at particular cutting speed. The intercept is regarded as the ploughing force and is shown in figure 2.6 for a particular value of cutting speed. The coefficient of friction values thus found are shown in figure 4.5. The coefficient of friction was observed to be decreasing with the increasing feed rate during machining of the alloys as shown in figure 4.5. The reduction in the friction coefficient is due to the chip's hot softening and

subsequent reduction in the chip's resistance to sliding along the tool rake (Hong et al., 2001b).

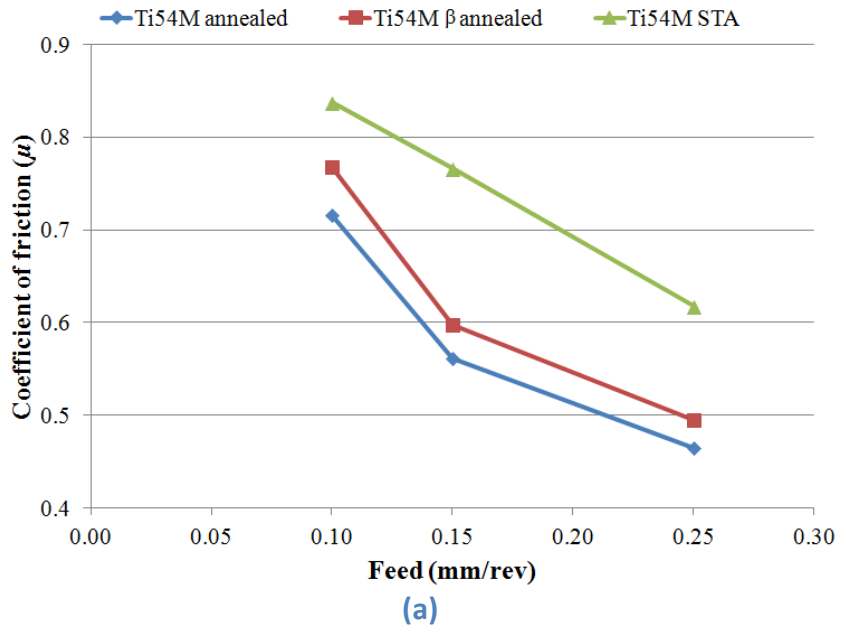

(a)

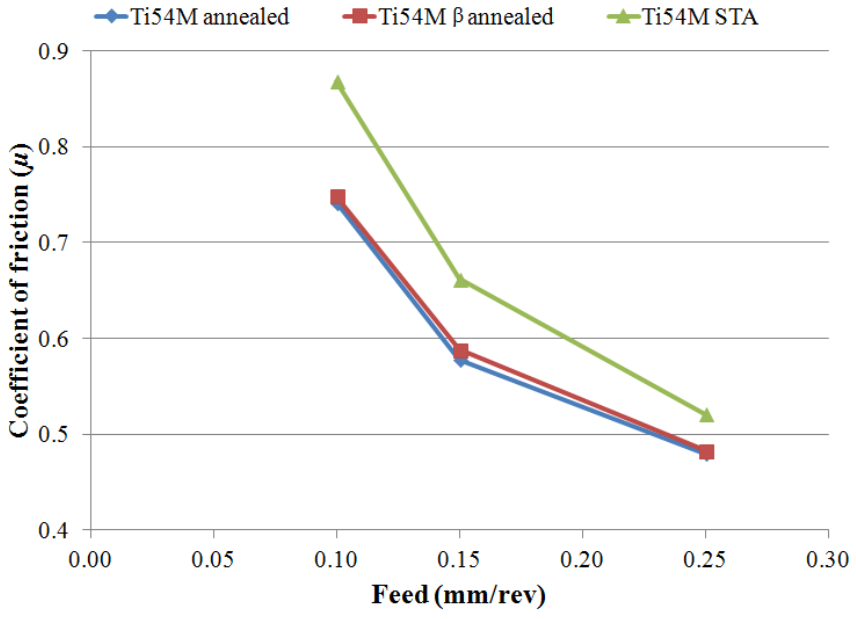

(b)

Figure 4.5. Apparent coefficient of friction for all the Ti54M titanium alloys at cutting speed of (a) 40 m/min and (b) 80 m/min

Coefficient of friction is highest for the Ti54M STA condition followed by β annealed and annealed alloys as seen in figure 4.5. This is due to the high hardness achieved in STA conditions as explained earlier. Therefore, higher tool wear is expected in machining Ti54M STA alloy. Tool condition was observed at the end of each test. The observations are shown in figure 4.6 for all alloys. Start of wear can be observed on the tool used for machining Ti54M STA alloy (Figure 4.6(c)).

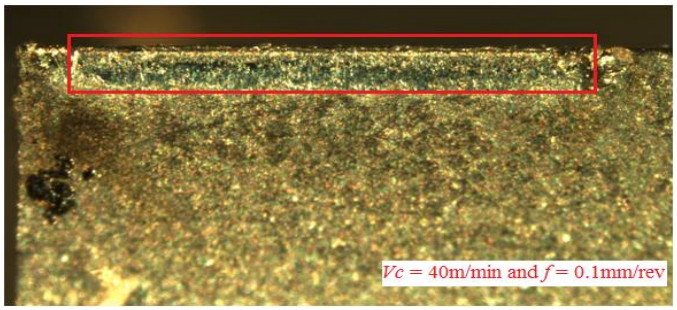

(a)

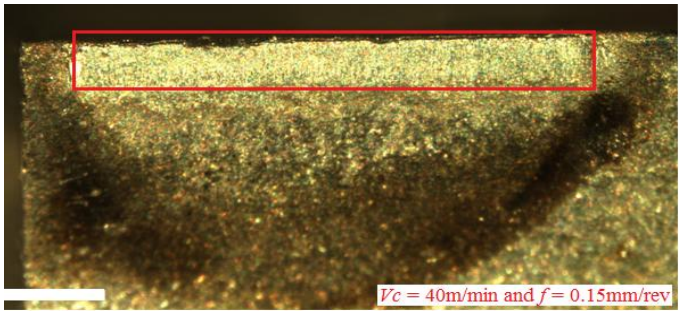

(b)

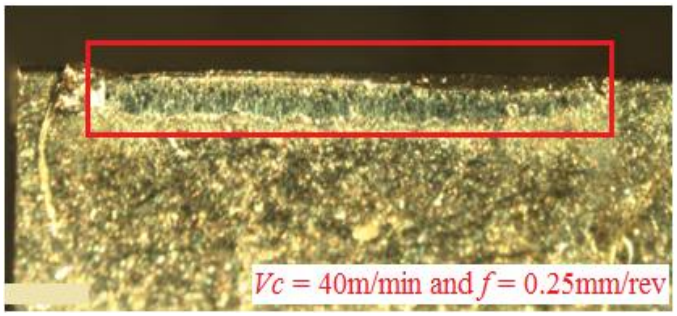

(c)

Figure 4.6. Flank face after 5 second for Ti54M titanium alloy in (a) annealed (b) β annealed, and (c) STA conditions

However, the tool at the end of the tests was in good condition and it can be said that the machining tests were within the useful tool life specified in ISO 3685. Therefore, it can be predicted that the prolonged machining of Ti54M STA alloy will lead to early tool failure compared to the other two alloys.

4.4.3. Cutting tool temperature

Interfacial temperatures in machining play a major role in tool wear and can also result in modifications to the properties of the workpiece and tool materials. As there is a general move towards dry machining for environmental reasons, it is increasingly important to understand how machining temperatures are affected by the process variables involved (cutting speed, feed rate, etc.) and by other factors such heat treatment conditions (Davies et al., 2007; Armendia et al., 2010).

The cutting tool temperature for all the analyzed titanium alloys at cutting speeds of 40m/min and 80m/min are shown in figure 4.7 (a) and (b) respectively. The temperature values were extracted for the last one second of cut as it is closer to a stationary behaviour.

At higher cutting parameters, very similar temperature values were observed for the analyzed alloys. Arrazola et al., (2005) observed that the specific feed force (K_k) indicates the friction and rubbing effects over the rake surface and hence explains the amount of heat generated at the tool/chip contact zone. Therefore, higher temperatures were expected in the machining of Ti54M STA and Ti54M β annealed alloys compared with Ti54M annealed alloy. At high cutting conditions, the cutting tool temperature reached above 1000^0C for all

the three different heat treated Ti54M alloys. The Ti54M alloy in STA condition showed the highest value of 1040^0C (Figure 4.8).

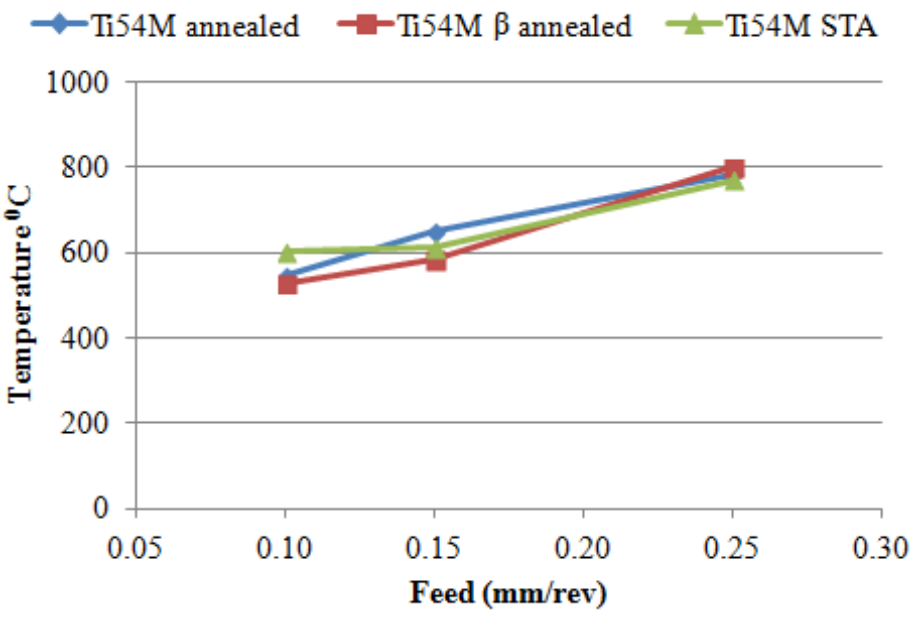

(a)

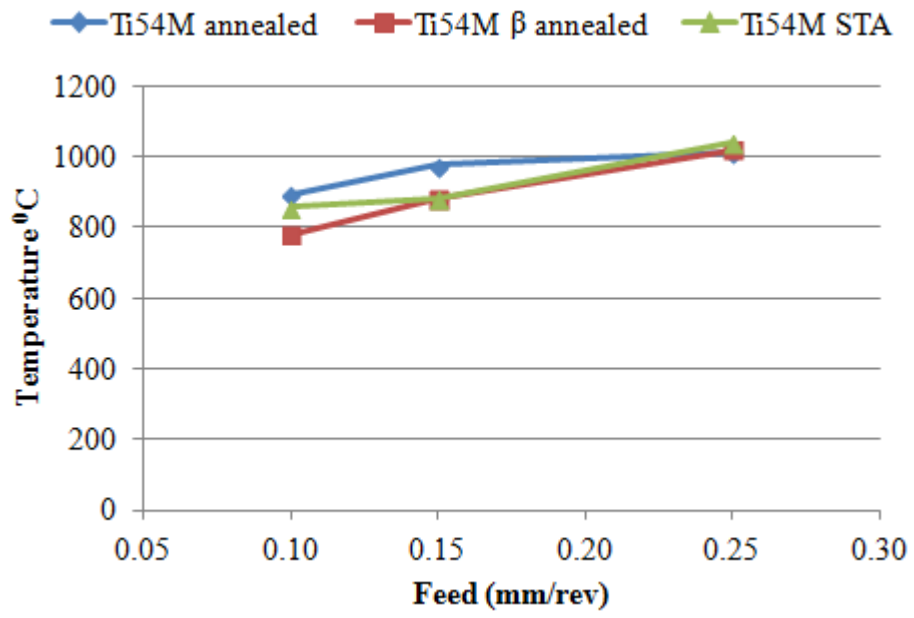

(b)

Figure 4.7. Cutting tool temperature for all the Ti54M titanium alloys at cutting speed of (a) 40 m/min and (b) 80 m/min

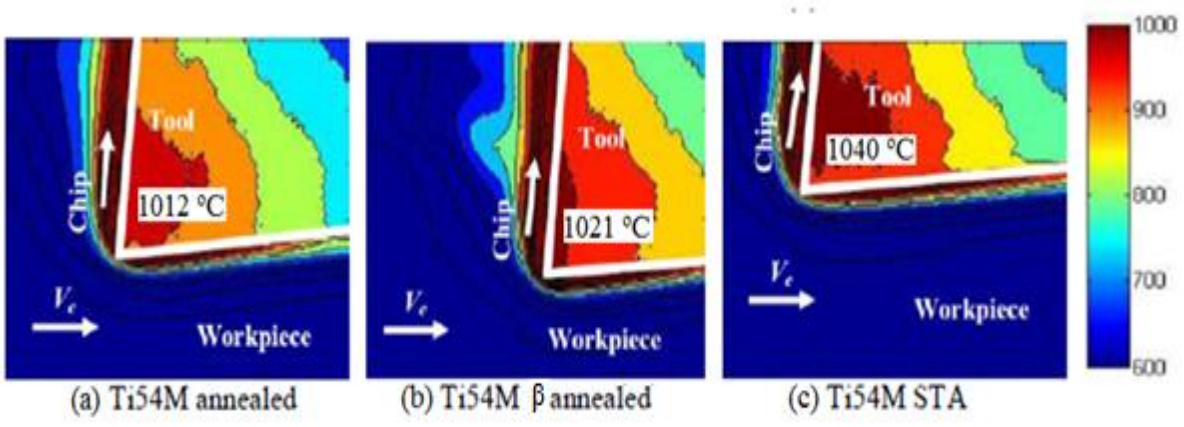

Figure 4.8. Thermal maps for all the Ti54M titanium alloys at cutting speed of 80 m/min and 0.25mm/rev feed rate

However, due to the uncertainty (±50ºC) in thermal measurement system, it cannot be stated effectively that the temperatures generated in the machining of the Ti54M alloy in STA and β annealed conditions are higher than Ti54M alloy in annealed condition. These uncertainties were attributed to fluctuations around the mean emissivity, stray light from other sources, surface location fluctuations, and focus conditions due to the low Young's modulus of titanium alloys. No clear conclusions are obtained in the temperature measurement study.

4.4.4. Chip morphology analysis

The different heat treatment conditions and different machining parameters produced different chip morphologies as shown in figures 4.9 (a), (b) and (c). Nurul Amin et al. (2007) related serrated teeth shape with the amplitude of chatter (a measure of machinability). Ti54M in annealed condition exhibits good plastic deformability at low cutting parameters resulting in continuous chip formation (Figure 4.9 (a)).

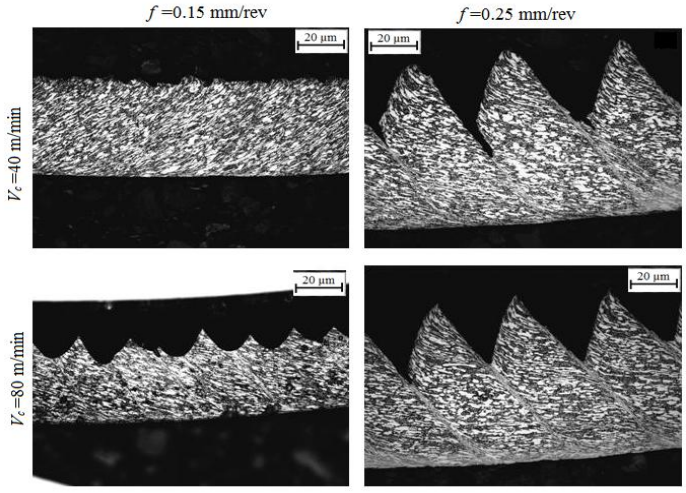

(a)

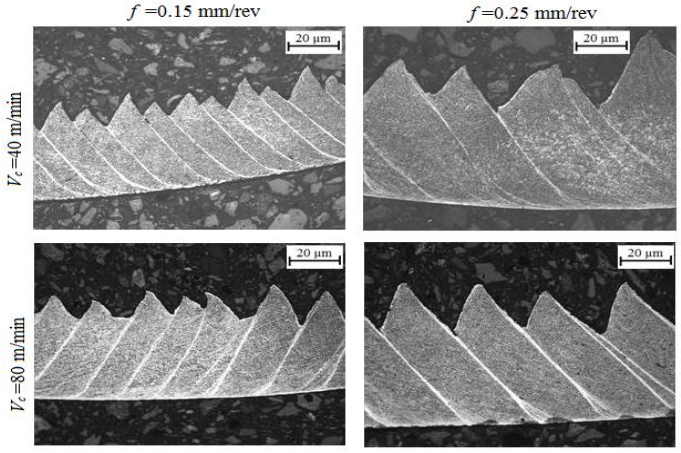

(b)

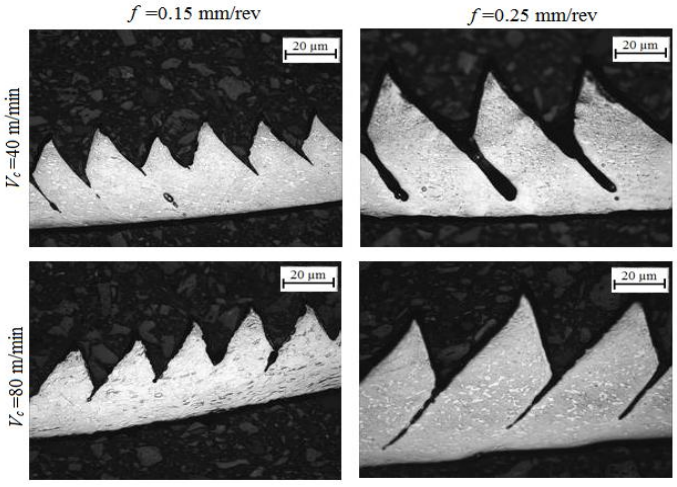

(c)

Figure 4.9. Chip morphology as a function of feed and cutting speed for Ti54M titanium alloy in (a) annealed (b) β annealed, and (c) STA conditions

This also indicates low tool vibrations. Periodic segmented chips were produced at 0.25 mm/rev feed rate. The β annealed heat treatment condition exhibits poor plastic deformability at all cutting parameters, therefore, resulting in segmented chips. The coarse microstructure consisting of layers of α and β laths are the reasons for poor plastic deformability. It can be observed from figure 4.9 (b) that there is uneven spacing of the serrated chip elements of irregular sizes indicating an intensive chatter at all cutting parameters.

A clear difference in chip morphology is observed at higher feed rates in the STA condition (Figure 4.9(c)). The segments of Ti54M STA chips were partially separated. This distinction coincides well with a recognizable difference in the specific feed force (Figure 4.4) and coefficient of friction (Figure 4.5). High specific feed force (K_k) indicates high friction over the rake surface which consequently shows the amount of heat generated at the tool/chip interface (Arrazola et al., 2005). Therefore, higher tool wear is expected in the Ti54M STA condition followed by Ti54M β annealed and Ti54M annealed alloys. Intensive chattering was observed during the machining of Ti54M STA and Ti54M β annealed alloys.

It can be observed that the shear band spacing varies with the change in feed rate, cutting speed and heat treatment. The similar trends have been observed in the turning of Ti6Al4V by Siemers et al. (2007) and Molinari et al. (2002) for cutting speed and depth of cut. Kosaka and Fox (2004) explained that the shear band spacing is a factor of microstructure in addition to cutting speed and depth of cut. The present study indicates that feed rate also affects shear band spacing. The effect of heat treatment on the chatter was also observed in this research.

The observable difference in the shear localized bands in the chips of the analyzed alloys can be seen more clearly by using Leica Z16 APO optical magnifier at cutting speed of 80 m/min and feed rate of 0.25 mm/rev as shown in figure 4.10.

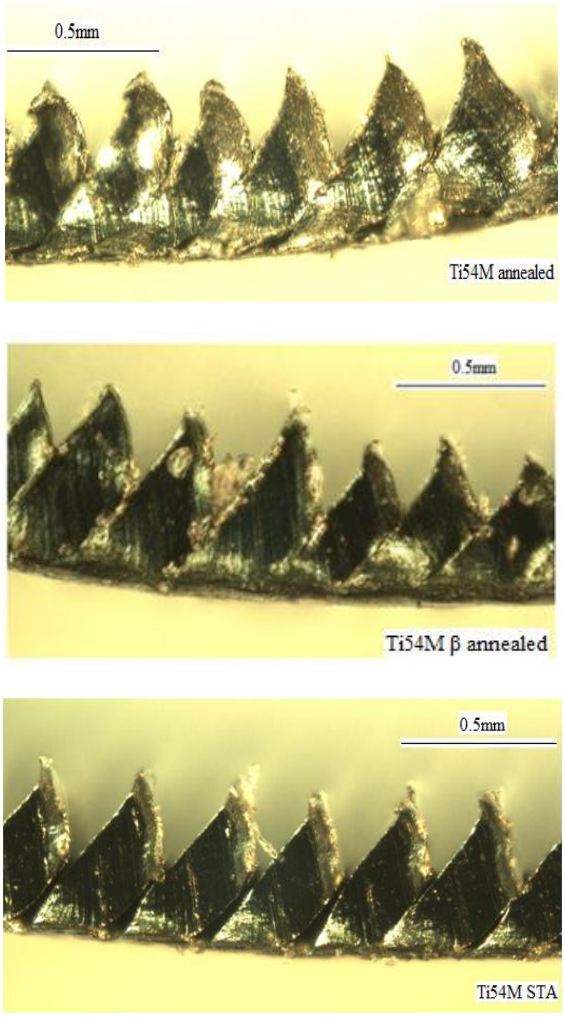

Figure 4.10. Chip cross-sections showing shear bands for all the Ti54M titanium alloys

4.5. Statistical Analysis of Results Using ANOVA

An analysis of variance (ANOVA) was conducted to verify the statistical significance of results of the previous section. The tables show sum of square (SS), degree of freedom (DF), mean square (MS), F values (F), and the P-values associated with each factor and

interaction. Statistical significance of the source values was evaluated by the P-values of ANOVA. When P-values are less than 0.05, the source effect on response is considered to be statistically significant at 95% confidence level (Ozel et al., 2005). The significance of the F value is that the larger the F value for a particular parameter, the greater the effect on the performance characteristic due to the change in that process parameter.

Table 4.3 shows the main and interaction effects of the feed rate and cutting speed on specific cutting force for all heat treated conditions. It is found that the effect of feed rate is statistically significant on the specific cutting forces for all the three alloys.

Table 4.3. ANOVA for specific cutting force for Ti54M titanium alloy in (a) annealed (b) β annealed and (c) STA conditions

(a)

Source	SS	DF	MS	F	P-value
f	588128.1	2	294064.1	1327.60	0.000
Vc	15138	1	15138	68.34	0.000
f Vc*	20533	2	10266.5	46.35	0.000
Within	2658	12	221.5		
Total	626457.1	17			

(b)

Source	SS	DF	MS	F	P-value
f	521656.8	2	260828.4	602.30	0.000
Vc	13833.39	1	13833.39	31.94	0.000
f Vc*	8610.11	2	4305.06	9.94	0.003
Within	5196.67	12	433.06		
Total	549296.9	17			

(c)

Source	SS	DF	MS	F	P-value
f	843024	2	421512	191.63	0.000
Vc	85560.06	1	85560.06	38.89	0.000
f Vc*	5303.11	2	2651.56	1.20	0.332
Within	26395.33	12	2199.61		
Total	960282.5	17			

Similarly, the effect of cutting speed is statistically significant for all the three alloys. The effects of two-factor interactions of the feed rate and the cutting speed is statistically significant for the specific cutting forces in annealed and β annealed conditions only. F value for the feed rate factor is larger than that of the cutting speed, i.e., the larger contribution to the specific cutting force is due to the feed rate.

Table 4.4 shows that the main and interaction effects of the feed rate and cutting speed on specific feed force for all heat treated conditions. It is found that the effect of feed rate on specific feed force is statistically significant (P-value ~ 0) for all the three alloys.

Table 4.4. ANOVA for specific feed force for Ti54M titanium alloy in (a) annealed (b) β annealed and (c) STA conditions

(a)

Source	SS	DF	MS	F	P-value
f	1812344	2	906172.2	24.86	0.000
Vc	5066.89	1	5066.89	0.14	0.723
f Vc*	81752.44	2	40876.22	1.12	0.361
Within	437493.3	12	36457.78		
Total	2336657	17			

(b)

Source	SS	DF	MS	F	P-value
f	1970306	2	985153.2	1041.51	0.000
Vc	6962	1	6962	7.36	0.022
f Vc*	471	2	235.5	0.25	0.781
Within	11350.67	12	945.89		
Total	1989090	17			

(c)

Source	SS	DF	MS	F	P-value
f	2296292	2	1148146	201.35	0.000
Vc	95776.06	1	95776.06	16.79	0.001
f Vc*	27052.11	2	13526.06	2.37	0.142
Within	68428	12	5702.33		
Total	2487549	17			

The effect of cutting speed is significant for β annealed and STA heat treated conditions, and insignificant for annealed condition (P-value = 0.723). F value for the feed rate factor is larger than that of the cutting speed, i.e., the larger contribution to the specific feed force is due to the feed rate. The interactions between cutting speed and feed rate are observed to be insignificant with respect to the specific feed force for Ti54M in all the heat treated condition.

Table 4.3 shows the main and interaction effects of the feed rate and cutting speed on cutting tool temperature for all heat treated conditions. It is found that the effect of feed rate and cutting speed on tool temperature is statistically significant (P-value ~ 0) for all the three alloys.

Table 4.5. ANOVA for cutting tool temperature for Ti54M titanium alloy in (a) annealed (b) β annealed and (c) STA conditions

(a)

Source	SS	DF	MS	F	P-value
f	94230.78	2	47115.39	407.34	0.000
Vc	407102.7	1	407102.7	3519.62	0.000
f Vc*	12326.78	2	6163.39	53.29	0.000
Within	1388	12	115.67		
Total	515048.3	17			

(b)

Source	SS	DF	MS	F	P-value
f	206566.3	2	103283.2	660.4252	0.000
Vc	297992	1	297992	1905.455	0.000
f Vc*	4381	2	2190.5	14.00675	0.001
Within	1876.667	12	156.3889		
Total	510816	17			

(c)

Source	SS	DF	MS	F	P-value
f	111880.1	2	55940.06	108.88	0.000
Vc	316277.6	1	316277.6	615.598	0.000
f Vc*	230.11	2	115.08	0.228	0.810
Within	6165.33	12	513.78		
Total	434553.1	17			

It can be seen that the interaction between feed rate and cutting speed ($f \times V_c$) has significant effect on cutting tool temperature for annealed and β annealed heat treated conditions but not for STA condition (P-value = 0.8). The ANOVA result shows that the F value for the factor cutting speed is larger than that of the other cutting parameter (feed rate), i.e., the larger contribution to the cutting tool temperature for all the heat treated conditions is due to the cutting speed.

4.6. Conclusions

The experimental studies carried out on Ti54M titanium alloy in as-received annealed, β annealed and STA conditions show that the chip morphology differs considerably with the different heat treated conditions of the Ti54M titanium alloy. There are clear indications that the machinability of Ti54M in annealed condition is better than that of β annealed and STA conditions. This distinction coincides well with the recognizable differences observed in the specific feed force and friction coefficient. However, the experimental results in term of cutting tool temperature and specific cutting force show irregular trends in machinability for the three heat treated conditions at different cutting speeds and feed rates. More experiments need to be carried out at different cutting speeds and feed rates to get clear trends in term of cutting tool temperature and specific cutting force. The ANOVA results have shown that most of the experimental results are statistically significant in term of feed rate and cutting speed variations. Feed rate has been found to have more significance than the cutting speed for specific cutting and feed forces in all heat treated conditions. Cutting speed has been found to be more significant for cutting tool temperature.

Chapter 5

Machinability Studies on Ti10.2.3 Titanium Alloys

5.1. Introduction

Metastable β titanium alloys form one of the most versatile classes of materials with respect to processing, microstructure and mechanical properties (Boyer and Briggs, 2005).These alloys are having better properties like excellent strength/density, strength/toughness, higher corrosion resistance, better balance between ductility and toughness, and attainment of very high strength levels during aging; which make these alloys technically better than commonly used titanium alloys in many aerospace and automotive applications like engines, power transmission components of automobile, aircraft landing gears, bogie beams or lower and upper torque links (Machai and Biermann, 2011; Boyer and Briggs, 2005; Donachei, 2004). Metastable β titanium alloys like Ti5553 and Ti10.2.3 are significantly more difficult to cut than α+β titanium alloys like Ti6Al4V.

5.2. Background

β titanium alloys have been available since the 1950's (Ti-13V-11Cr-3Mo or B120VCA), but significant applications of these alloys have been slow. The first commercial application is reported in SR-71 Blackbird (Lockheed Corporation) in year 1966. The next significant usage of β alloys did not occur until the mid-1980s on the B-1B bomber (Boeing). This aircraft used Ti-15V-3Cr-3Al-3Sn sheet due to its capability for strip rolling, improved formability and higher strength than Ti6Al4V. The next major usage has been on the Boeing

777 and Boeing 787 commercial aircrafts where Ti10.2.3 high-strength forgings have been extensively used (Boyer and Briggs, 2005). The properties of various metastable β titanium alloys can be altered by specific heat treatment. Most of the metastable β titanium alloys can be solution treated plus aged to increase their strength and hardness (Weiss and Semeatin, 1998).

Recent work has shown that heat treatment can have a significant impact on machinability of Ti10.2.3 alloys and these alloys in annealed condition exhibit superior machinability compared to STA condition (Machai and Biermann, 2011b). It was realized that the machinability of the alloys depends on the alloy chemistry and heat treatment conditions (strength and microstructure) (Kosaka and Fox, 2004). Ti10.2.3 alloy in STA condition is more difficult-to-cut than in annealed condition. The main reason for this poor machinability in STA condition is the emergence of secondary α phase within the microstructure (Machai and Biermann, 2011b). This phase has an abrasive impact as the particles strike the cutting edge and leads to catastrophic tool failure. Machai and Biermann (2011b) concluded that cutting speeds of 100 m/min and 50 m/min are most suitable while machining Ti10.2.3 in the solution treated and STA conditions respectively. Machai and Biermann (2011a) also showed during the machining of Ti10.2.3 with cryogenic coolant, using carbon dioxide snow, that the machinability of this alloy cannot be improved beyond a cutting speed of 100 m/min due to rapid tool wear causing catastrophic tool failure. These studies confirm that the poor machinability of Ti10.2.3 titanium alloys is a significant manufacturing hurdle preventing increasing usage of these alloys. Donachie (2004) also stated that the machinability depends on the heat treatment condition of the material. Donachie (2004) recommended low cutting speed values during turning operation on the titanium alloys in

STA condition as compared to the annealed condition. Ezugwu (2004) reported that aging process decreases the tool life due to the abrasive effect of the emerging microstructure. It suggests that the variation in the machinability must be linked to the difference in heat treatment conditions. However, only a limited amount of work has been done to check the machinability of metastable β titanium alloys in different heat treated conditions.

The strength and machinability relationship depends on the heat treatment condition which provides variations in the microstructure. There are three types of heat treatments usually recommended for metastable β Ti10.2.3 titanium alloys – solution treatment (annealing), solution treated plus aged (STA) and solution treated plus over aged (STOA) (Chandler, 2006). Strengthening during aging is primarily due to the small secondary α precipitates (Terlinde et al., 1980) and mechanical properties are controlled by the size and volume fraction of these precipitates. The solution treated plus over aged (STOA) condition refers to the aging above the standard aging temperature but below the β transus temperature. It is used to obtain modest increase in strength while maintaining satisfactory toughness and dimensional stability (Chandler, 2006).

Arrazola et al. (2009) found that uncoated cemented carbide tools loose a considerable amount of useful life when machining a metastable β titanium alloy. These tools used for machining solution treated and aged Ti5553 alloy have about 56% of their ordinary useful life when compared with Ti6Al4V alloy in a quenched and annealed condition. Fanning (2005) also observed tool wear as the main problem during machining of metastable β titanium alloys in the STA condition. The purpose of this study is to analyze the effect of heat treatment on the machinability of Ti10.2.3 alloys in terms of specific forces, friction coefficient and cutting tool temperature.

5.3. Workpiece Materials

Titanium alloys can be classified from the value of the aluminum and molybdenum equivalent parameters. The molybdenum equivalent (Mo Equiv.) and aluminum equivalent (Al Equiv.) parameters are defined by the following equations (Arrazola et al., 2009),

Aluminum equivalent value (wt. %) = $Al + Sn/3 + Zr/6 + 10(O^2 + N^2)$ (5.1)

Molybdenum equivalent value (wt. %) = $Mo + 2V/3 + Nb/3 + 3(Fe + Cr)$ (5.2)

While the molybdenum equivalent value reflects the capacity to attain an ultimate tensile strength (UTS) and hardness in aged condition and indicates the β stability of an alloy. The aluminum equivalent value specifies the capacity of the alloy to obtain a given hardness. Regarding the composition, a proportion of β stabilizers are higher in Ti10.2.3 alloy as compared to widely used titanium alloy Ti6Al4V resulting an increase of molybdenum equivalent value and decrease of β transus temperature. The β transus temperature is almost 195^0C lower than that of Ti6Al4V alloy. The titanium phase stability diagram (Figure 5.1) shows this difference. This figure shows that Ti6Al4V belong to the α+ β alloy group, while Ti5553 and Ti10.2.3, have a metastable β structure and belongs to the family of near β alloys. It is desirable to maintain the higher strength of the titanium parts without sacrificing their machinability. The experimental tests are conducted on Ti10.2.3 in three different heat treatment conditions. These conditions are those used in industrial application for this alloy. Chemical composition and mechanical properties of Ti10.2.3 titanium alloy are summarized in table 5.1. It is observed that Ti10.2.3 alloys have a molybdenum equivalent value of twelve. This value explains the higher mechanical properties of this metastable β titanium alloy as compared to α+β titanium alloys.

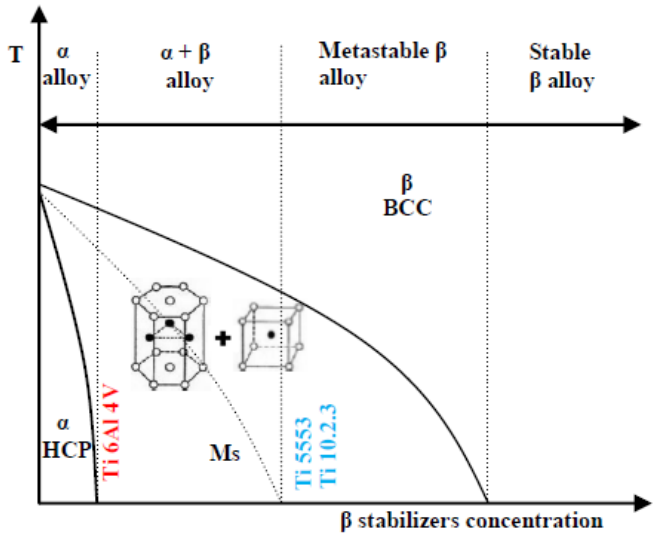

Figure 5.1. Titanium phase stability as a function of temperature and β stabilizers

The details of Ti10.2.3 alloy in as received annealed, STA and STOA heat treatment conditions are presented in table 5.2.

Table 5.1. Chemical composition and mechanical properties of the Ti10.2.3 alloy

Titanium Alloy	Chemical Composition (%)				Al Equiv. Value (wt.%)	Mo Equiv. Value (wt.%)	Transus β (°C)	TYS (MPa)	UTS (MPa)	Elongation (%)
	Al	Mo	V	Fe						
Ti10.2.3	3	-	10	2	3	12	800	1100	1200	9

Table 5.2. Details of different heat treatments performed on Ti10.2.3 alloy

Material	Heat Treatment	Hardness (HRC ±3)
Ti 10.2.3	Annealed 760°C	32
	STA (770°C (2h) – water quench + 500°C (8h) – air cool)	38
	STOA (750°C (2h) – air cool+ 565°C (8h) – air cool)	32

5.4. Experimental Methodology

Machai and Biermann (2011b) used a fine-grained, uncoated cemented carbide tool for turning of Ti10.2.3 alloy. The depth of cut and feed rate were fixed at 0.3 mm and 0.1 mm/rev respectively. Experimental investigations were carried out at cutting speeds (V_c) of 50 m/min, 100 m/min and 150 m/min. Emulsion with a concentration of 6% was applied for flood cooling and lubrication. Rashid et al. (2011) tested the machinability of a near β Ti25Nb3Mo3Zr2Sn titanium alloy at wide range of cutting speeds with constant feed rate of 0.19 mm/rev and depth of cut of 0.1 mm. Arrazola et al. (2009) performed the machinability tests on a metastable β Ti5553 alloy at a cutting speeds ranging from 40 m/min to 60 m/min at constant feed rate and depth of cut of 0.1 mm/rev and 2 mm respectively as shown in table 5.3.

Table 5.3. Summary of recent research work on machinability of β titanium alloys

Heat treatment condition	Insert/Grade	Cutting parameters			Author(s)
		Cutting speed m/min	Feed mm/rev	Depth of cut mm	
STA (Ti5553)	Uncoated cemented carbide (grade K15 micrograin)	40-60	0.1	2	Arrazola et al., (2009)
STA (Ti10.2.3)	Coated and uncoated cemented carbide CNMG 120404	50-150	0.1	0.3	Machai and Biermann (2011a)
STA/ST (Ti25Nb3Mo3Zr2Sn)	Carbide tool	Up to 190	0.19	1	Rachid et al., (2011)
STA/ST (Ti10.2.3)	Uncoated cemented carbide CNMG 120404	50-100-150	0.1	0.3	Machai and Biermann (2011b)

Experimental investigations were carried out at the two cutting speeds (40 m/min and 80 m/min) and three feed rates (0.1 mm/rev, 0.20 mm/rev and 0.25 mm/rev) It is again worthwhile to mention that the commercial availability of these alloys is limited and titanium producer (TIMET) provided limited material to carry out research at these crucial parameters. The experiments were carried out on the LAGUN vertical CNC machining centre and as explained in chapter 3 and 4. The cutting conditions and tooling details are given in table 4.2.

5.5. Results and Discussion

This section provides the results and discussion of the experimental investigations at different cutting speeds and feed rates in terms of specific forces, friction coefficient, and cutting tool temperature.

5.5.1. Specific forces

The significance of determining specific forces has already been discussed in the previous chapters. The specific forces are calculated from the measured forces using equations 2.1and 2.2. The specific cutting force (K_c) for all the analyzed titanium alloys at cutting speeds of 40 m/min and 80 m/min are shown in figure 5.2. The specific feed force (K_k) for all the Ti10.2.3 alloys at cutting speeds of 40 m/min and 80 m/min are shown in figure 5.3. Results plotted for the specific forces represent the mean values observed from the three experimental tests at each condition.

It can be seen from figure 5.2 that the specific cutting force decreases with the increase in feed rate. This trend is followed in all heat treatment conditions.

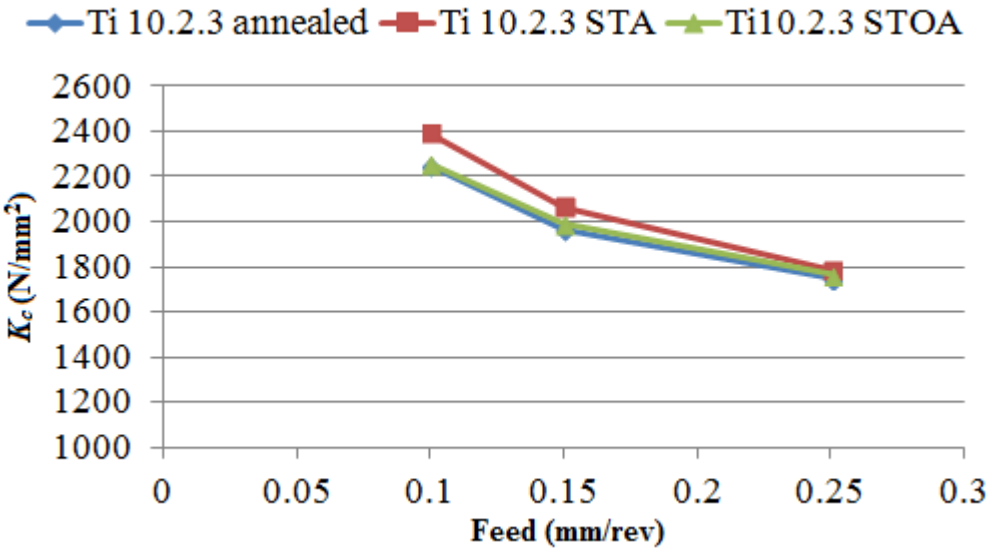

(a)

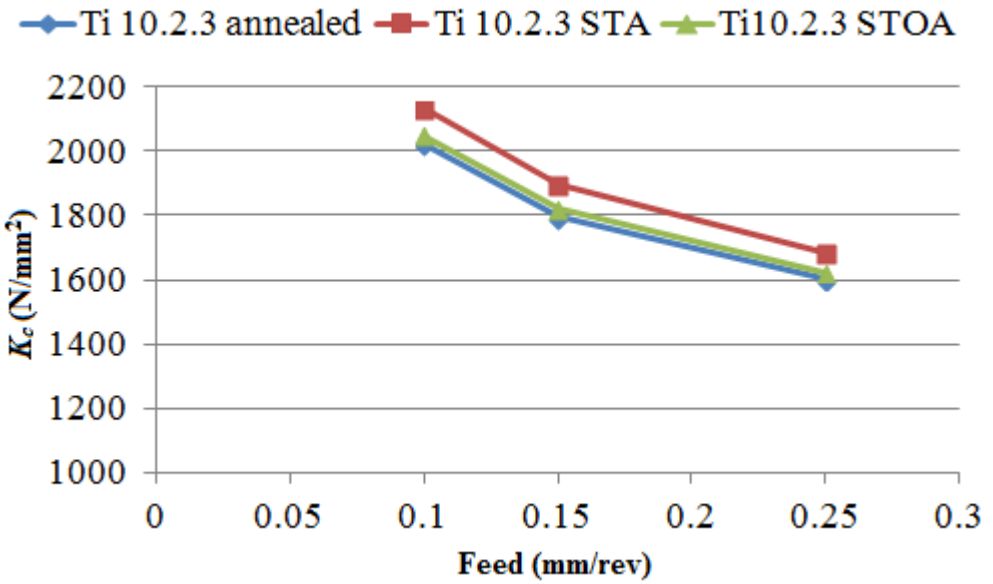

(b)

Figure 5.2. Specific cutting force K_c for all the Ti10.2.3 titanium alloys at cutting speed of (a) 40 m/min and (b) 80 m/min

The highest specific cutting forces were noticed for Ti10.2.3 STA at all feed rates. At cutting speed of 80 m/min, the specific cutting force for the Ti10.2.3 alloy in STA condition was slightly higher than those for the annealed and STOA heat treatment conditions, with an

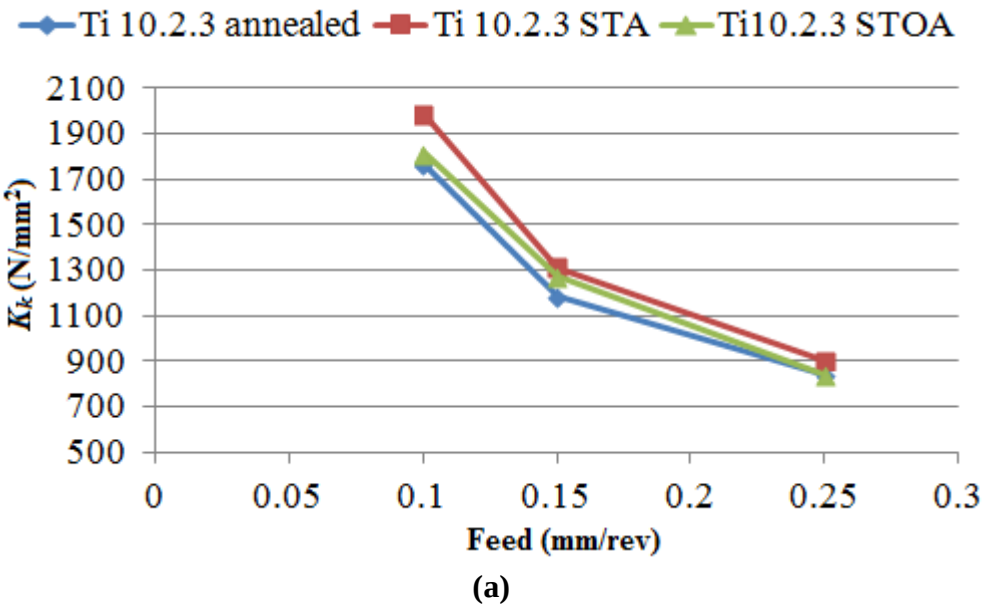

(a)

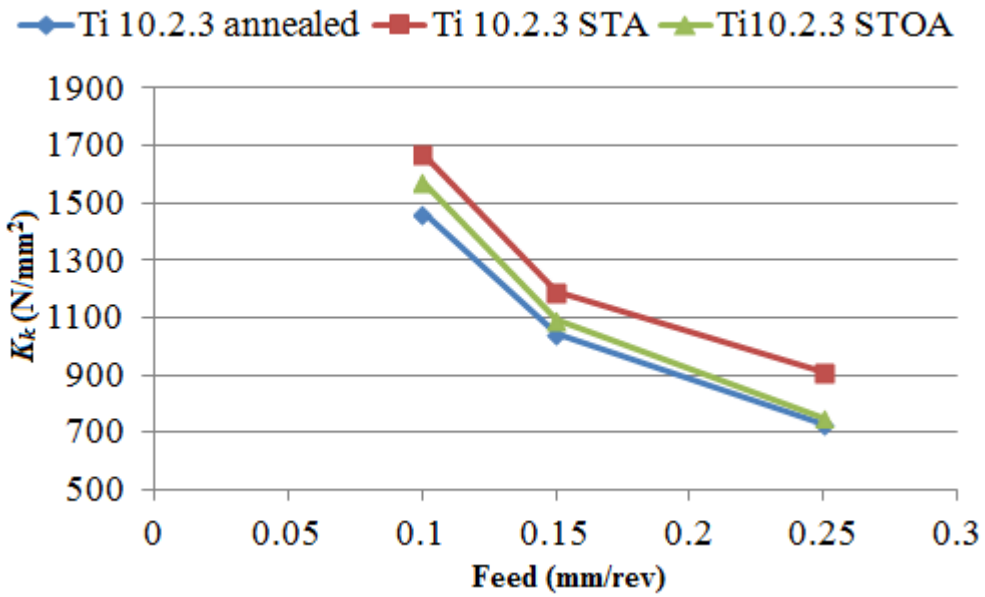

(b)

Figure 5.3. Specific feed force K_k for all the Ti10.2.3 titanium alloys at cutting speed of (a) 40 m/min and (b) 80 m/min

average difference of around 100 N/mm^2 and 70 N/mm^2 respectively. These results correspond well with the hardness obtained after the respective heat treated conditions.

The specific feed force (figure 5.3) decreases rapidly with the increase of feed rate and gets almost halved on increasing the feed value from 0.1 mm/rev to 0.25 mm/rev. At cutting speed of 40 m/min, the highest specific feed forces were observed for Ti10.2.3 STA followed by STOA and annealed conditions. Same trend was observed at cutting speed of 80 m/min. It is also observed that both specific cutting force and feed force values have similar effect of heat treatment. Lowest values are obtained for the alloy Ti10.2.3 in annealed condition and the highest ones are obtained for the alloy Ti10.2.3 in STA condition. For instance, at the cutting speed (V_c) of 40m/min and feed rate (f) of 0.1mm/rev the specific cutting force (K_c) varies from 2248 N/mm^2 for the Ti10.2.3 annealed to 2254 N/mm^2 for the Ti10.2.3 STOA and 2391 N/mm^2 for the Ti10.2.3 STA. The specific feed force (K_k) varies from 1769 N/mm^2 for the Ti10.2.3 annealed to 1818 N/mm^2 for the Ti10.2.3 STOA and 1989 N/mm^2 for the Ti10.2.3 STA. Thus, the differences among the different heat treated conditions are more apparent in the case of the specific feed force (K_k) than in the specific cutting force (K_c).

A drop in specific cutting force was observed with increasing cutting speed from 40 m/min to 80 m/min. This is because of the thermal softening effect. This drop in force is significant in the cutting as well as feed directions. This observation gives an indication of strong thermal softening effect within the tested cutting speed range. Ti10.2.3 alloy in STA heat treatment condition seems too strong to give in to thermal softening than the Ti10.2.3 in annealed and STOA heat treatment conditions at higher feed rates. The values of specific feed force at 40 m/min and 80 m/min are very similar for STA condition at feed rate of 0.25 mm/rev.

5.5.2. Friction coefficient

The effect of friction on the machining process is characterized by the friction coefficient. The calculation of coefficient of friction (μ) for an orthogonal cutting condition is done by using equations 4.1 - 4.3.

Figure 5.4 shows that the variation in coefficient of friction with feed rate for Ti10.2.3 titanium alloys in different heat treated conditions. The coefficient of friction was found to decrease with the increase of feed rate. This drop in the friction coefficient is due to the chip's hot softening and consequent reduction in the chip's resistance to sliding along the tool rake surface, as explained in the previous chapter. The larger decrease in friction coefficient was observed when the feed rate changes from 0.1 mm/rev to 1.5 mm/rev in comparison to the change in feed rate from 0.15 mm/rev to 0.25 mm/rev for both the cutting speeds. At V_c = 80 m/min, the data consistently shows that the μ is highest for Ti10.2.3 STA and lowest for Ti10.2.3 annealed.

In dry cutting, the coefficient of friction is known to decrease with the increase in cutting speed. Rashid et al. (2011) reported a decrease in the coefficient of friction from 0.80 to 0.60 while increasing the cutting speed from 5 m/min to 100 m/min when cutting Ti25Nb3Mo3Zr2Sn titanium alloy. Hong et al. (2001) also reported a reduction in the friction coefficient from 0.54 to 0.40 as the cutting speed is increased from 60 m/min to 180 m/min during Ti6Al4V machining. The reduction in the coefficient of friction is attributed to thermal softening of the workpiece. Similar trends have been observed in this research, except for STA heat treated condition at feed rate of 0.25 mm/rev. At this cutting condition friction coefficient increased with increase in cutting speed.

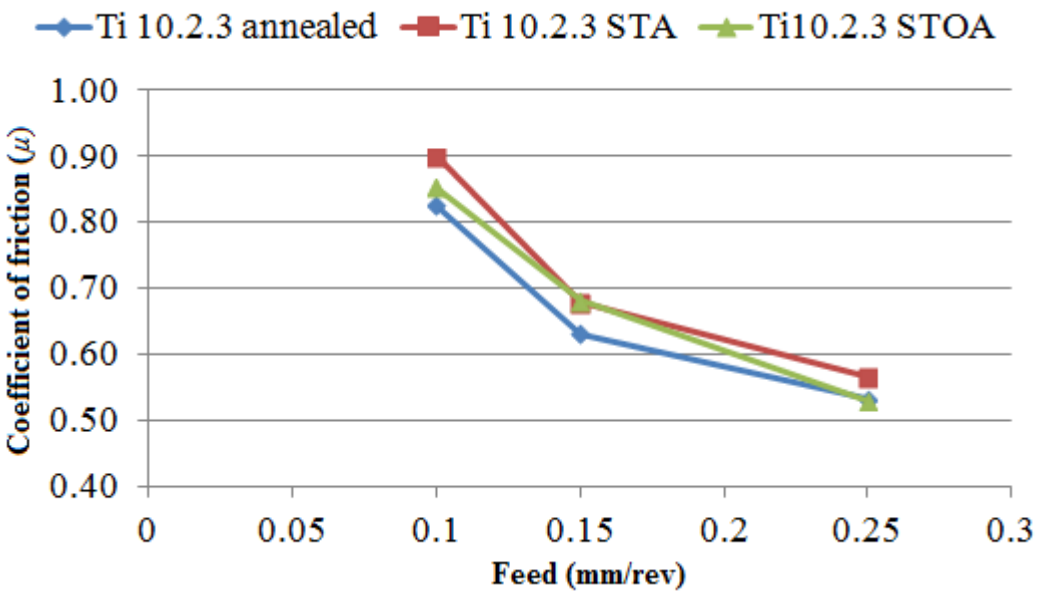

(a)

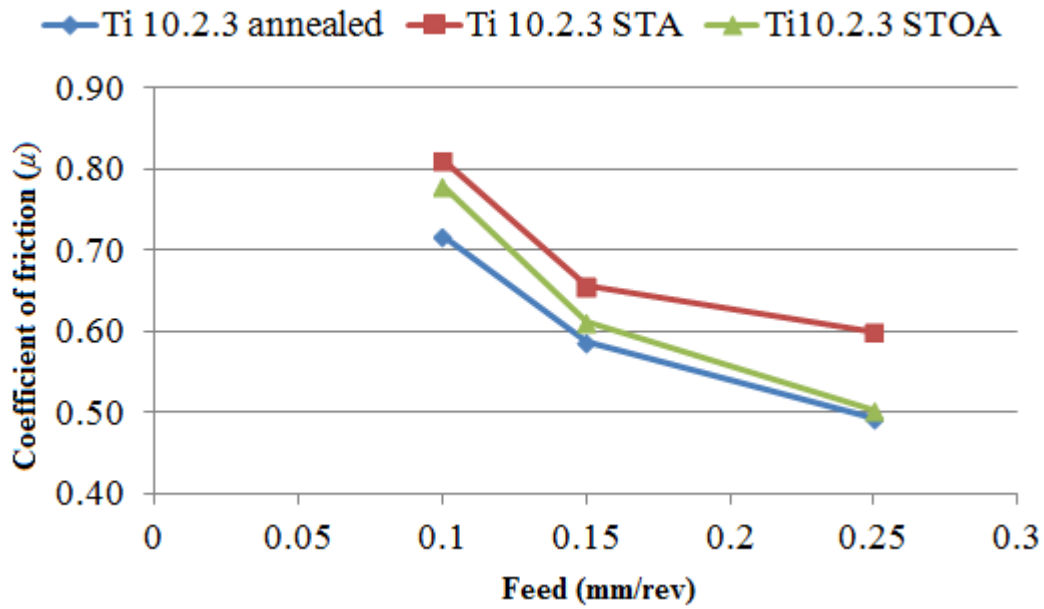

(b)

Figure 5.4. Apparent coefficient of friction for all the Ti10.2.3 titanium alloys at cutting speed of (a) 40 m/min and (b) 80 m/min

STA heat treated condition strengthens the workpiece more as compared to the other heat treatment conditions. It reduces thermal softening effect at higher temperatures and can

increase friction. Therefore, it is clear that higher cutting speed and thermal softening reduce the friction between the chip/tool interface and STA heat treatment condition restricts the thermal softening effect and increases friction as compared to other heat treatment conditions.

5.5.3. Cutting tool temperature

The influence of cutting parameters and heat treatment conditions on the cutting tool temperature is shown in figure 5.5. These values are the averages of three readings for each cutting condition.

The heat generated during a machining operation is a result of both the plastic deformation due to chip formation at the cutting tool tip and the friction between the cutting tool rake face and the surface of the newly formed chip (Ezugwu and Wang, 1997). This heat generation is significant and for the Ti10.2.3 alloy temperatures exceeding 1000 °C are reached at higher cutting speeds and feed rates with the given depth of cut. Figure 5.5 depicts a tendency of higher heat generation as the feed rate and cutting speed are increased. At V_c = 80 m/min and f = 0.25 mm/rev, the cutting tool temperature reached above 1200^{o}C for the Ti10.2.3 STA alloy. The cutting tool temperature values of Ti10.2.3 alloy in STA condition are higher as compared to other heat treated conditions. It can be attributed to lower hardness value due to annealing and over aging. This reduction in hardness during over aging process is due to the coalescence of the precipitates into bigger particles which cause fewer impediments to the movement of dislocation. However, due to the uncertainty in thermal measurement system, no clear differences have been observed between the temperatures generated in the machining of the Ti10.2.3 annealed and Ti10.2.3 STOA alloys

at all cutting speeds. Young's modulus of the titanium alloys decreases as the temperature of the titanium alloy workpiece increases (Komanduri and Hou, 2001). Fluctuation in the tool/chip interface during titanium machining due to this reduction in Young's modulus is one of the probable cause of this uncertainty in the thermal measurement system.

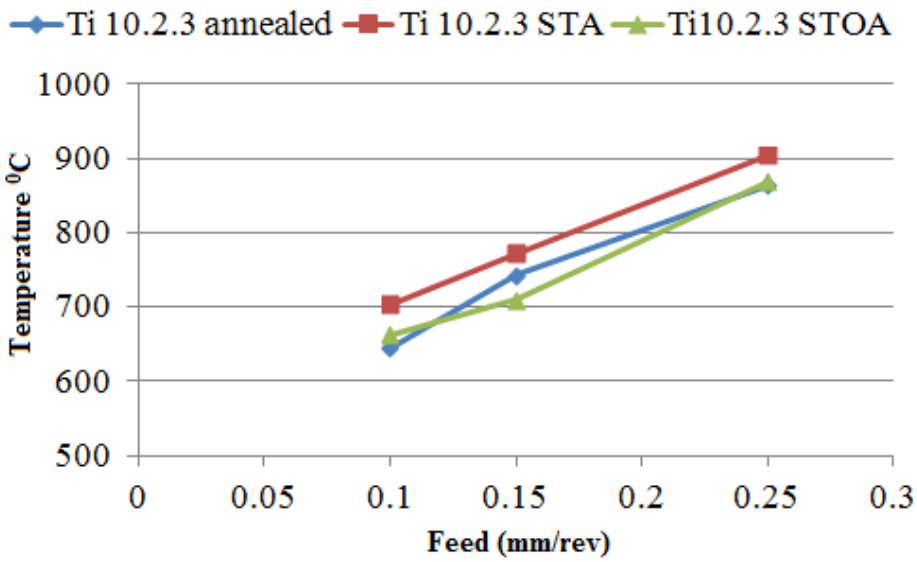

(a)

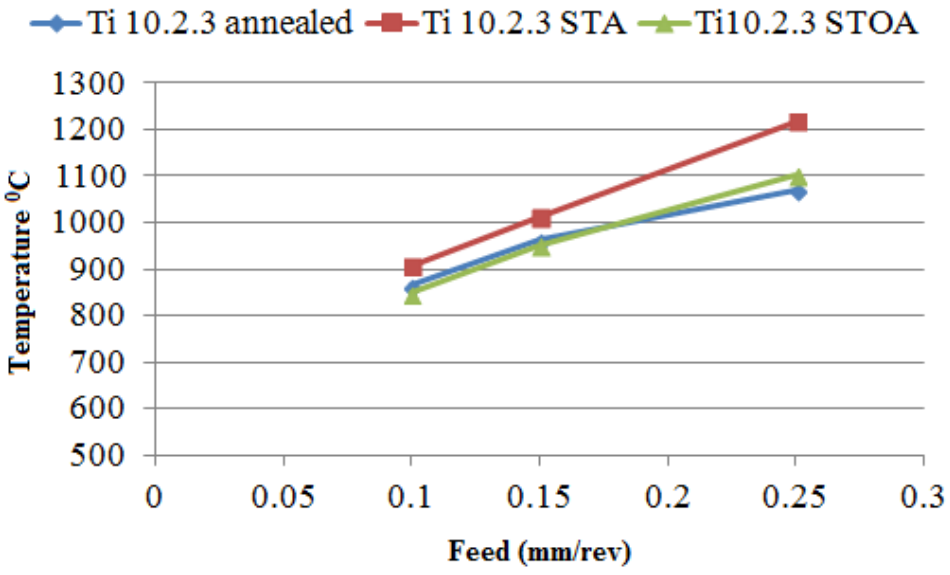

(b)

Figure 5.5. Cutting tool temperature for all the Ti10.2.3 titanium alloys at cutting speed of (a) 40 m/min and (b) 80 m/min

This research shows that for STA heat treated condition the corresponding temperature increase is linear over the investigated cutting speeds. The rise in temperature is sufficiently high to dominate strain rate hardening. There is found to be an exception at the feed rate of 0.25 mm/rev where strain hardening effect showed its dominance over thermal softening effect regardless of very high temperature for Ti10.2.3 in STA condition. However, it is clear that thermal softening begins to dominate strain rate hardening for other two heat treatment conditions at given cutting speeds, because of the decrease in cutting forces and hardness. From aforementioned discussion it is clear that the alloying with more β stabilizers and STA heat treatment condition makes the material to retain its strength with rise in cutting tool temperature, and, therefore, reduce the values of permissible cutting parameters.

5.6. Statistical Analysis of Results Using ANOVA

The experimental results obtained in the previous section were analyzed for statistical significance using analysis of variance (ANOVA). The results of ANOVA for the specific cutting force, specific feed force and cutting tool temperature are shown in Tables 5.4, 5.5 and 5.6 respectively. This analysis was carried out for a significant level of 0.05 (95% confidence level).

Table 5.4 shows the main and interaction effects of the feed rate and cutting speed for all heat treatment conditions. It is found that the effect of feed rate is statistically significant on the specific cutting forces for all the three alloys (P-value ~ 0). Similarly, the effect of cutting speed is statistically significant for all the three alloys. Also, the effects of two-factor interactions of the feed rate and the cutting speed are statistically significant for the specific cutting forces in all conditions. The F values clearly indicate that the feed rate is more

significant factor compared to the cutting speed, i.e. the larger contribution to the specific cutting force for all the heat treatment conditions is due to the feed rate. The interactions between feed rate and cutting speed ($f \times V_c$) are comparatively more significant for the Ti54M in STA condition.

Table 5.4. ANOVA for specific cutting force for the Ti10.2.3 titanium alloy in (a) annealed (b) STA and (c) STOA conditions

(a)

Source	SS	DF	MS	F	P-value
f	636089.3	2	318044.7	785.72	0.000
V_c	147424.5	1	147424.5	364.21	0.000
$f * V_c$	5217.33	2	2608.67	6.44	0.014
Within	4857.33	12	404.78		
Total	793588.5	17			

(b)

Source	SS	DF	MS	F	P-value
f	834365.8	2	417182.9	1744.72	0.000
V_c	142756.1	1	142756.1	597.02	0.000
$f * V_c$	18544.44	2	9272.22	38.78	0.000
Within	2869.33	12	239.11		
Total	998535.6	17			

(c)

Source	SS	DF	MS	F	P-value
f	629724.1	2	314862.1	2349.71	0.000
V_c	138864.5	1	138864.5	1036.30	0.000
$f * V_c$	2977	2	1488.5	11.11	0.002
Within	1608	12	134		
Total	773173.6	17			

Table 5.5 shows that the main and interaction effects of the feed rate and cutting speed on specific feed force for all heat treatment conditions. It is found that the effect of feed rate and cutting speed on specific feed force is statistically significant (P-value ~ 0) for all the three alloys. The interactions between cutting speed and feed rate are observed to be

significant with respect to the specific feed force. These results show that the F value for the factor feed rate is larger than that of cutting speed, i.e. the larger contribution to the specific feed force for all the heat treatment conditions is due to the feed rate. This interaction is comparatively more significant for the annealed and STA heat treatment conditions.

Table 5.5. ANOVA for specific feed force for the Ti10.2.3 titanium alloy in (a) annealed (b) STA and (c) STOA conditions

(a)

Source	SS	DF	MS	F	P-value
f	2118697	2	1059349	1062.95	0.000
V_c	151800.5	1	151800.5	152.31	0.000
$f * V_c$	31712.33	2	15856.17	15.91	0.000
Within	11959.33	12	996.61		
Total	2314170	17			

(b)

Source	SS	DF	MS	F	P-value
f	2625425	2	1312713	415.40	0.000
V_c	93312	1	93312	29.52	0.000
$f * V_c$	78220.33	2	39110.17	12.37	0.001
Within	37921.33	12	3160.11		
Total	2834879	17			

(c)

Source	SS	DF	MS	F	P-value
f	2450002	2	1225001	702.50	0.000
V_c	136242	1	136242	78.13	0.000
$f * V_c$	17672.33	2	8836.17	5.07	0.033
Within	20925.33	12	1743.78		
Total	2624842	17			

Table 5.6 shows the main and interaction effects of the feed rate and cutting speed on cutting tool temperature for all heat treated conditions. It is found that the effect of feed rate and cutting speed on tool temperature is statistically significant (P-value ~ 0) for all the three alloys.

It can be seen that the interactions between feed rate and cutting speed ($f \times V_c$) have significant effect on tool temperature for STA heat treatment condition only. F value for the factor cutting speed is larger than that of the feed rate factor, i.e. the larger contribution to the cutting tool temperature is due to the cutting speed. This analysis shows that the effect of cutting parameters on the specific forces and cutting tool temperature are remarkably significant.

Table 5.6. ANOVA for cutting tool temperature for the Ti10.2.3 titanium alloy in (a) annealed (b) STA and (c) STOA conditions

(a)

Source	SS	DF	MS	F	P-value
f	134230.8	2	67115.39	426.28	0.000
V_c	206724.5	1	206724.5	1313	0.000
$f * V_c$	210.33	2	105.17	0.67	0.531
Within	1889.33	12	157.44		
Total	343054.9	17			

(b)

Source	SS	DF	MS	F	P-value
f	202474.3	2	101237.2	1480.31	0.000
V_c	284760.9	1	284760.9	4163.84	0.000
$f * V_c$	9230.11	2	4615.06	67.48	0.000
Within	820.67	12	68.39		
Total	497286	17			

(c)

Source	SS	DF	MS	F	P-value
f	164022.3	2	82011.17	167.21	0.000
V_c	215168	1	215168	438.72	0.000
$f * V_c$	2704.33	2	1352.17	2.75	0.102
Within	5885.33	12	490.44		
Total	387780	17			

5.7. Conclusions

The experimental studies carried out on Ti10.2.3 titanium alloy in as-received annealed, STA and STOA conditions show that this alloy has the poorest machinability in the STA heat treated condition as the specific forces, friction coefficient and cutting tool temperature are higher in this condition. It is also found that the specific feed force is more sensitive to variations in feed rates than the specific cutting force. The over aging treatment improves the machinability of this alloy because of reduction in hardness as a consequence of coalescence of the precipitates into the bigger particles causing fewer impediments to the movement of dislocations. Thermal softening plays a dominant role for all the heat treated conditions except for STA condition at 0.25 mm/rev feed rate. At this particular feed rate Ti10.2.3 STA showed resistance to thermal softening. The ANOVA results have shown that most of the experimental results are statistically significant in term of feed rate and cutting speed variations. Feed rate has been found to have more significance than the cutting speed for specific cutting and feed forces in all heat treated conditions. Cutting speed has been found to be more significant for cutting tool temperature. The interactions between the feed rate and cutting speed have significant effect on the specific cutting and feed forces as well as on the cutting tool temperature for the STA condition.

Chapter 6

Machinability Studies on Ti6Al4V Titanium Alloys and Comparative Machinability Analysis of Ti6Al4V, Ti54M and Ti10.2.3 Alloys

6.1. Introduction

This chapter presents the machinability studies on the most widely used titanium alloy, Ti6Al4V. This is followed by the comparison of machinability studies of Ti54M and Ti10.2.3 titanium alloys with the Ti6Al4V alloy. The machinability studies on Ti54M and Ti10.2.3 titanium alloys are relatively new and few, therefore, the comparison of these new machinability results with the well researched Ti6Al4V alloy is expected to provide new directions in the research as well as the adoption of these alloys in industries. Ti10.2.3 alloy has a comparative poor machinability (Donachei, 2004) which needs to be overcome so as to maintain at least the same productivity levels as of Ti6Al4V. Comparative studies are important to investigate the effect of chemical composition, heat treatment conditions and cutting parameters. The comparative studies are expected to add value to the existing knowledge bank on titanium machining.

6.2. Machinability Studies on Ti6Al4V Titanium Alloys

Ti6Al4V alloy accounts for more than 50% of the titanium alloy production (Boyer, 1996; Yang and Liu, 1999; Rahman et al., 2003). Detailed review on machining of Ti6Al4V titanium alloy has been discussed in chapter 2. However, the exact chemical composition

and mechanical properties of the Ti6Al4V titanium alloy used in the experimental work are summarized in table 6.1. It is observed that the Ti6Al4V alloys have a molybdenum equivalent value of 3.1. This lower value of molybdenum equivalent, as discussed in chapter 5, explains the lower mechanical properties of this α+β titanium alloy as compared to β titanium alloys.

The various experimental studies were carried out at feed rates of 0.1 mm/rev, 0.15 mm/rev and 0.25 mm/rev at 40 m/min and 80 m/min cutting speeds. Depth of cut is taken as 2 mm. The effect of these cutting parameters was studied in term of specific forces, friction coefficient, cutting tool temperature, and chip morphology. The results and discussion of these experiments are given next.

6.2.1. Specific forces

The significance of determining specific forces has already been discussed in the previous chapters. The specific forces are calculated from the measured forces using equations 2.1 and 2.2. The specific cutting and feed forces (K_c and K_k) at cutting speeds of 40 m/min and 80 m/min are shown in figure 6.1. Results plotted for the specific forces represent the mean values observed from the three experimental tests at each condition.

Table 6.1. Chemical composition and mechanical properties of the Ti6Al4V alloy

Titanium Alloy	Chemical Composition (%)				Al Equiv. Value (%)	Mo Equiv. Value (%)	Hardness (HRC ±3)	TYS (MPa)	UTS (MPa)	Elongation (%)	RA (%)
	Al	V	Fe	O							
Ti6Al4V	6	4	0.15	0.18	6	3.1	31	990	910	18	39

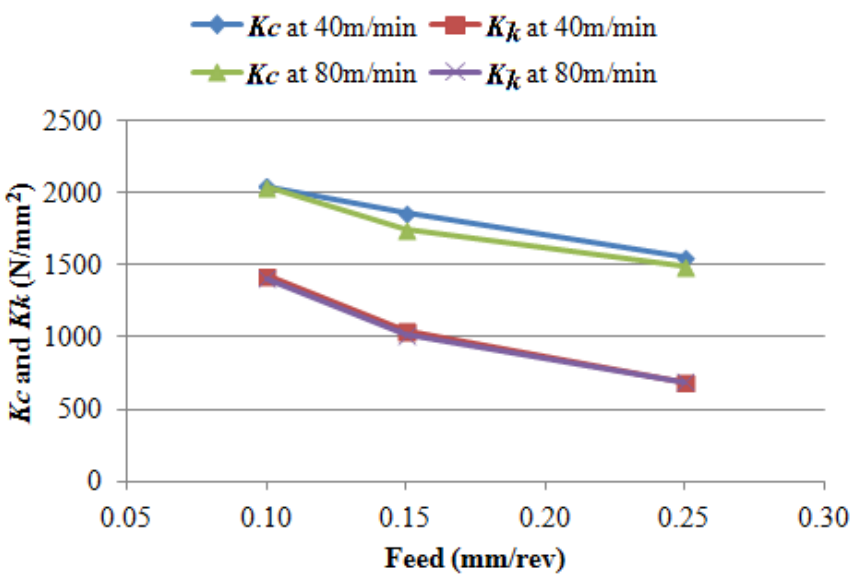

Figure 6.1. Specific cutting force (K_c) and feed force (K_k) for Ti6Al4V titanium alloy at cutting speed of 40 m/min and 80 m/min

It can be seen from figure 6.1 that the specific cutting force decreases with the increase in feed rate. Specific feed force also decreases with the increase of feed rate and gets almost halved on increasing the feed value from 0.1 mm/rev to 0.25 mm/rev. However, the specific feed force are much lower than the specific cutting force. It is observed that with increasing cutting speed, the specific feed force show almost similar values. This proves that the Ti6Al4V titanium alloys maintain their strength at higher temperatures because in this case strain hardening is balancing the thermal softening (Sun et al., 2009).

6.2.2. Friction coefficient

It is necessary to evaluate the friction coefficient in order to characterize the effect of friction on the machining process to evaluate the effect of various cooling fluids. The calculation of friction coefficient (μ) has been developed for the situation of two-dimensional orthogonal cutting by using equations 4.1 - 4.3.

Figure 6.2 shows the variation of coefficient of friction with the change in feed rate at different cutting speeds for the Ti6Al4V titanium alloy. The coefficient of friction is found to be decreasing with the increasing feed rate. This drop in the friction coefficient is due to the chip's hot softening and consequent reduction in the chip's resistance to sliding with the tool rake surface, as explained in the previous chapters. The larger decrease in friction coefficient was observed when the feed rate changes from 0.1 mm/rev to 1.5 mm/rev in comparison to the change in feed rate from 0.15 mm/rev to 0.25 mm/rev for both the cutting speeds. It is also found that in spite of increasing cutting speed, there is not much effect on the friction coefficient.

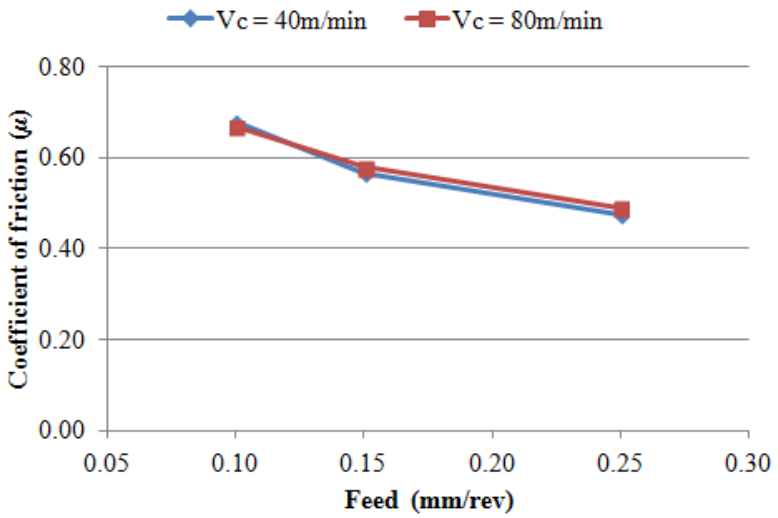

Figure 6.2. Apparent coefficient of friction for Ti6Al4V alloy at cutting speed of 40 m/min and 80 m/min

6.2.3. Cutting tool temperature

The influence of cutting parameters on the cutting tool temperature is shown in figure 6.3. These values are the averages of three readings for each cutting condition. As it can be depicted from figure 6.3, a tendency of a higher heat generation rate at higher feed rates and

cutting speeds is experienced. At higher machining conditions, the cutting tool temperature reached above 900°C for the Ti6Al4V alloy.

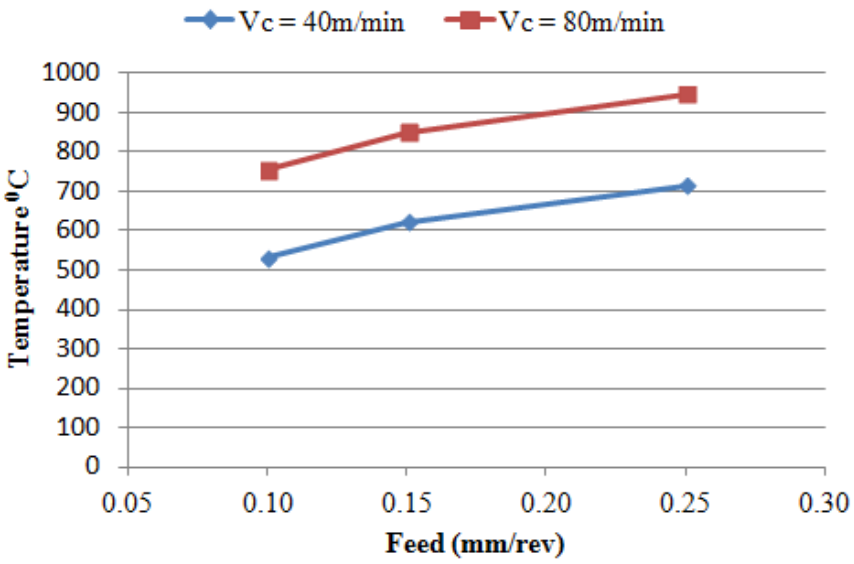

Figure 6.3. Cutting tool temperature for Ti6Al4V alloy at cutting speed of 40 m/min and 80 m/min

A consistent increase in the cutting tool temperature by approximately 230°C has been observed with increase in cutting speed from 40 m/min to 80 m/min at all feed values.

6.2.4. Chip morphology

Optical microscopy of chip cross-sections obtained at different feed rates and cutting speeds for Ti6Al4V alloy are shown in section 6.3.4. The localized adiabatic shear-band formation in the chips of Ti6Al4V alloy at all cutting speeds has been observed. Similar results have been reported already by Barry et al. (2001). It is found that with low values of cutting speed and feed, aperiodic segmented chips were produced. A transition from aperiodic to periodic segmentation occurred with the increase of both cutting parameters.

6.2.5. Statistical analysis of results using ANOVA

An analysis of variance (ANOVA) was conducted to verify the statistical significance of results. Table 6.2 shows the main and interaction effects of the feed rate and cutting speed on specific cutting force. Investigating these effects based on 5% level of significance, it is found that the effect of feed rate, cutting speed and interaction among them are statistically significant for the specific cutting force as P-values are less than 0.05. F value for the feed rate factor is larger than that of the cutting speed, i.e., the larger contribution to the specific cutting force is due to the feed rate.

Table 6.2. ANOVA for specific cutting force for Ti6Al4V titanium alloy

Source	SS	DF	MS	F	P-value
f	804979	2	402489.5	830.07	0.000
V_c	16320.22	1	16320.22	33.66	0.000
f*V_c	7760.11	2	3880.06	8.001	0.006
Within	5818.67	12	484.89		
Total	834878	17			

Table 6.3 shows the main and interaction effects of the feed rate and cutting speed on specific feed force. It is found that the effect of feed rate is statistically significant on the specific feed force. The effects of cutting speed and two-factor interactions of the feed rate and the cutting speed are found to be statically insignificant on the specific feed force which is evident from their P-values of 0.373 and 0.841 respectively.

Table 6.3. ANOVA for specific feed force for Ti6Al4V titanium alloy

Source	SS	DF	MS	F	P-value
f	1585824	2	792912.1	527.78	0.000
V_c	1317.56	1	1317.56	0.87	0.373
f*V_c	518.11	2	259.06	0.17	0.841
Within	18028	12	1502.33		
Total	1605688	17			

Table 6.4 shows ANOVA results for cutting tool temperature. It can be seen that the feed and cutting speed have significant effect on cutting tool temperature as P-values are less than 0.05 (P~0). The interaction effect between the feed rate and the cutting speed is insignificant as evident from the P-value of 0.932. The ANOVA result shows that the F value for the factor cutting speed is larger than that of the other cutting parameter (feed rate), i.e., the larger contribution to the cutting tool temperature for is due to the cutting speed.

Table 6.4. ANOVA for cutting tool temperature for Ti6Al4V titanium alloy

Source	SS	DF	MS	F	P-value
f	106785.4	2	53392.72	132.56	0.000
V_c	232334.7	1	232334.7	576.83	0.000
f*V_c	56.78	2	28.39	0.07	0.932
Within	4833.33	12	402.78		
Total	344010.3	17			

6.3 Machinability Comparison of Ti54M and Ti6Al4V Titanium Alloys

Armendia et al. (2010a) studied the comparative machinability performance of Ti54M alloy in forged condition and Ti6Al4V alloy in mill annealed condition with uncoated cemented carbide tools. Lower wear rates and cutting force values for the Ti54M alloy were observed, which confirmed its better machinability. The difference in the microstructure of these alloys leads to different machinabilities of these alloys. Kosaka and Fox (2004) studied the drilling performance of these two alloys under different heat treatment conditions. They also confirmed the better machining behavior of Ti54M alloy. The influence of microstructure (totally laminar microstructures) of β annealed samples showed higher cutting forces and tool wear rates. However, Rahim and Sharif (2006) claimed better machinability of Ti6Al4V alloy than Ti54M alloy during drilling operation using uncoated carbide drills. Armendia et al. (2010b) studied the influence of microstructure on the machinability of Ti54M and

Ti6Al4V alloys using uncoated cemented carbide tools. Both the materials were tested in four different heat treatment conditions (as forged, mill annealed, β annealed, and duplex annealed). The alloys in the β annealed condition were found to be least machinable. Lower tool life and higher cutting forces were observed while machining both the alloys in β annealed condition. Preliminary study of cutting temperatures generated during machining of these alloys using a micro-thermal imaging system was also performed. These studies did not show any significant differences in temperature generation during machining. Low resolution of 30 μm used in the study was found to be the reason for the insignificant difference, which is too coarse to analyze in detail the tool/chip interface. The extremely short contact length common in the machining of these materials makes the resolution of 10 μm appropriate to analyze the tool/chip interface in detail. In this section, comparison of the heat treatment effect on the machinability of Ti54M titanium alloy for the as-received annealed, β annealed and STA conditions with the commonly used Ti6Al4V in annealed condition is investigated. The comparison is carried in terms of microstructure, specific forces, cutting tool temperature (at 10 μm resolution), and chip morphology as given next.

6.3.1. Material microstructure

[1] Both Ti54M and Ti6Al4V alloys belong to the α+β alloy group. These alloys have very similar chemical composition and mechanical properties. Due to the presence of higher concentration of β stabilizers (Fe, V and Mo) in Ti54M alloy, the β transus temperature is almost 30^0C lower than that of Ti6Al4V. Microstructure detail of Ti6Al4V in annealed condition and Ti54M alloys in annealed, β annealed and STA heat treated conditions are shown in figure 6.4.

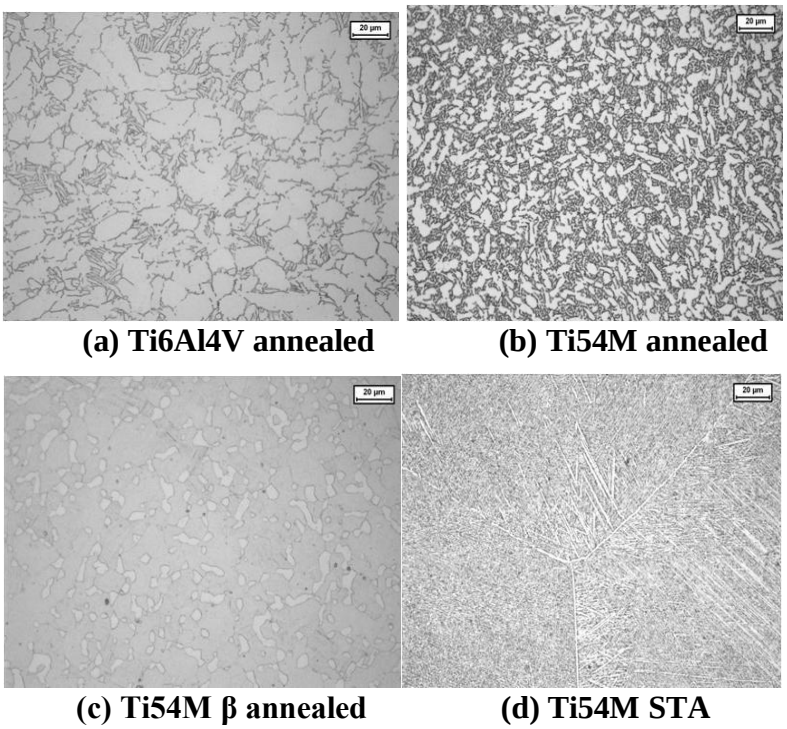

(a) Ti6Al4V annealed **(b) Ti54M annealed**

(c) Ti54M β annealed **(d) Ti54M STA**

Figure 6.4. Microstructure of different Ti54M and Ti6Al4V titanium alloys

6.3.2. Specific forces

The specific cutting force (K_c) and the specific feed force (K_k) for all the analyzed titanium alloys at cutting speeds of 40 m/min and 80 m/min are shown in figures 6.5(a) and (b) respectively. Results plotted for the specific forces represent the average values obtained from the three experimental tests at each condition. The uncertainty in the force measurements is shown by the error bars.

It can be seen from figure 6.5(a) that the specific cutting force decreases with the increase in feed rate. This trend is followed in all heat treated conditions. However, the difference among the cutting forces is higher at higher feed rates for all alloys. The highest specific cutting forces were noticed for Ti54M in β annealed condition at high feed rates. The lower specific cutting forces were observed for Ti54M in STA condition at 80 m/min cutting

speed. Same trends were observed (Figure 6.5 (a)) at cutting speed of 40 m/min except at lower feed rate, where Ti54M in STA heat treatment condition showed highest value.

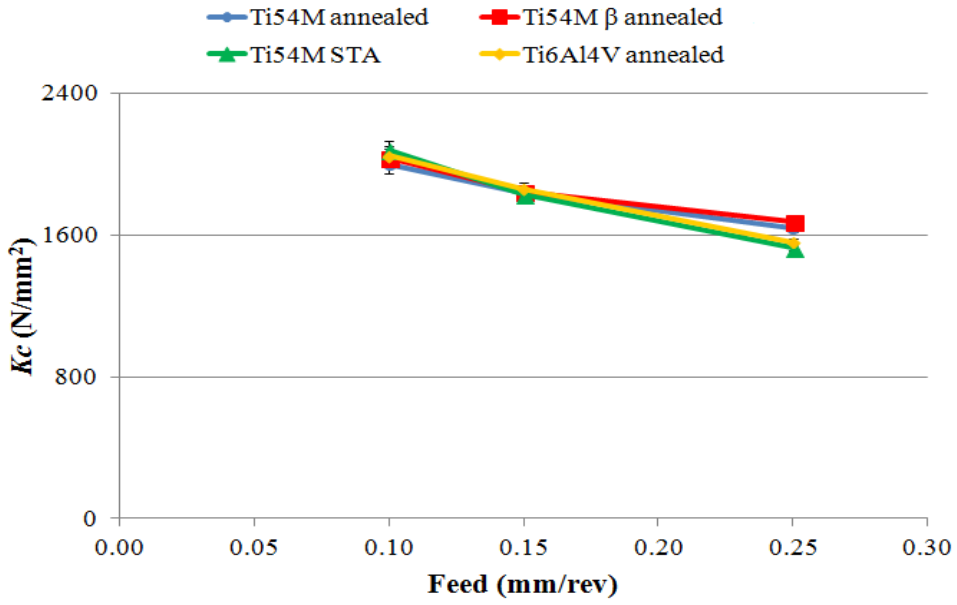

(a)

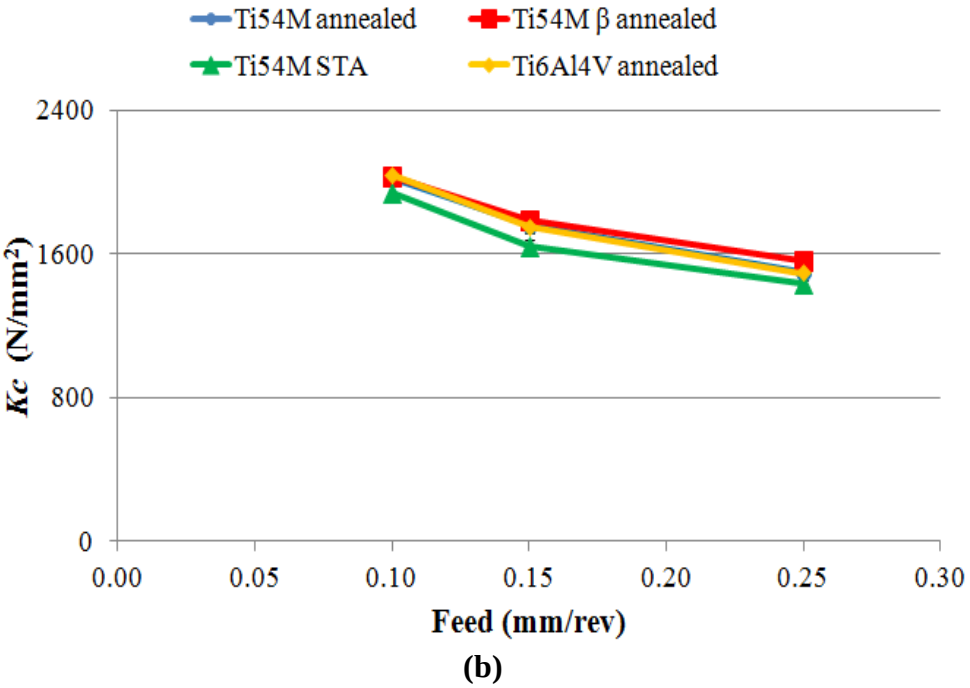

(b)

Figure 6.5. Specific cutting (K_c) force for Ti54M and Ti6Al4V titanium alloys at cutting speed of (a) 40 m/min and (b) 80 m/min

In addition, all the titanium alloys show steady decrease in specific cutting force even when hardness and tensile strength differ due to the different heat treated conditions. For annealed heat treatment condition at the lower feed rates, specific cutting force is lower during the machining of the Ti54M alloy as compared to Ti6Al4V alloy. However, at higher feed rate specific cutting force for Ti54M alloy is higher than Ti6Al4V. Same trend is observed for Ti54M β annealed and Ti6Al4V annealed alloys. Similar trends were also observed by Aermendia et al. (2010b) for the Ti54M and Ti6Al4V alloys in forged condition.

Variation in the specific feed force (Figure 6.6) follows the same trend and decreases rapidly with the increase of feed rate and gets almost halved on increasing the feed value from 0.1 mm/rev to 0.25 mm/rev. It is found that the specific feed force is higher for the Ti54M in all heat treated conditions than Ti6Al4V alloy at all cutting parameters except at V_c = 40 m/min and f = 0.15 mm/rev; where Ti54M in annealed condition showed lesser value than Ti6Al4V alloy. It is observed that the specific feed forces are more sensitive to change in feed rate than specific cutting forces for both Ti54M and Ti6Al4V alloys. The specific feed force (K_k) values correlated well with the mechanical properties of the alloys, as higher values were obtained for the Ti54M STA alloy. Clear influence on specific feed (K_k) forces has been observed for the Ti54M with STA heat treatment condition.

6.3.3. Cutting tool temperature

Interfacial temperatures in machining play a major role in tool wear and can also result in modifications of the workpiece and tool material properties.

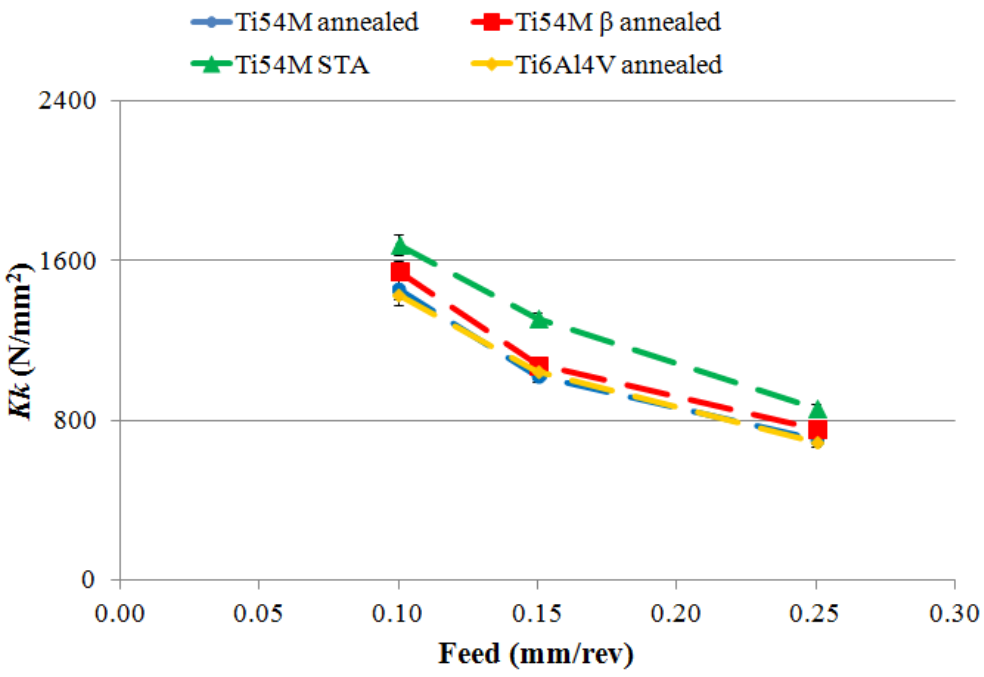

(a)

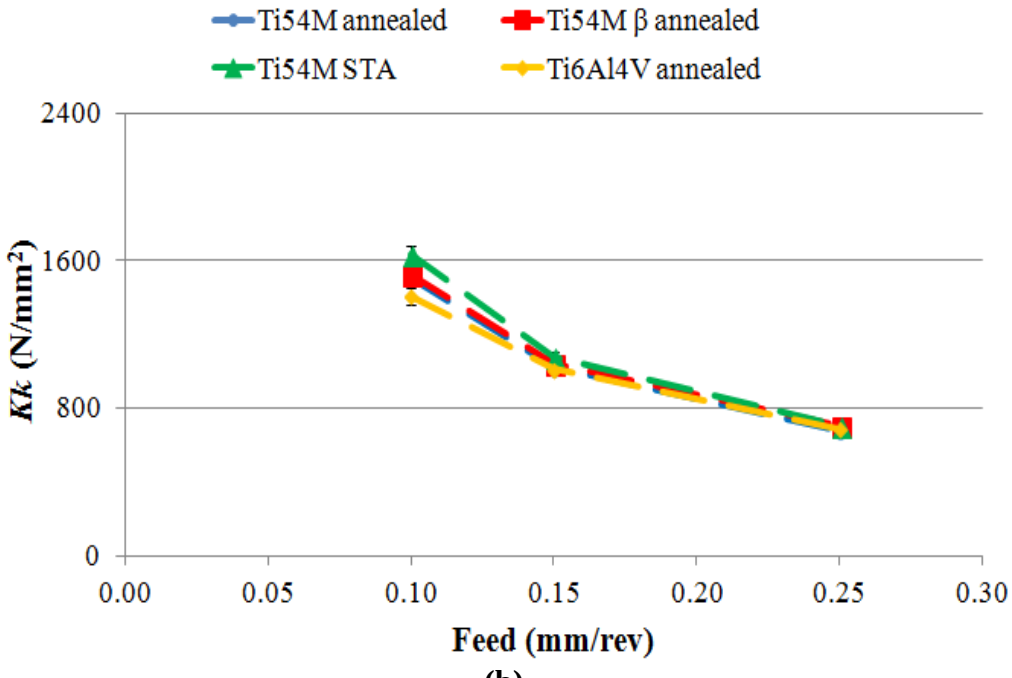

(b)

Figure 6.6. Specific feed (K_k) force for Ti54M and Ti6Al4V titanium alloys at cutting speed of (a) 40 m/min and (b) 80 m/min

As there is a general move towards dry machining (Davies et al., 2007), for environmental reasons, it is increasingly important to understand how machining temperatures are affected by the process variables involved (cutting speed, feed rate, etc.) and by other factors such as heat treatment conditions (Armendia et al., 2010a).

The cutting tool temperature for all the analyzed titanium alloys at cutting speeds of 40 m/min and 80 m/min are shown in figure 6.7. Temperature plots represent the average values observed from the experimental tests. The uncertainty in thermal measurements is revealed by the error bars. Figure 6.7 shows a tendency of higher heat generation rate as the feed rate and cutting speed are increased. At cutting speeds of 40 m/min and 80 m/min and feed rate of 0.25 mm/rev, the cutting tool temperature for all the three different heat treated Ti54M alloys was found to be greater by 50^0C over the temperature obtained for Ti6Al4V alloy.

At lower cutting values, similar temperature values were observed for the analyzed alloys. Arrazola et al. (2005) observed that the specific feed force (K_k) indicates the friction and rubbing effects over the rake surface and hence explains the amount of heat generated at the tool/chip contact zone. Therefore, higher temperatures are expected in the machining of Ti54M in STA and β annealed conditions as compared with other analyzed alloys. But machining of both the alloys along with Ti54M annealed produced higher temperature than the Ti6Al4V alloy at the higher cutting speeds (Figure 6.7 (a) and (b)). However, due to the uncertainty in thermal measurement system, it cannot be stated effectively that the temperatures generated in the machining of the Ti54M alloys are higher than Ti6Al4V at higher cutting speeds. From the results presented above, it is clear that factors determining the rise in temperature are heat treatment, cutting forces and friction during machining.

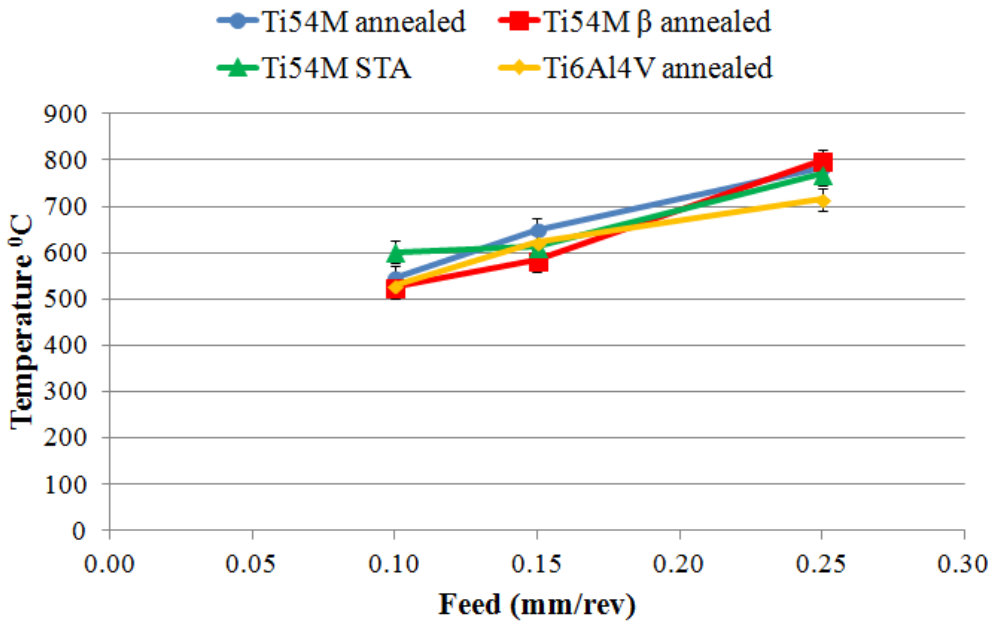

(a)

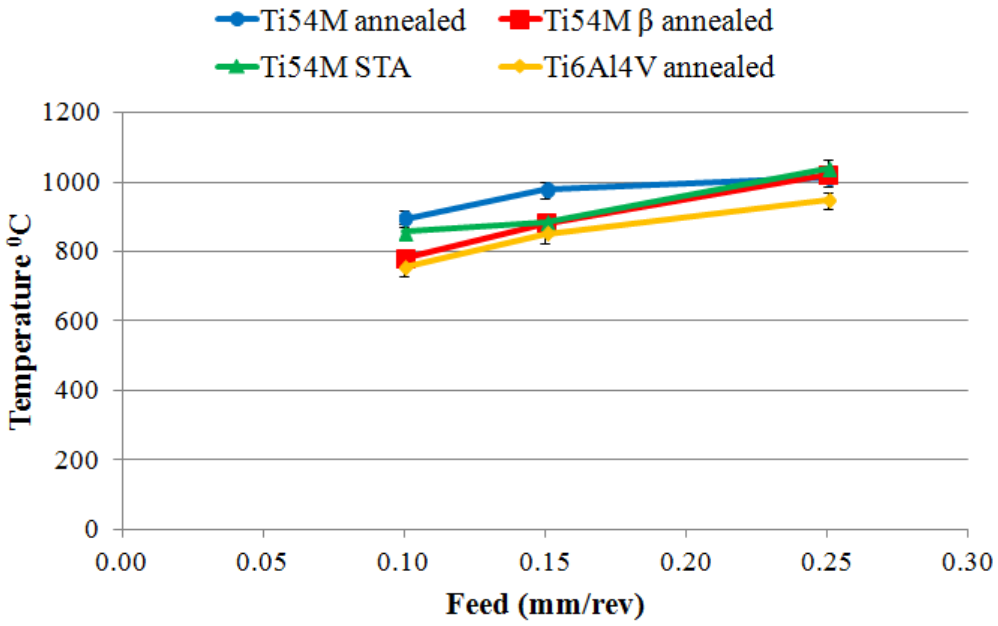

(b)

Figure 6.7. Temperature graph for Ti54M and Ti6Al4V titanium alloys at cutting speed of (a) 40 m/min and (b) 80 m/min

It is observed that the maximum cutting tool temperature (Figure 6.8) is located near to the cutting tool edge on the rake surface. The aforementioned discussion shows an apparent relation between the microstructure of the analyzed titanium alloys and the cutting tool temperature.

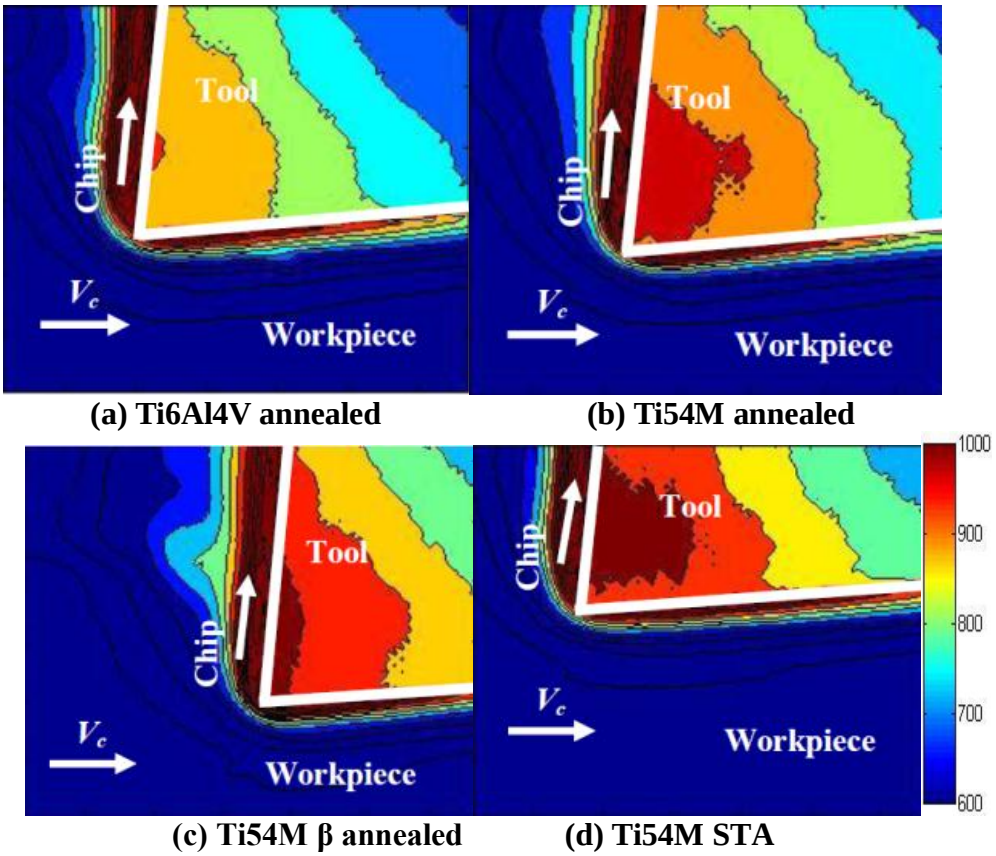

Figure 6.8. Thermal maps for Ti54M and Ti6Al4V titanium alloys at cutting speed of 80 m/min and 0.25 mm/rev feed rate

6.3.4. Chip morphology

Optical microscopy of chip cross-sections obtained for different alloys are shown in figure 6.9. The different heat treatment conditions and different machining parameters produced different chip morphologies.

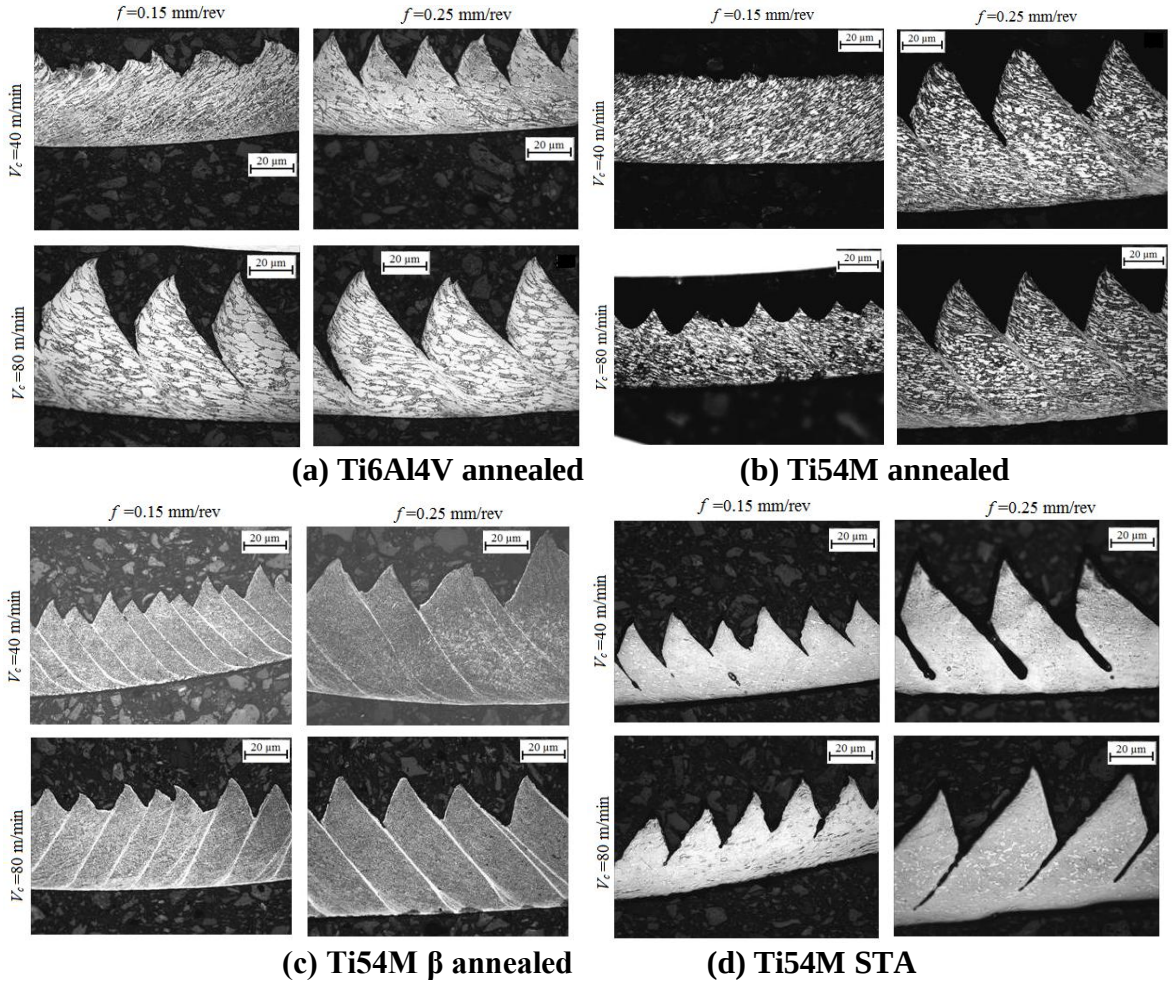

Figure 6.9. Chip morphology of Ti54M and Ti6Al4V titanium alloys at different feed rates and cutting speeds

Several authors have analyzed chip formation on titanium alloys. The most significant characteristic is the formation of adiabatic shear bands, a typical trend in the machining of hardened steels at high cutting speeds. Barry et al. (2001) analyzed the adiabatic shear band formation during the cutting of the Ti6Al4V alloy and confirmed that this phenomenon occurs at all the cutting conditions. The same conclusion has been achieved in the present study because this phenomenon appears in the chips of both Ti6Al4V and Ti54M alloys in different heat treated conditions as well as at all cutting conditions. It may be observed for Ti6Al4V alloy that with low values of cutting speed and feed, aperiodic segmented chips

were produced. A transition from aperiodic to periodic segmentation occurred with the increase of cutting speed and feed rate.

Chips produced from Ti54M annealed alloy at lower values of cutting parameters (V_c = 40 m/min and f = 0.15 mm/rev) were fairly of uniform thickness (continuous) but at higher cutting conditions segmented chips were produced. Segmented chips were obtained in the machining of Ti54M β annealed alloy at all cutting conditions. Chips produced for Ti54M STA at higher cutting speed and feed rate exhibit a much larger deformed volume at primary shear zone compared to the lower cutting parameters. It indicates a greater amount of microstructural deformation and overheating. This result matches with recent study by Bermingham et al. (2011) on the β annealed Ti6Al4V alloy. It is found that segmented chips are not always periodic for all the alloys at same cutting conditions.

6.4 Machinability Comparison of Ti10.2.3 and Ti6Al4V Titanium Alloys

In this section, comparison of the heat treatment effect on the machinability of Ti10.2.3 titanium alloy for the as-received annealed, solution treated plus aged (STA) and solution treated plus over aged (STOA) conditions with the commonly used Ti6Al4V in annealed condition is investigated. Ti10.2.3 alloy in solution treated plus aged condition shows the least machinability (in terms of specific forces and cutting tool temperature) among all the analyzed alloys. This is due to the strengthening effect, which is a consequence of interference with the motion of dislocation due to the formation of secondary α precipitates (Terlinde et al., 1980). The comparison is carried out in terms of specific forces and cutting tool temperatures as given next.

6.4.1. Specific forces

The specific cutting (K_c) and specific feed (K_k) forces for all the heat treated titanium alloys at cutting speeds of 40 m/min and 80 m/min are shown in figures 6.10 and 6.11 respectively. The difference among the specific cutting forces is higher at higher feed rates for all the alloys. The highest specific cutting forces were noticed for Ti10.2.3 in STA condition at all feed rates. The lower specific cutting forces were observed for Ti6Al4V except at cutting speed of 80 m/min and feed rate of 0.1 mm/rev.

At cutting speed of 40 m/min, the highest specific feed forces were observed for Ti10.2.3 STA followed by Ti10.2.3 alloy in STOA and annealed conditions. Same trend was observed at cutting speed of 80 m/min.

It is observed that specific cutting force (K_c) and specific feed force (K_k) values are dependent on the mechanical properties. The lowest values are obtained for the Ti6Al4V alloy and the highest are obtained for the Ti10.2.3 STA alloy. For instance, at the cutting speed (V_c) of 40 m/min and feed rate (f) of 0.1 mm/rev the specific cutting force (K_c) varies from 2047 N/mm^2 in the case of the Ti6Al4V to 2248 N/mm^2 for the Ti10.2.3 annealed, 2254 N/mm^2 for the Ti10.2.3 STOA, and 2391 N/mm^2 for the Ti10.2.3 STA. The specific feed force (K_k) varies from 1426 N/mm^2 in the case of the Ti6Al4V to 1769 N/mm^2 for the Ti10.2.3 annealed, 1818 N/mm^2 for the Ti10.2.3 STOA and 1989 N/mm^2 for the Ti10.2.3 STA. Thus, the differences between the Ti6Al4V and the Ti10.2.3 titanium alloy in different heat treated conditions are more apparent in the case of the specific feed force (K_k) than in the specific cutting force (K_c).

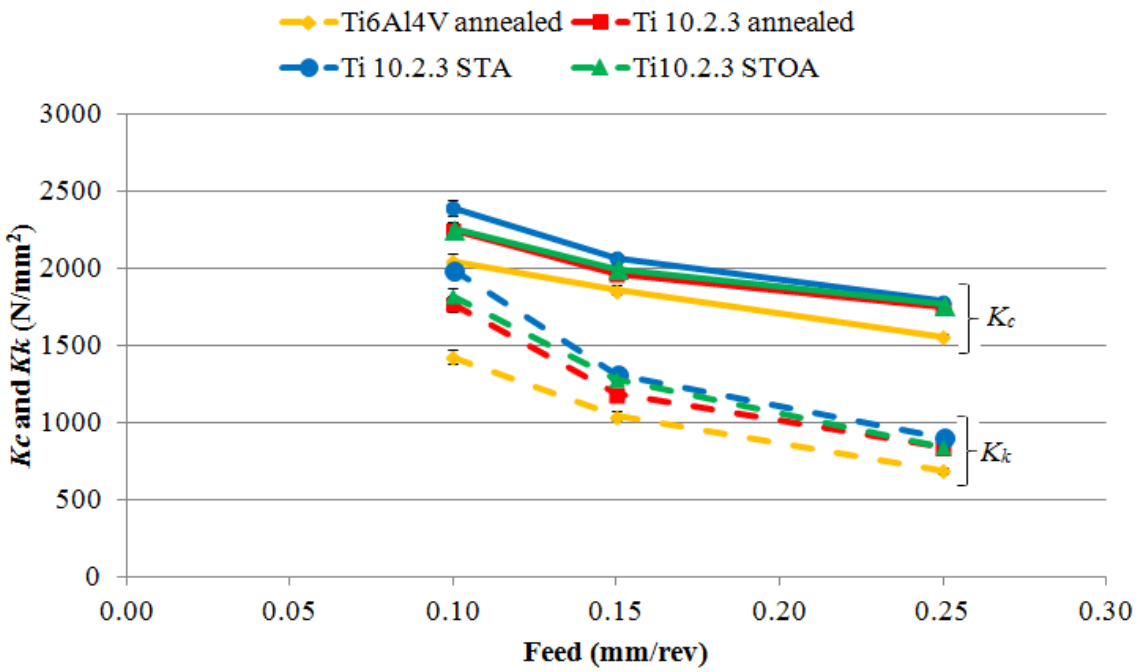

Figure 6.10. Specific cutting (K_c) and specific feed (K_k) forces for Ti10.2.3 and Ti6Al4V titanium alloys at cutting speed of 40 m/min

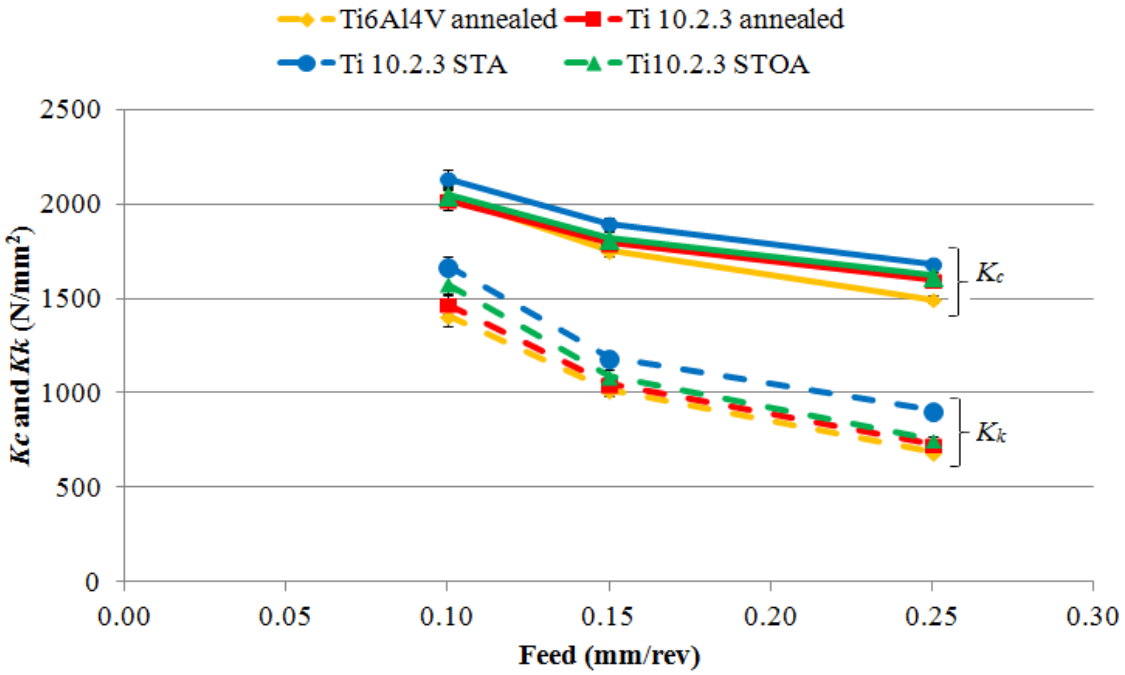

Figure 6.11. Specific cutting (K_c) and specific feed (K_k) forces for Ti10.2.3 and Ti6Al4V titanium alloys at cutting speed of 80 m/min

6.4.2. Cutting tool temperature

The influence of cutting parameters and heat treatment conditions on the cutting tool temperature is shown in figure 6.12 and figure 6.13. These values are the averages of three readings for each cutting condition. The uncertainty in thermal measurements is shown by the error bars.

A tendency of higher heat generation is depicted as the feed rate and cutting speed are increased (Figure 6.12 and Figure 6.13). At higher machining conditions; the cutting tool temperature reached above 1200^{o}C for the Ti10.2.3 STA alloy. The cutting tool temperature values of Ti10.2.3 STA alloy which have relatively higher hardness value are higher than those of lower hardness alloys (Figure 6.12 and Figure 6.13). Annealing and over aging heat treatments of Ti10.2.3 alloy resulted in lower hardness value and this, in turn reduced cutting tool temperature values when compared to Ti10.2.3 alloy in STA condition, at all cutting parameters.

At all cutting experiments, high temperature values were observed for the Ti10.2.3 STA alloy. A temperature difference of 270^{0}C was observed between Ti10.2.3 STA and Ti6Al4V alloys at higher cutting parameters. However, due to the uncertainty in thermal measurement system, no clear differences were observed between the temperatures generated in the machining of the Ti10.2.3 in annealed and Ti10.2.3 in STOA heat treatment conditions at all cutting speeds. As mentioned in the previous chapters these uncertainties were attributed to fluctuations around the mean emissivity, stray light from other sources, surface location fluctuations, and focus conditions due to the low modulus of elasticity of titanium alloys.

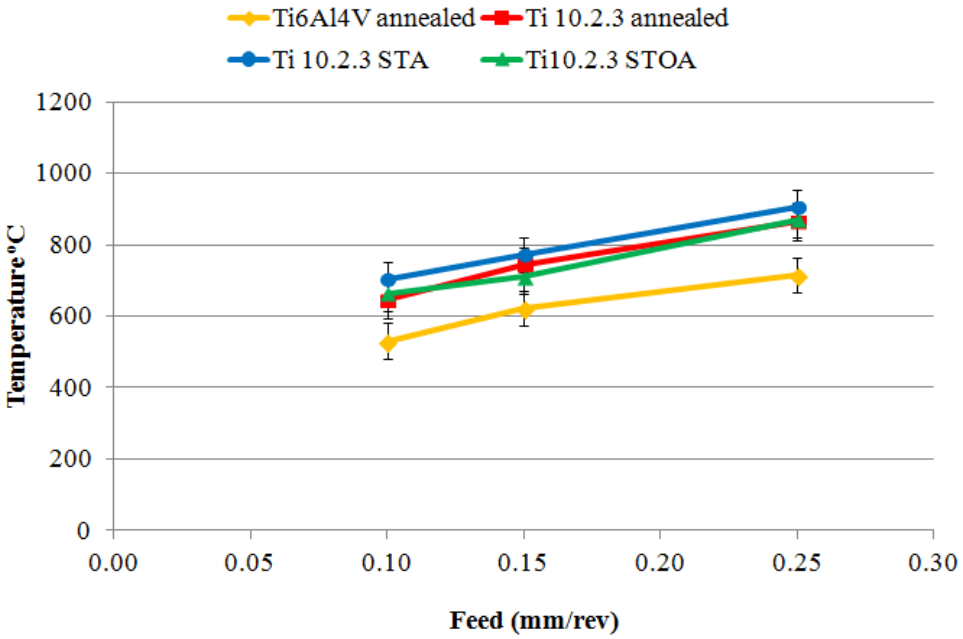

Figure 6.12. Cutting tool temperature graph for Ti10.2.3 and Ti6Al4V titanium alloys at cutting speed of 40 m/min

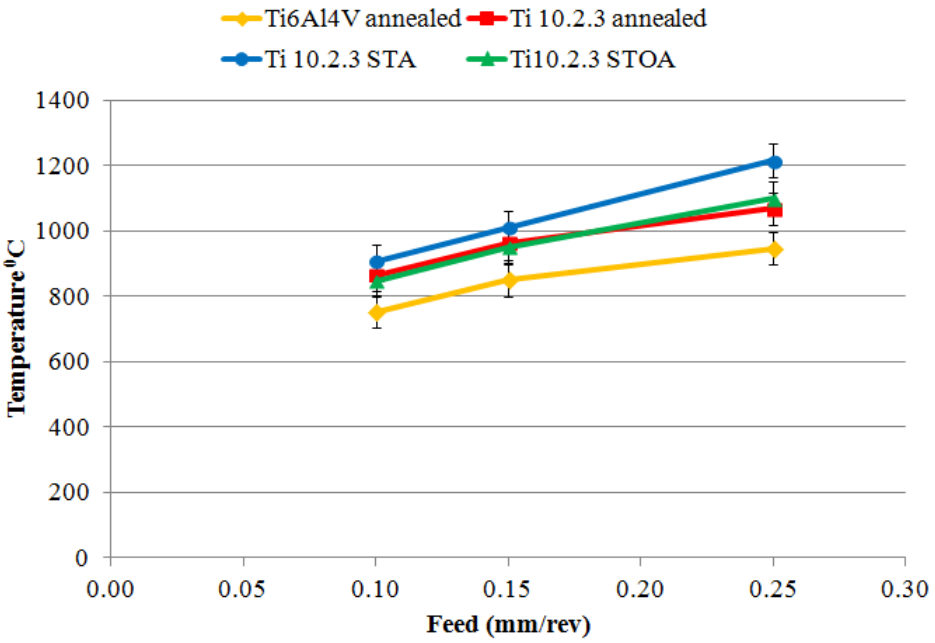

Figure 6.13. Cutting tool temperature graph for Ti10.2.3 and Ti6Al4V titanium alloys at cutting speed of 80 m/min

From aforementioned discussion it is clear that the effect of alloying with more β stabilizers and STA condition is to raise the cutting tool temperature and reduce the permissible machining parameters for any set of cutting conditions. The poor machinability of Ti10.2.3 in STA heat treated condition is due to the strengthening effect as a result of interference with the motion of dislocation due to the formation of secondary α precipitates (Terlinde et al., 1980). Over aging decreases the hardness of the alloy (Donachei, 2004). This might be due to coalescence of the precipitates into bigger particles which cause fewer impediments to the movement of dislocation.

6.5 Machinability Comparison of Ti54M and Ti10.2.3 Titanium Alloys

In this section, the effect of heat treatment on the machinability of α+β (Ti54M) and β (Ti10.2.3) titanium alloys is compared for the annealed and solution treated plus aged (STA) conditions. Ti10.2.3 alloy showed poorer machinability than Ti54M alloy in both the heat treated conditions due to the presence of higher content of β stabilizer elements (V and Fe).

6.5.1. Specific forces

The specific cutting (K_c) and specific feed (K_k) forces for both the analyzed titanium alloys in annealed heat treatment condition at cutting speeds of 40 m/min and 80 m/min are shown in figures 6.14 (a) and (b) respectively. The specific cutting (K_c) and specific feed (K_k) forces for both the analyzed titanium alloys in STA heat treatment condition at cutting speeds of 40 m/min and 80 m/min are shown in figures 6.15 (a) and (b) respectively. Results plotted for the specific forces represent the average values obtained from the three experimental tests at each cutting condition.

An examination of the specific forces with respect to the feed rate revealed a number of general trends. During dry machining, from the lowest feed rates the forces tended to decrease rapidly up to the feed rate of 0.15 mm/rev, after which the forces tends to decrease slightly with further increase in feed rate. The reduction in specific forces with increasing feed rate is a well observed phenomenon and is believed to occur because of the size effects of the cutting edges.

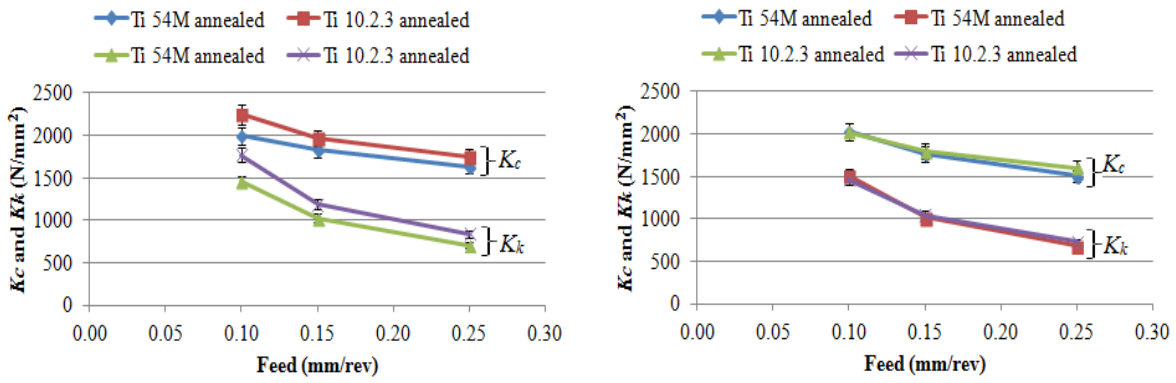

(a) **(b)**

Figure 6.14. Specific forces K_c and K_k for Ti54M and Ti10.2.3 titanium alloys at cutting speed of (a) 40 m/min and of (b) 80 m/min

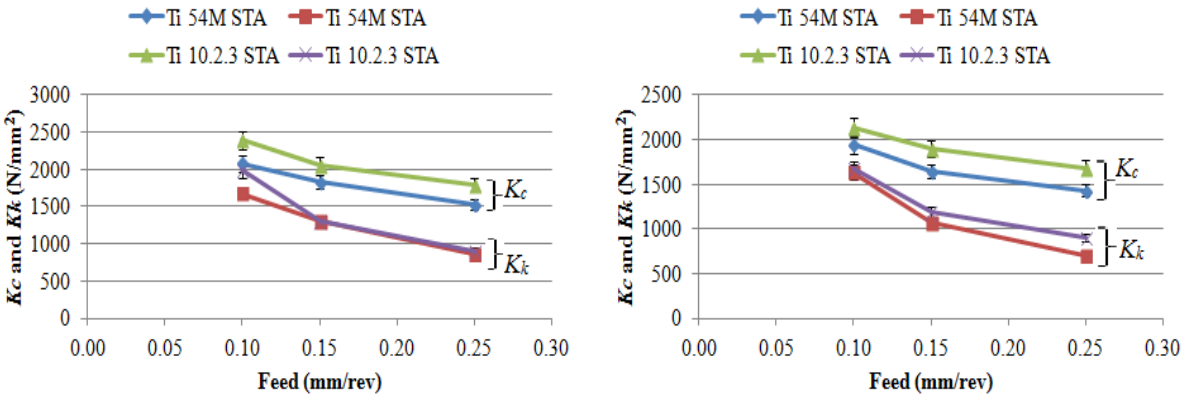

(a) **(b)**

Figure 6.15. Specific forces K_c and K_k for Ti54M and Ti10.2.3 titanium alloys at cutting speed of (a) 40 m/min and of (b) 80 m/min

It is observed that specific cutting force (K_c) values are dependent on the alloy composition and heat treatment conditions as observed in previous section. The lower values are obtained for the alloy Ti54M and the higher values are obtained for the Ti10.2.3 alloy. As expected, higher specific forces were observed for the Ti10.2.3 alloy than the Ti54M alloy at all cutting parameters and heat treated conditions except in annealed heat treatment condition where Ti54M alloy showed higher specific force values than Ti10.2.3 alloy at certain cutting parameter values. For instance, at the cutting speed (V_c) of 80 m/min and feed rate (f) of 0.1 mm/rev, the specific cutting force (K_c) is 2028 N/mm^2 in the case of the Ti54M in annealed condition and 2021 N/mm^2 for the Ti10.2.3 in annealed condition. The specific feed force (K_k) value is 1509 N/mm^2 in the case of the Ti54M in annealed condition and 1469 N/mm^2 for the Ti10.2.3 annealed at same cutting speed. The effect of heat treatment on the Ti54M and the metastable β Ti10.2.3 titanium alloy is more evident in the case of the specific feed force (K_k) than in the specific cutting force (K_c).

A drop in specific forces was observed with increase in cutting speed from 40 m/min to 80 m/min for all the analyzed alloys. This is because of the thermal softening effect. This drop in force is significant in the cutting as well as feed directions. This observation gives an indication of strong thermal softening effect within the tested cutting speed range. The exception is for Ti54M alloy in annealed condition at feed of 0.1 mm/rev because of dominance of strain hardening effect over thermal softening effect. Ti10.2.3 alloy in STA heat treatment condition seems too strong to give-in to thermal softening at higher feed rates.

6.5.2. Cutting tool temperature analysis

The temperature data plotted in figure 6.16 (a) and (b) shows a clear increase in cutting tool temperature with cutting speed for the machined materials. Higher temperature values were found during machining of Ti10.2.3 alloy than Ti54M alloy. However, at cutting speed of 80 m/min and at feed rates of 0.1 mm/rev and 0.15 mm/rev the temperatures observed were higher for Ti54M. This distinction coincides well with a recognizable difference in the specific feed force (Figure 6.14 (b)).

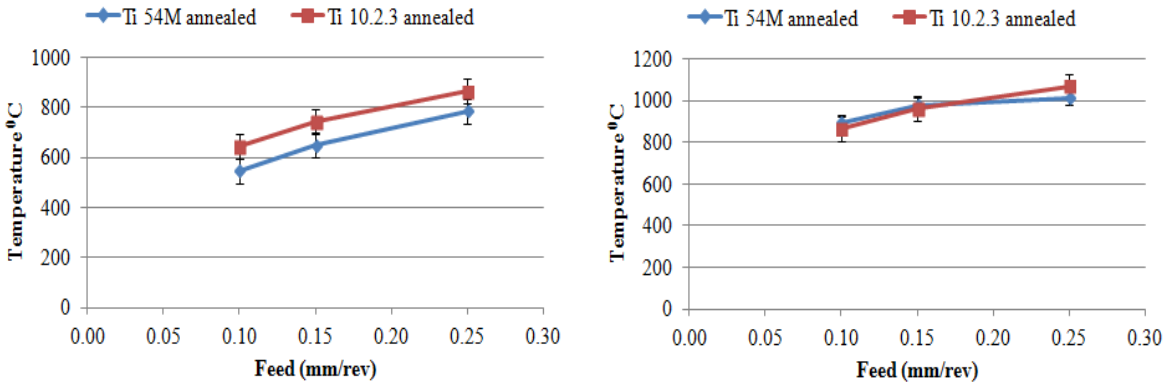

(a) **(b)**

Figure 6.16. Cutting tool temperature for Ti54M and Ti10.2.3 titanium alloys at cutting speed of (a) 40 m/min and of (b) 80 m/min

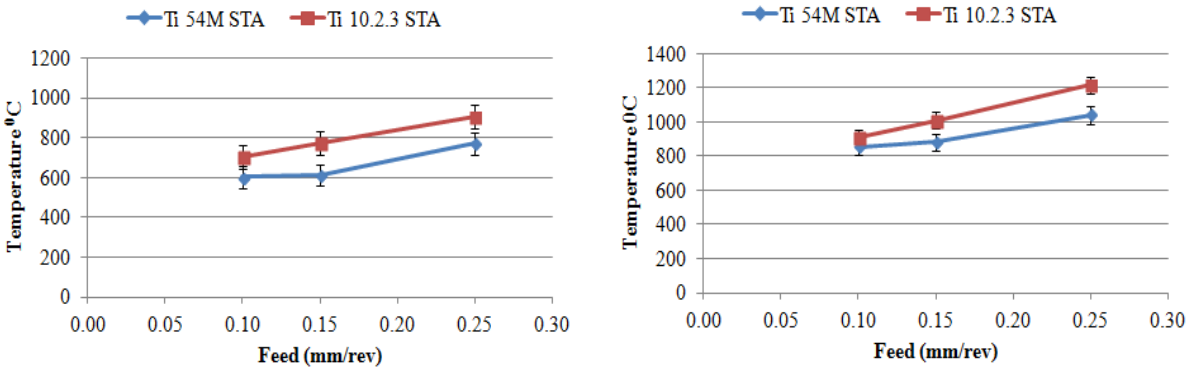

(a) **(b)**

Figure 6.17. Cutting tool temperature for Ti54M and Ti10.2.3 titanium alloys at cutting speed of (a) 40 m/min and of (b) 80 m/min

The cutting tool temperature values of Ti10.2.3 STA alloy which have relatively higher hardness values are higher than Ti54M alloy in STA condition (Figure 6.17 (a) and (b)). Therefore, high tool wear is expected in the Ti10.2.3 STA alloy as compared with Ti54M alloy in STA conditions because of friction and rubbing effects over the rake surface leading to high heat generation at the tool chip contact zone (Arrazola et al., 2005).

It is observed that the cutting tool temperature is more sensitive to change in cutting speed than feed rate. From aforementioned discussion it is clear that the effect of alloying with more β stabilizers and STA condition is to raise the cutting tool temperature for any set of cutting conditions, and, therefore, reduces the permissible machining parameters i.e. machinability.

6.6 Machinability Comparison of Ti10.2.3, Ti54M and Ti6Al4V Titanium Alloys

In this section, machinability of the heat treated α+β (Ti6Al4V and Ti54M) and metastable β (Ti10.2.3) titanium alloys is compared for the experimental results obtained in the previous chapters. The idea is to provide visual glimpses of results at one place. It is already clear that the titanium alloys with STA heat treatment condition are having least machinability, therefore, alloys in STA heat treatment conditions are excluded from this comparison. The comparison in term of specific forces and cutting tool temperature is given next.

6.6.1. Specific cutting and feed forces

The results of specific cutting (K_c) and specific feed (K_k) forces for all the analyzed titanium alloys at two cutting speeds (40 m/min and 80 m/min) are shown in figures 6.18 (a) and (b), respectively at feed rates of 0.1 mm/rev. 0.15 mm/rev and 0.25 mm/rev. Results plotted for

the specific forces represent the mean values observed from the experimental tests at each cutting condition.

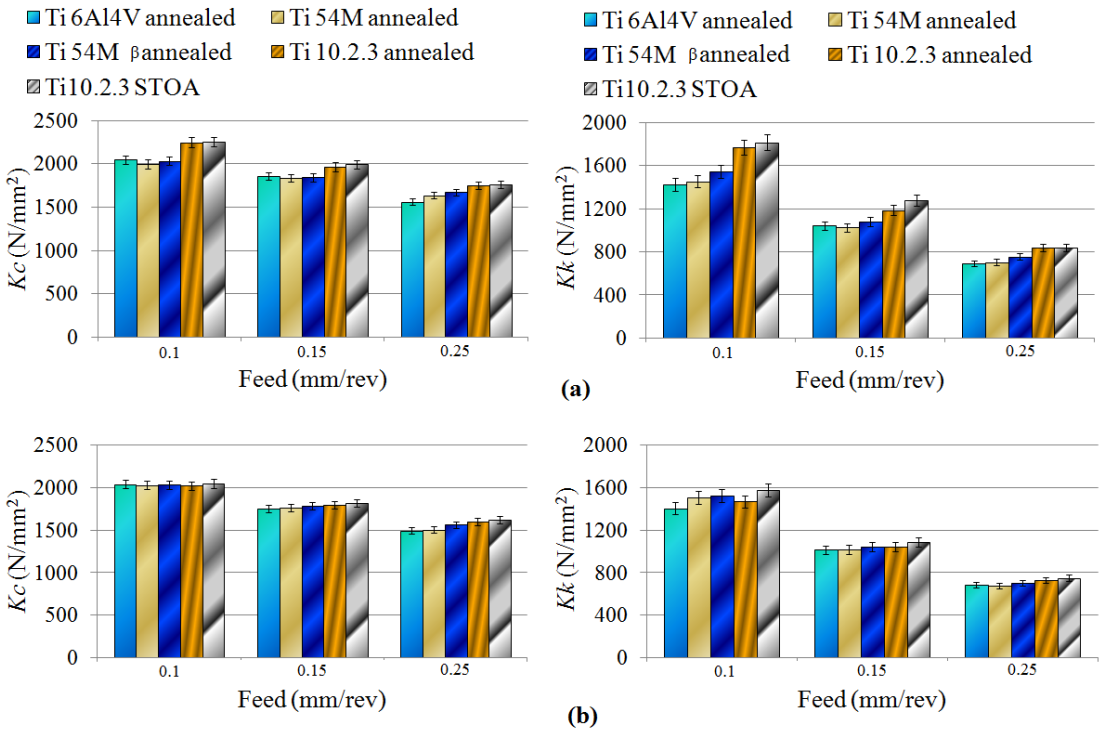

Figure 6.18. Specific cutting and feed forces at cutting speed of (a) 40 m/min and of (b) 80 m/min for different titanium alloys

The highest specific cutting forces were noticed for Ti10.2.3 STOA at all cutting parameters. The force components experience fall in magnitude from 40 m/min to 80 m/min at higher feed rates. This observation gives a hint of occurrence of thermal softening effect at the selected cutting speeds. Furthermore, no built-up-edge was experienced for any experimental run on any material. The specific feed force values correlated well with the mechanical properties of the alloys, as higher values were obtained for the Ti10.2.3 alloy. Thus, the differences between the α+β and the metastable β titanium alloys in different heat treated conditions are comparatively more apparent in the case of the specific feed force than in the specific cutting force.

6.6.2. Cutting tool temperature analysis

The influence of cutting parameters along with heat treatment conditions on the cutting tool temperature is shown in figures 6.19 (a) and (b).

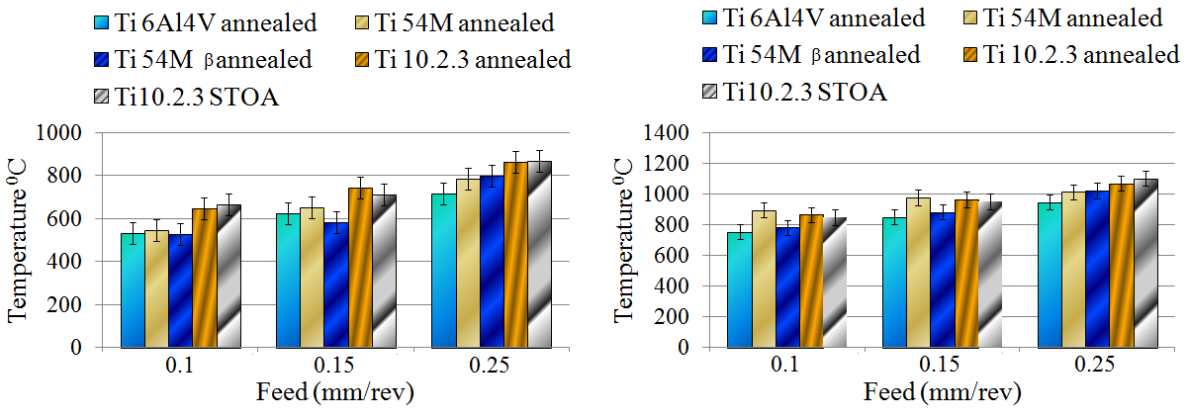

Figure 6.19. Cutting tool temperature at cutting speed of (a) 40 m/min and of (b) 80 m/min for different titanium alloys

As expected, cutting temperatures are considerably higher in the machining of Ti10.2.3 than in machining of Ti54M and Ti6Al4V titanium alloy. Due to the thin chip and short contact length typical of the machining of titanium alloys (Dearnley and Grearson, 1986) the high temperatures are concentrated in a small area near to the tool edge. The cutting tool temperature values of both the Ti10.2.3 alloys, having relatively higher strength values, are higher than α+β alloys (Figure 6.19 (a)). Therefore, high tool wear are expected in the Ti10.2.3 alloys as compared with α+β titanium alloys. The cutting tool temperature observed at cutting speed of 80 m/min does not provide clear differences among different alloys at different feed rates (Figure 6.19 (b)). This distinction does not coincide well with an identifiable difference in the specific feed forces (Figure 6.18 (b)). However, this might be due to the uncertainty in thermal measurement method. As mentioned, these uncertainties

were attributed to fluctuations around the mean emissivity, stray light from other sources, surface location fluctuations, and focus conditions due to the low modulus of elasticity of titanium alloys. This work reconfirmed the influence of heat treatment and chemical composition on the machinability of the analyzed alloys.

6.7. Conclusions

The experimental studies carried out on Ti6Al4V titanium alloy in as-received annealed conditions show that there is not much effect of the increase of cutting speed on thermal softening. The ANOVA results have shown that feed rate experimental results of Ti6Al4V are statistically significant in term of specific forces and cutting tool temperature. The effect of cutting speed is statistically significant for specific cutting force and cutting tool temperature. Feed rate has been found to have more significance than the cutting speed for specific cutting and feed forces. Cutting speed has been found to be more significant for cutting tool temperature.

The comparison of titanium alloys in different heat treated conditions shows that Ti10.2.3 has poor machinability than Ti54M and Ti6Al4V alloys. This is due to the chemical composition of this alloy. Ti54M alloy in annealed condition has better machinability than Ti6Al4V alloy in term of chip morphology at lower feed rates. The differences among all the seven analyzed titanium alloys in different heat treated conditions are more apparent in the case of the specific feed force than the specific cutting force. There is a significant influence of chemical composition and the metallurgical state, and the modification of the heat treatment plan can improve the machinability of the titanium alloys.

Chapter 7

Interrupted Machining Studies on Ti6Al4V and Ti5553 Titanium Alloys Using Physical Vapour Deposition (PVD) Coated Carbide Tools

7.1. Introduction

Interrupted cutting is widely used in machine tool manufacturing industry. Recently, interrupted cutting of die and mould steel has been widely used to generate high-quality and intricate sculptured surfaces. Because of the intermittent nature of interrupted cutting, tool wear is usually more severe and the cutting mechanism is different from continuous cutting. While the application of interrupted cutting has increased, there is relatively little research effort on interrupted cutting of titanium alloys (Wang et al., 2009). Machining process variables like, tool geometry (cutting edge radius and rake angle) and cutting parameters (feed rate, cutting speed and depth of cut) have significant influence on the cutting performance while machining titanium alloys.

Cutting tool manufacturers pay particular attention to tool geometry (Saoubi and Chandrasekaran, 2004). The design of tool cutting edge and its effect on machining performance are given more consideration by the researchers (Bouzakis et al., 2000; Wyen and Wegener, 2010). Cutting edge radius is one of the important variables in predicting the machining behaviour. The machining performance of titanium alloys can be enhanced by using rounded cutting edge tools. Although some experimental investigations have been

conducted to quantify the best cutting edge preparation, very few studies have tried to explain the influence of cutting edge preparation on coated tools during interrupted cutting (Bouzakis et al., 1998; Bradbury and Huyanan, 2000; Derrico et al., 1998). Vargas Pérez (2005) found that abrasion, adhesion, and fatigue as wear mechanisms of the tungsten carbide inserts during face milling of γ -TiAl alloy. Jawaid et al. (2000) have investigated the performance and wear mechanisms of coated carbide tools during face milling of Ti6Al4V and found that CVD coated tools have better performance than PVD coated tool. Zhang et al. (2010) found that wear mechanisms of PVD-coated (TiN + TiAlN) tools during face milling of TC18 alloy were mainly adhesion, diffusion and crater wear, and the main failure mode of uncoated carbide tool was tipping. Niu et al. (2012) indicated that during face milling TA19 alloy, PVD-coated (TiN + TiAlN) inserts had more advantages than other carbide inserts. Thermal cycling is considered to be the one of the reasons for tool wear and coating delamination during interrupted cutting. Bouzakis et al. (2002) checked the cutting performance of PVD coated cemented carbide inserts with cutting edge radii of 13 µm, 18 µm, 23 µm and 28 µm during milling. Physical Vapour Deposition (PVD) has been preferred among several deposition techniques because thinner coatings can be deposited, and sharp edges and complex shapes can be easily coated at lower temperatures (Bouzakis et al., 2009).

The key cutting tool characteristics during interrupted machining are toughness, oxidation resistance and compressive residual stresses in the tool material. In order to avoid negative influences on substrate properties associated with high coating-process temperatures, PVD coatings are used very frequently (Wertheim, 1998). Titanium nitride (TiN) was the first commercial PVD coating and since then majority of the industrial coatings has been based

on nitrides (Wang, 1992). The evolution of TiAlN, by adding aluminum to the TiN base composition, offered not only a higher hardness, but also an extraordinary improvement of high temperature strength. Oxidation and hardness heat resistance up to approximately 900 °C, contributed to essential cutting conditions improvement (Bouzakis et al., 2012). The first generation PVD coating on carbide used TiN hard coatings and was used in the milling operation of steel (interrupted cutting condition). Following their success in milling applications, their use was extended to other machining operations like threading, grooving, boring, turning and parting. The second and third generation of PVD coatings utilized TiCN and TiAlN that have further boosted productivity (Jindal et al., 1999). Instead of single homogeneous coatings of TiN, TiCN and TiAlN, a new class of coating that have multiple layers of coating material deposited on a carbide substrate have shown better tribological and mechanical properties. The thin films of material are alternatively deposited on a micro or nano-thickness scale and have the same total thickness as a single layer (Ducros et al., 2003). The high potential to increase the cutting performance of coated tools demands the optimization of a variety of tool parameters (Klocke, 1999; Toenshoff et al., 2001). One of the important parameters is cutting edge roundness (Bouzakis et al., 2000). This fact is a motivation to further investigate the effect of the cutting edge radius on the machining performance of titanium alloys during interrupted cutting.

Another significant cutting parameter, which determines the tool/chip contact area, is rake angle. A positive rake edge is recommended for finishing and semi-finishing operations. Positive rake geometry reduces work hardening of the machined surface by shearing the chip away from the workpiece in an efficient way besides minimizing built-up-edge (Ezugwu, 2004). Increasing rake angle from small values up to certain optimum value

causes reduction in tool/chip contact length, and, therefore, forces and temperature are likely to be reduced (Saglam et al., 2007). In recent research work on machining of titanium alloys, Ozel and Sima (2010); Bermingham et al. (2011); Cotterell and Byrne (2010); Arrazola et al. (2009); Sun et al. (2009); Machai and Biermann (2011) used 0^0, 6°, 6.5°, 7°, 15°, 15° rake angle carbide tools respectively. Wagner et al. (2011) worked on optimizing the edge preparation and rake angle of coated carbide tools for machining of the Ti5553 alloy. A tool with sharp edge having a rake angle of 20° and a feed value more than edge preparation was found to be the best choice.

In this chapter, the effects of multi-layered PVD coated (TiAlN-TiN) cemented carbide inserts with selected edge preparations (cutting edge radius) and rake angles on cutting forces and cutting tool temperature at different cutting parameters have been studied. These inserts are having higher hardness, higher abrasive resistance and are suited for dry machining applications (Niu et al., 2013). Results of this study would be helpful for the tool manufacturers in designing novel geometries for coated cutting tools used to machine wide range of α+β and β titanium alloys.

7.2. Workpiece Materials

Ti6Al4V has been studied extensively because of its high strength, low density and good corrosion resistance. As mentioned earlier, it accounts for more than 50% of the titanium alloy production. Industry has started taking interest in Ti5553, a metastable β titanium alloy. This alloy is a derivative of Russian VT22 and later VT22-1 titanium alloys. It has been reported by Baili et al. (2011) that Messier–Dowty uses the Ti5553 beta titanium alloy for landing gear applications. More recent work at Boeing has focused on the development

of Ti5553, a high-strength alloy that can be used at higher strength than Ti10.2.3 and is much more robust. It has a much wider or friendlier processing window (Boyer and Briggs, 2005). Ti5553 alloy is appreciably more difficult to cut than Ti6Al4V alloy because of phase compositions (Arrazola et al., 2009; Fanning, 2005; Boyer and Briggs, 2005). It has been found from the literature that there is a limited research on interrupted machining of Ti6Al4V and Ti5553 alloys using the PVD coated tools.

Table 7.1 shows categorization of the analyzed alloys. High mechanical properties of Ti5553 titanium alloy as compared with the mill annealed Ti6Al4V alloy can be observed from the table 7.1. The higher concentration of β stabilizers (Mo and V) is present in Ti5553 alloy as compared to the Ti6Al4V alloy. This resulted in approximately seven times higher value of molybdenum equivalent value in Ti5553 alloy than that of the Ti6Al4V alloy leading to higher mechanical properties of this near β titanium alloy compared with the traditional Ti6Al4V alloy (Arrazola et al., 2009).

Table 7.3. Chemical composition and mechanical properties of Ti6Al4V and Ti5553 titanium alloys used for interrupted cutting

Titanium Alloy	Chemical Composition (%)				Al Equiv. Value (wt. %)	Mo Equiv. Value (wt. %)	TYS (MPa)	UTS (MPa)	Elongation (%)	Hardness (HV)
	Al	Mo	V	Cr						
Ti6Al4V (α+β)	6	-	4	-	6	2.7	931	1014	14	351
Ti5553 (β)	5	5	5	3	5	17.3	1170	1290	6	417

7.3. Experimental Methodology

Orthogonal dry interrupted machining was carried out on the LAGUN vertical CNC machining centre (Figure 3.1). Orthogonal tests of 5 second duration were conducted. Tests

were conducted on Ti6Al4V using three different cutting edge radii (15 µm, 30 µm and 60 µm), three different rake angles (0^0, 15^0, 30^0), two feed rates (0.1 mm/rev and 0.15 mm/rev), and fixed cutting speed of 40 m/min. Further experiments were carried out to compare Ti6Al4V and Ti5553 interrupted machining performance at two feed rates (0.1 mm/rev and 0.15 mm/rev) keeping cutting edge radius and rake angle at constant value of 15 µm and 0^0 respectively. The cutting speeds for Ti6Al4V were taken as 40 m/min and 70 m/min while the cutting speed for Ti5553 were taken as 25 m/min and 40 m/min. The cutting parameters were chosen after considering the cutting tool manufacturer's recommendations. It is worthwhile to mention that the commercial availability of these coated inserts is also limited and cutting tool manufacturer (SECO Tools) provided limited inserts (PVD coated (TiAlN-TiN) cemented carbide inserts ISO TPUN160308 F40M) to carry out research for the company at these parameters. To perform the interrupted machining, the specially prepared workpieces were used as shown in figure 3.3. All the alloys were machined keeping a 1 mm depth of cut.

7.4. Results and Discussion

7.4.1. Effect of cutting tool edge radius during interrupted machining of Ti6Al4V alloy

The measured forces (cutting and feed) at different cutting edge radii are shown in figure 7.1(a). High values of cutting forces are observed at large edge radius of 60 µm. The tool with large cutting edge radii needs higher forces for material shearing as observed by Yen et al. (2004) during machining of 0.2% plain carbon steel. The change in cutting force is almost negligible for the change in cutting edge radius from 15 µm to 30 µm. The results of feed force with respect to the change in cutting edge radius are not consistent for the two

feed rates. The feed forces for 15 µm and 60 µm are little more for higher feed rate but for 30 µm the value of feed force is higher for lower feed rate. The cutting edge radius seems to have more effect on feed forces than cutting forces. As the cutting edge radius increases from 15 µm to 60 µm, the increase in feed force and cutting force are about 100% and 13% respectively.

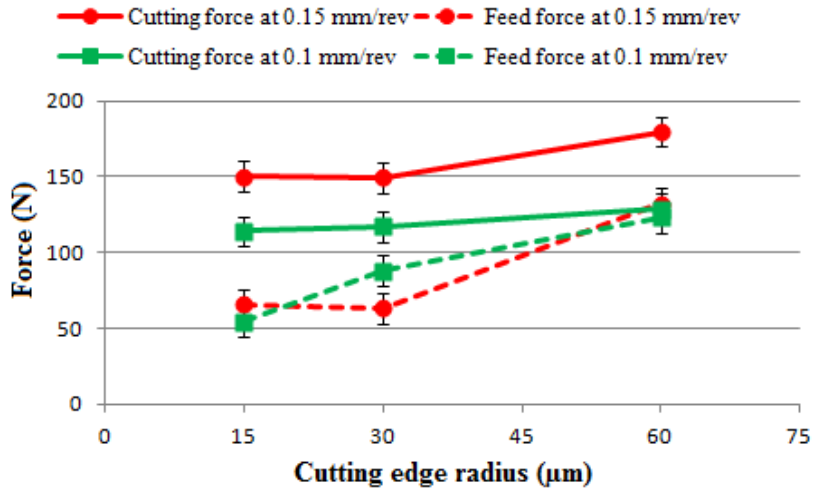

(a)

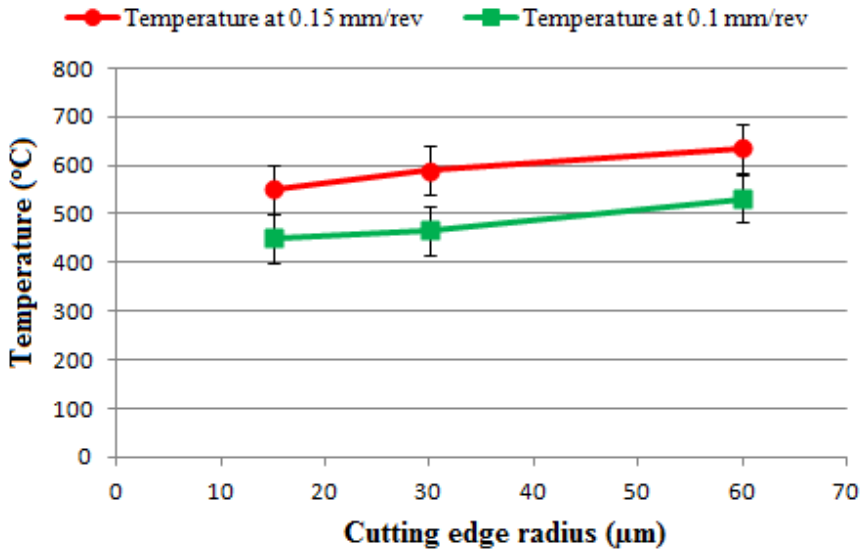

(b)

Figure 7.1. Cutting edge radius effect on (a) cutting and feed forces and (b) cutting tool temperature for Ti6Al4V titanium alloys at cutting speed of 40 m/min and 0^0 rake angle

Similar trends were reported by Wyen and Wegener (2010) in the uninterrupted cutting of the Ti6Al4V alloy using tungsten carbide tools with different cutting edge radii (10 µm, 20 µm, 30 µm, 40 µm, and 50 µm) at cutting speed of 70 m/min. From figure 7.1(a), it is observed that by increasing the value of edge radius by 4 times (15 µm – 60 µm), the feed force value gets doubled irrespective of the feed rate.

When machining titanium alloys, high heat is concentrated at very short distance from cutting tool tip (Ezugwu and Wang, 1997). The cutting tool temperature increases almost linearly with increasing cutting edge radius as shown in figure 7.1(b). Moreover, the temperature increases with the increase in feed rate. Increase in cutting edge radius from 15 µm to 60 µm induces an approximate 80°C increase of the cutting tool temperature on the rake face. This is due to the increased deformation near tool/chip boundary (Yen et al., 2004). Energy required for this deformation is more in case of higher cutting edge radius values (Wyen and Wegener, 2010).

7.4.2. Effect of tool rake angle during interrupted machining of Ti6Al4V alloy

Cutting and feed forces decrease with the increase in cutting tool rake angle as shown in figure 7.2(a). Decrease in tool/chip contact area is the main cause of this behaviour. The cutting forces are higher for higher feed rate. The rake angle seems to have more effect on feed forces than cutting forces. As the rake angle increases from 0^0 to 30^0, there is 87% decrease in feed force and 33% in cutting force at 0.15 mm/rev. Similar trend has been observed at the feed rate of 0.1 mm/rev. However, the change in feed forces for change in feed rate is not much pronounced and, in fact, the feed forces at 15 degree and 30 degree rake angles are lower for higher feed rates.

The cutting tool temperature decreases with the increase in rake angle as shown in figure 7.2(b). The increase in rake angle in positive direction decreases the tool/chip contact length. It causes a decrease in cutting tool temperature due to reduction in area available for friction. The extent of temperature reduction is not much evident with the increasing rake angle from 0^0 to 30^0, particularly for lower feed rate of 0.1 mm/rev. However, there is need to find the optimum value of rake angle for the machining of titanium alloys with different cutting conditions as higher rake angles decrease the cutting tool strength and accelerates its wear.

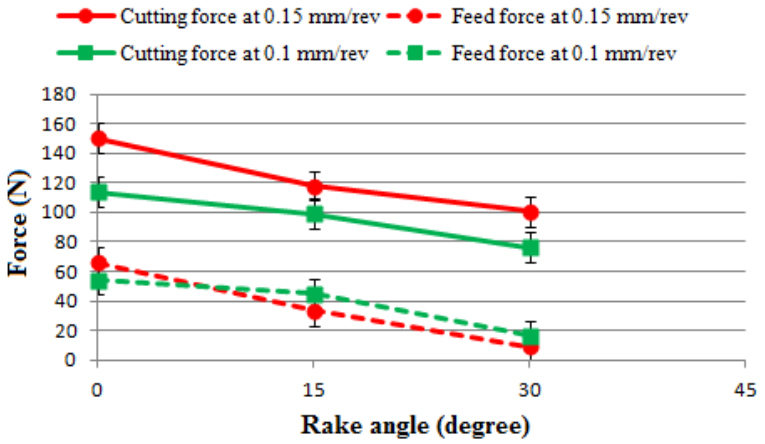

(a)

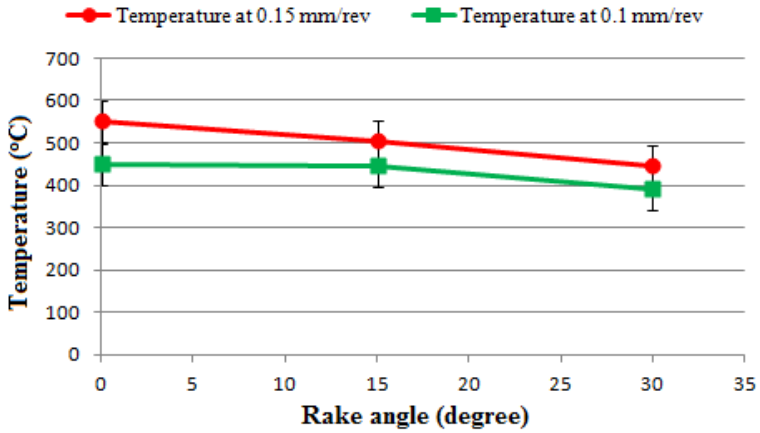

(b)

Figure 7.2. Rake angle effect on (a) cutting and feed forces and (b) cutting tool temperature for Ti6Al4V titanium alloys at cutting speed of 40 m/min and 15 µm edge radius

7.4.3 Feed rate effect on Ti6Al4V and Ti5553 alloys during interrupted machining

It can be observed from figure 7.3(a) that cutting and feed forces increase with increasing feed rate. It is because there is more material to remove due to increase in cutting area. Figure 7.3(a) shows that the force values associated perfectly with the mechanical properties which depend on the microstructure. Higher values of forces are found for Ti5553 as compared to the Ti6Al4V alloy because of its higher Mo equivalent value as mentioned earlier. The cutting force changes with the change in cutting speed are not much pronounced for Ti6Al4V alloy. The feed forces are higher at higher cutting speeds for Ti6Al4V alloy.

An increase in temperature with increasing feed rate has been observed (Figure 7.3(b)) because a large volume of material gets removed at higher feed rates. This shows a considerable influence of feed rate on cutting tool temperature. Similar results have been reported in past research works also (Korkut et al., 2007; Li and Liang, 2006). Ti5553 alloy shows higher temperature at 25 m/min cutting speed as compared with Ti6Al4V at 40 m/min cutting speed because of its high hardness and strength acquired due to the higher concentration of β stabilizers. It promotes wear and tear of the cutting tool material.

Another important observation to differentiate Ti6Al4V and Ti5553 machining is in term of deviations observed during on-line monitoring of the cutting forces for these two alloys as shown in figure 7.4. It is observed that the Ti6Al4V alloy at 40 m/min shows less fluctuation in the cutting forces as compared to the Ti5553 alloy at 25 m/min. This is because frequency of formation of the adiabatic shear bands is much higher for Ti5553 than for Ti6Al4V alloy (Arrazola et al., 2009). The significant fluctuations in the cutting forces observed while machining Ti5553 alloy in comparison to Ti6Al4V are due to the creation of adiabatic shear

bands at higher rate (Arrazola et al., 2009). The high dynamic loads resulting due to the higher segmentation frequency for Ti5553 appear to be consistent with the poor machining performance observed for this material when compared to Ti6Al4V.

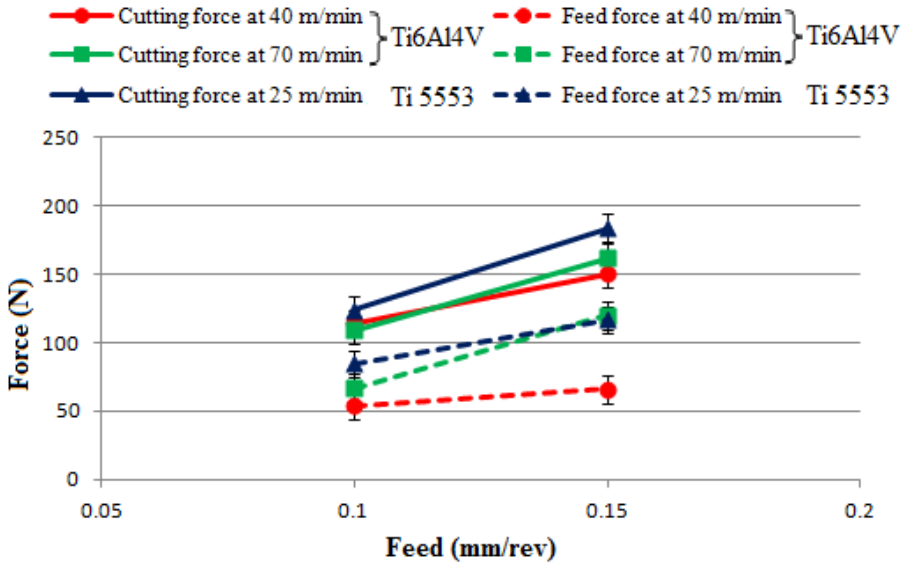

(a)

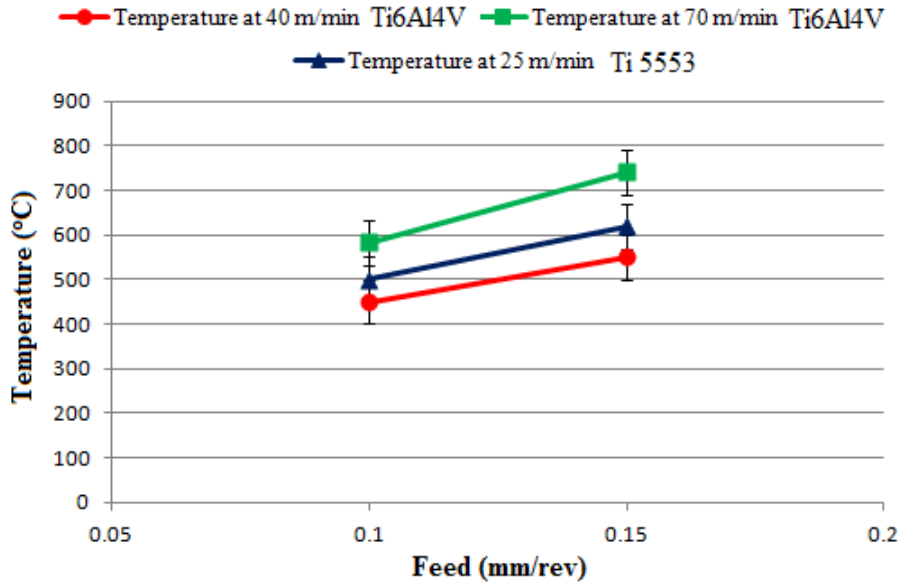

(b)

Figure 7.3. Feed rate effect on (a) cutting and feed forces, and (b) cutting tool temperature for Ti6Al4V and Ti5553 titanium alloys at 15µm cutting edge radius and 0^0 rake angle

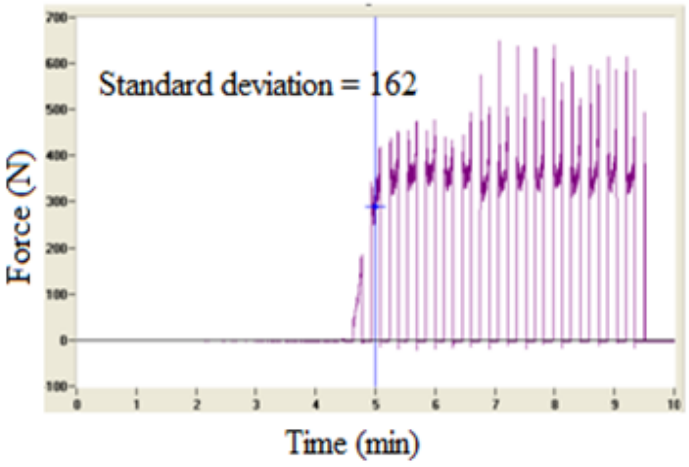

(a)

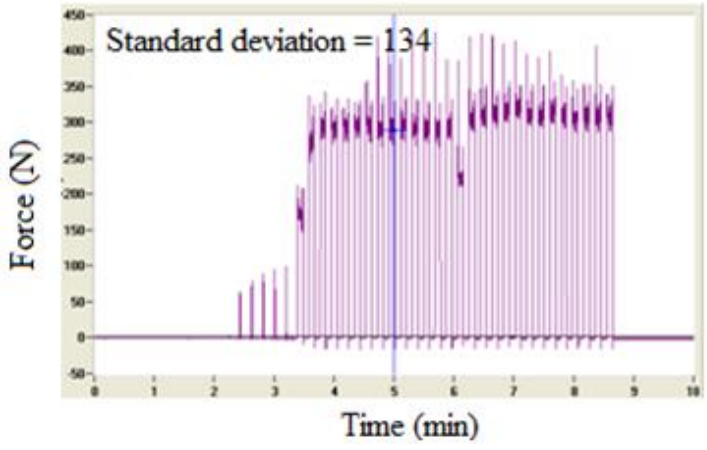

(b)

Figure 7.4. Variation in cutting forces with time at same feed rate of 0.15 mm/rev (a) for Ti5553 at cutting speed of 25 m/min and (b) for Ti6Al4V at cutting speed of 40m/min

7.4.4. Cutting speed effect on cutting tool temperature during interrupted machining of Ti6Al4V and Ti5553 alloys

Figure 7.5 shows the cutting tool temperature at different cutting parameters. The cutting tool temperature for Ti6Al4V significantly increases from 551^0C at 40 m/min cutting speed to 741^0C at 70 m/min at high feed rates. The large increase is attributed to the poor heat conductivity of these alloys.

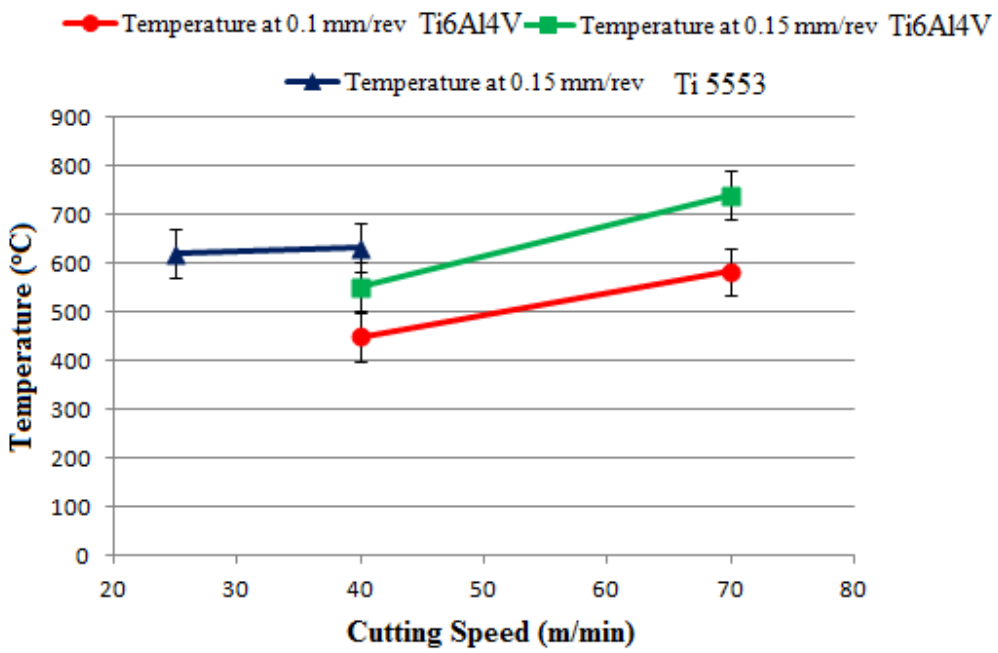

Figure 7.5. Cutting speed effect on temperature for Ti6Al4V and Ti5553 titanium alloys at cutting edge radius of 15 µm and 0^0 rake angle

Higher temperature values are observed (Figure 7.5) during the machining of Ti5553 alloy as compared with Ti6Al4V alloy. An increase in the temperature can be perfectly correlated with increasing feed rate. It is clear from figure 7.3(b) that as feed value increases from 0.1 mm/rev to 0.15 mm/rev temperature increases from 501^0C to 620^0C for Ti5553 alloy. In contrast, figure 7.5 shows that as cutting speed increases from 25 m/min to 40 m/min, temperature rises from 620^0C to 633^0C. This indicates that the feed rate impacts cutting tool temperature and has dominance over the cutting speed. Moreover, for Ti5553 at cutting speed value of 25 m/min and feed value of 0.15 mm/rev, cutting tool temperature is higher (620^0C) than obtained for Ti6Al4V (583^0C) at cutting speed value of 40 m/min and feed value of 0.15 mm/rev (Figure 7.6). Higher heat generation is observed in secondary shear zone during machining Ti5553 as compared to Ti6Al4V (Figure 7.6) which further increases

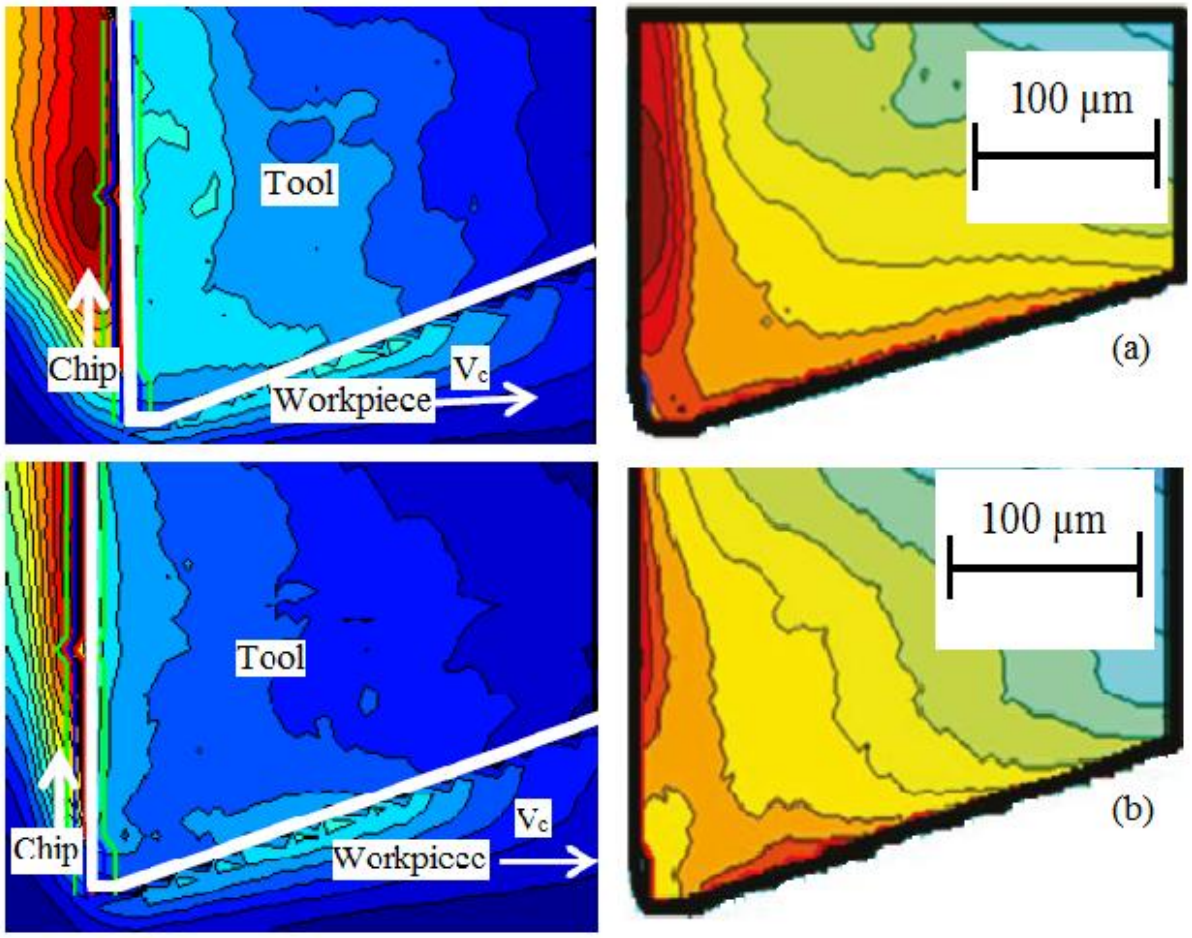

Figure 7.6. Thermal maps at feed rate of 0.15mm/rev for (a) Ti5553 alloy at 25 m/min cutting speed and (b) Ti6Al4V alloy at 40 m/min cutting speed

the temperature of the cutting tool (Ugartea et al., 2012). This higher tool temperature during machining of Ti5553 is the consequence of its high mechanical properties.

7.5. Conclusions

The interrupted machining analysis of Ti6Al4V and Ti5553 titanium alloys using PVD coated cemented carbide inserts shows the poor machinability of Ti5553 as compared to the Ti6Al4V; as higher forces and temperature are observed in the machining of Ti5553 alloy as compared to Ti6Al4V alloy; due to its high mechanical properties which further depends on

the microstructure. The online monitoring of the forces has shown higher fluctuations during machining of Ti5553 alloys even at the lower cutting speeds as compared to Ti6Al4V alloy.

It has also been found that the cutting and feed forces, and cutting tool temperature increase with increase in cutting edge radius and decrease with increase in rake angle. It is observed that the feed forces are more sensitive to variation in tool geometry and feed rates than the cutting forces. There is a significant influence of the cutting edge preparation and rake angle on the machining performance of PVD coated inserts and the modification of the insert geometry can improve the machinability of the titanium alloys.

Chapter 8
Conclusions

Planned heat treatment is a promising technique for improving the mechanical properties as well as the machinability of the different titanium alloys. In the present study, experimental studies are carried out to analyze the effect of heat treatment conditions on the machinability of the increasingly used titanium alloys. The effects of tool geometry and edge preparation of PVD coated cemented carbide tools on the machining performance of titanium alloys (Ti6Al4V and Ti5553) are also presented. Titanium alloys from different (α+β and β) groups with different heat treatments are used. This data will be useful to increase the productivity and to reduce machining costs for machining titanium alloys.

The experimental studies carried out on Ti54M titanium alloy in as-received annealed, β annealed and STA conditions show that the chip morphology differs considerably with the different heat treated conditions of the Ti54M titanium alloy. There are clear indications that the machinability of Ti54M in annealed condition is better than that of β annealed and STA conditions. This distinction coincides well with the recognizable differences observed in the specific feed force and friction coefficient. However, the experimental results in term of cutting tool temperature and specific cutting force show irregular trends in machinability for the three heat treated conditions at different cutting speeds and feed rates. More experiments need to be carried out at different cutting speeds and feed rates to get clear trends in term of cutting tool temperature and specific cutting force. The ANOVA results have shown that most of the experimental results are statistically significant in term of feed rate and cutting

speed variations. Feed rate has been found to have more significance than the cutting speed for specific cutting and feed forces in all heat treated conditions. Cutting speed has been found to be more significant for cutting tool temperature.

The experimental studies carried out on Ti10.2.3 titanium alloy in as-received annealed, STA and STOA conditions show that this alloy has the poorest machinability in the STA heat treated condition as the specific forces, friction coefficient and cutting tool temperature are higher in this condition. It is also found that the specific feed force is more sensitive to variations in feed rates than the specific cutting force. The over aging treatment improves the machinability of this alloy because of reduction in hardness as a consequence of coalescence of the precipitates into the bigger particles causing fewer impediments to the movement of dislocations. Thermal softening plays a dominant role for all the heat treated conditions except for STA condition at 0.25 mm/rev feed rate. At this particular feed rate Ti10.2.3 STA showed resistance to thermal softening. The ANOVA results have shown that most of the experimental results are statistically significant in term of feed rate and cutting speed variations. Feed rate has been found to have more significance than the cutting speed for specific cutting and feed forces in all heat treated conditions. Cutting speed has been found to be more significant for cutting tool temperature. The interactions between the feed rate and cutting speed have significant effect on the specific cutting and feed forces as well as on the cutting tool temperature for the STA condition.

The experimental studies carried out on Ti6Al4V titanium alloy in as-received annealed conditions show that there is not much effect of the increase of cutting speed on thermal softening. The ANOVA results have shown that feed rate experimental results of Ti6Al4V are statistically significant in term of specific forces and cutting tool temperature. The effect

of cutting speed is statistically significant for specific cutting force and cutting tool temperature. Feed rate has been found to have more significance than the cutting speed for specific cutting and feed forces. Cutting speed has been found to be more significant for cutting tool temperature.

The comparison of titanium alloys in different heat treated conditions shows that Ti10.2.3 has poor machinability than Ti54M and Ti6Al4V alloys. This is due to the chemical composition of this alloy. Ti54M alloy in annealed condition has better machinability than Ti6Al4V alloy in term of chip morphology at lower feed rates. The differences among all the seven analyzed titanium alloys in different heat treated conditions are more apparent in the case of the specific feed force than the specific cutting force. There is a significant influence of chemical composition and the metallurgical state, and the modification of the heat treatment plan can improve the machinability of the titanium alloys.

The interrupted machining analysis of Ti6Al4V and Ti5553 titanium alloys using PVD coated carbide inserts shows the poor machinability of Ti5553 as compared to the Ti6Al4V; as higher forces and temperature are observed in the machining of Ti5553 alloy as compared to Ti6Al4V alloy; due to its high mechanical properties which further depends on the microstructure. The online monitoring of the forces has shown higher fluctuations during machining of Ti5553 alloys even at the lower cutting speeds as compared to Ti6Al4V alloy.

It has also been found that the cutting and feed forces, and cutting tool temperature increase with increase in cutting edge radius and decrease with increase in rake angle. It is observed that the feed forces are more sensitive to variation in tool geometry and feed rates than the cutting forces. There is a significant influence of the cutting edge preparation and rake angle

on the machining performance of PVD coated inserts and the modification of the insert geometry can improve the machinability of the titanium alloys.

Major Contributions of the Thesis

- Machinability data on the Ti54M, Ti10.2.3, Ti5553 and Ti6Al4V titanium alloys in different heat treated conditions determined experimentally.
- To the best of my knowledge, cutting temperature data has been provided for the first time while machining Ti10.2.3 alloy in different heat treated conditions. The experimental data for machining Ti10.2.3 in STOA heat treated condition is presented to the scientific community.
- Intermittent machining tests are performed using PVD coated carbide tools with different edge preparations and tool geometry.
- The major benefits will be an increase in productivity and the cost reduction for the suppliers of aerospace industry and end users

Limitations and future scope of the research

- The number of experimental tests performed were limited due to the limited commercial availability and high cost of the workpiece materials – Ti54M, Ti10.2.3, Ti5553 and Ti6Al4V titanium alloys and limited availability of the tailor-made tool inserts.
- The investigation of chip morphology in this study is based on optical microscopy analysis. In order to confirm the relationship between machinability and heat treatment under different set of cutting parameters, a detailed examination of chip morphology by Scanning Electron Microscope (SEM) is necessary.

- The chip morphology analysis was done for Ti54M and Ti6Al4V alloys only. The chip morphology analyses were not done for Ti10.2.3 and Ti5553 alloys. The comparison of chip morphology for all the investigated alloys may have provided more information on the machinability of these alloys.
- The experiments were conducted at few variables. More experimental tests with different phase compositions, cutting parameters and heat treated conditions are required to get the general trends and optimum machinability variables.
- There is need to design a temperature acquisition system which could be able to synchronize with tool deflection. This will help in measuring temperature even at intense cutting conditions.
- A mathematical model predicting the process temperature with microstructural changes is required to determine the thermal load on the cutting tool.
- It could be interesting to carry out tests with higher cutting parameters, laser assisted machining, cryogenic coolants, etc. in the future. It is suggested that a novel model needs to be developed in order to explain the relationship between thermo-mechanical treatments and machinability of the titanium alloys.

References

Ahmad-Yazid, A., Taha, Z., Almanar, I.P. A review of cryogenic cooling in high speed machining (HSM) of mold and die steels. *Scientific Research and Essays*. 2010, 5(5): 412-427.

Akir, O.C., Kiyak, M., Altan, E. Comparison of gases alications to wet and dry cutting in turning. *Journal of Materials Processing Technology*. 2004, 153(154): 35–41.

Albrecht, P. New developments in the theory of the metal cutting process. Part I. The ploughing process in metal cutting. *Journal of Engineering for Industry-Transactions of the ASME*. 1960, 82: 348–357.

Altintas, Y., Yellowley, I. In-process detection of tool failure in milling using cutting force models. *Journal of Engineering for Industry-Transactions of the ASME*. 1989, 111: 149–157.

Aluwihare, C.B., Armarego, E.J.A., Smith, A.J.R. A Predictive Model for Temperature Distributions in 'Classical' Orthogonal Cutting. *Transactions of the North American Manufacturing Research Institution of SME*. 2000, 28: 131-136.

Amontons, G. Histoire de l'Académie Royale des Sciences avec les Mémoires de Mathématique et de Physique. *Paris*. 1699.

Armendia, M., Garay, A., Iriarte, L.M., Arrazola, P.J. Comparison of the Machinabilities of Ti6Al4V and TIMETAL® 54M Using Uncoated WC-Co Tools. *Journal of Materials Processing Technology*. 2010a, 210: 197-203.

Armendia, M., Garay, A., Iriarte, L.M., Belloso, J., Turner, S., Osborne, P., Arrazola, P.J. The influence of heat treatment in the machinability of titanium alloys: Ti6Al4V and Ti-5Al-4V-0.6Mo-0.4Fe (Ti54M). *4th CIRP International Conference on High Performance Cutting, Japan*. 2010b, C:02.

Armendia, M., Garay, A., Villar, A. , Davies, M. A., Arrazola, P. J. High bandwith temperature measurement in interrupted cutting of difficult to machine materials. *CIRP Annals -Manufacturing Technology*. 2010c, 59(1): 97-100.

Arrazola, P.J., Garay, A., Iriarte, L.M., Armendia, M., Marya, S., Le Maître, F. Machinability of titanium alloys (Ti6Al4V and Ti555.3). *Journal of Materials Processing Technology*. 2009, 209: 2223-2230.

Arrazola, P.J., Meslin, F., Marya, S. Serrated chip prediction in numerical cutting models. *Proceedings of the CIRP Congress 8 WMMO*. 2005, 115–122.

Ay, H., Yang, W.J., Heat Transfer. Life of metal cutting tools in turning. *Int. J. Heat Mass Transf*. 1998, 41 (3): 613–623.

Baili, M., Wagner, V., Dessein, G., Sallaberry, J., Lallement, D. An experimental investigation of hot machining with induction to improve Ti-5553 machinability. *Applied Mechanics Materials*. 2011, 62:67–76.

Barrow, G. A review of experimental and theoretical techniques for assessing cutting temperatures. *CIRP Annals - Manufacturing Technology*. 1973, 22(2): 203-211.

Barry, J., Byrne, G., Lennon, D. Observations on chip formation and acoustic emission in machining Ti–6Al–4V alloy. *International Journal of Machine Tools and Manufacture*. 2001, 41: 1055–1070.

Bayoumi, A.E., Xie, J.Q. Some metallurgical aspects of chip formation in cutting Ti-6wt.%Al-4wt.%V alloy. *Journal of Materials Science and Engineering*. 1995, 190: 173-180.

Bermingham, M.J., Kirsch, J., Sun, S., Palanisamy, S., Dargusch, M.S. New observations on tool life, cutting forces and chip morphology in cryogenic machining Ti-6AL-4V. *Journal of Machine Tools and Manufacture*. 2011, 51: 500-511.

Boothroyd, G. Photographic Technique for the Determination of Metal Cutting Temperatures. *British Journal of Applied Physics*. 1961, 12: 238-242.

Boothroyd, G., Knight, W.A. *Fundamentals of Machining and Machine Tools*. 2nd ed. Marcel Dekker, New York. 1989, 83–86.

Bouzakis, K.D., et al. Fatigue failure mechanisms of multi and monolayer physically vapour-deposited coatings in interrupted cutting processes, *Surface and Coatings Technology*. 1998, 108-109: 526–534.

Bouzakis, K.D., et al. Alication in milling of coated tools with rounded cutting edges after the film deposition. *CIRP Annals - Manufacturing Technology*. 2009, 58: 61-64.

Bouzakis, K.D., et al. Effect of the Cutting Edge Radius and its Manufacturing Procedure, on the Milling Performance of PVD Coated Cemented Carbide Inserts. *CIRP Annals - Manufacturing Technology*. 2002, 51(1): 61–64.

Bouzakis, K.D., Michailidis, N., Skordaris, G., Bouzakis, E., Biermann, D., M'Saoubi, R. Cutting with coated tools: coating technologies, characterization methods and performance optimization, *CIRP Annals – Manufacturing Technology*. 2012, 61(2): 703–723.

Bouzakis, K.D., Michailidis, N., Vidakis, N., Efstathiou, K., Leyendecker, T., Erkens, G., Wenke, R., Fuss, H.G. Optimization of the cutting edge radius of PVD coated inserts in milling considering film fatigue fracture mechanisms. *Surface and Coatings Technology*. 2000, 133(134): 501-507.

Boyer, R.R. An overview on the use of titanium in the aerospace industry. *Materials Science and Engineering*. 1996, 213(A): 103-114.

Boyer, R.R. Attributes, Characteristics, and Applications of Titanium and its Alloys. *JOM*. 2010, 62(5): 21-24.

Boyer, R.R., Briggs, R.D. The Use of β Titanium Alloys in the Aerospace Industry. *Journal of Materials Engineering and Performance*. 2005, 14: 681–685.

Bradbury, S.R., T. Huyanan. Challenges facing surface engineering technologies in the cutting tool industry. *Vacuum*. 2000, 56: 173-177.

Byrant, W.A. Cutting tool for machining titanium and titanium alloys. US Patent 5,718,54, 17 February 1998.

Byrne, G., Dornfeld, D., Denkena, B. Advanced Cutting Technology. *CIRPAnnals-Manufacturing Technology*. 2003, 52(2): 483–507.

Chandler, H. *Heat Treater's Guide, Practices and Procedures for Nonferrous Alloys*. ASM International. 2006.

Che-Haron, C.H. Tool life and surface integrity in turning titanium alloy. *Journal of Materials Processing Technology*. 2001, 118: 231-237.

Che-Haron, C.H., Jawaid, A. The effect of machining on surface integrity of titanium alloy Ti–6% Al–4% V. *Journal of Materials Processing Technology*. 2005, 166: 188–192.

Colwell, L.V., Truckenmiller, W.C. Cutting Characteristics of Titanium and Its Alloys. *Mechanical Engineering*. 1953, 6: 461-480.

Cook, N.H. Chip formation in machining titanium. *Proceedings of the Symposium on Machine Grind Titanium*, Watertown Arsenal, MA. 1953, 1–7.

Cooke, A.L. High Bandwidth Thermal Microscopy of the Tool-Chip Interface During Machining. *Doctor of Philosophy in Mechanical Engineering, Charlotte*. 2008.

Corduan, N., Himbart, T., Poulachon, G., Dessoly, M., Lambertin, M., Vigneau, J., Payoux, B. Wear Mechanisms of New Tool Materials for Ti6AI4V High Performance Machining. *CIRP Annals - Manufacturing Technology*. 2003, 52: 73-76.

Cotterell, M., Byrne, G. Dynamics of chip formation during orthogonal cutting of titanium alloy Ti–6Al–4V. *CIRP Annals - Manufacturing Technology*. 2008, 57: 93–96.

Coullomb, C.A. Mémoires de Mathématique et de Physique de l'Académie Royale des Sciences. *Paris*. 1785.

Dandekar, C.R., Yung, C.S., John, B. Machinability improvement of titanium alloy (Ti–6Al–4V) via LAM and hybrid machining. *International Journal of Machine Tools & Manufacture*. 2010, 50: 174-182.

Davies, M.A., Cao, Q., Cooke., A.L., Ivester, R. On the Measurement and Prediction of Temperature Fields in Machining 1045 Steel. *CIRP Annals – Manufacturing Technology*. 2003a, 52(1): 77-80.

Davies, M.A., Cooke, A.L., Larsen, E.R. High bandwidth thermal microscopy of machining AISI 1045 steel. *CIRP Annals - Manufacturing Technology*. 2005, 54(1): 63-66.

Davies, M.A., Ueda, T.M., Mullany, R.B., Cooke, A.L. On the Measurement of Temperatures in Material Removal Processes. *CIRP Annals – Manufacturing Technology*. 2007, 56(2): 581-604.

Davies, M.A., Yoon, H., Schmitz, T.L., Burns, T.J., Kennedy, M.D. Calibrated thermal microscopy of the tool-chip interface in machining. *Journal of Machining Science and Technology*. 2003b, 7(2): 167-190.

Dearnley, P., Grearson, A. Evaluation of principal wear mechanisms of cemented carbides and ceramics used for machining titanium alloy IMI 318. *Materials Science and Technology*. 1986, 2: 47–58.

Derrico, G.E., Bugliosi, S., Guglielmi, E. Tool-life of cermet inserts in milling tests. *Journal of Materials Processing Technology*. 1998, 77: 337–343.

Dewes, R.C., Ng, E., Chua, K.S., Newton, P.G., Aspinwall, D.K. Temperature measurement when high speed machining hardened mould/die steel. J. Mater. Process. Technol. 1999, 92/93: 293–301.

Dhananchezian, M., Kumar, M.P. Cryogenic turning of the Ti-6Al-4V alloy with modified cutting tool inserts. *Cryogenics*. 2011, 51: 34-40.

Diack, M.I. Contribution a` l'E´tude de l'Usinage Grande Vitesse de l'Alliage de Titane TA6V. Th. Doctorat, Universite´ de Nantes. 1995.

Dinc, C. I, Serpenguzel, L. A. Analysis of thermal fields in orthogonal machining with infrared imaging. *Journal of Materials Processing Technology*. 2008, 198: 147–154.

Donachei, M.J. *Titanium-A Technical Guide*. 2nd ed. ASM International. 2004.

Ducros, C., Benevent, V., Sanchette, F. Deposition, Characterization and Machining Performance of Multilayer PVD Coatings on Cemented Carbide Cutting Tools. *Surface and Coatings Technology*. 2003, 163-164: 681-688.

Egorova, Y.B., Il'in, A.A., Kolachev, B.A., Nosov, V.K., Mamonov, A.M. Effect of the structure in the curability of titanium alloys. *Metal Science and Heat Treatment*. 2003, 45(3–4): 134–139.

Elbestawi, M.A., Papazafirou, T.A., Du, R.X. In-process monitoring of tool wear in milling using cutting force signal. *International Journal of Machine Tools & Manufacture*. 1991, 31: 55–73.

Eylon, D., Fulishiro, S., Postans, P.J., Froes, F.H. *J. Met*. 1984, 36(11): 55-62.

Eylon, D., Vassel, A., Combres, Y., Boyer, R.R., Bania, P.J., Schutz, R.W. Issues in the Development of Beta Titanium Alloys. *JOM*. 1994, 6: 14-15.

Ezugwu, E.O. High Speed Machining of Aero-Engine Alloys. *Journal of the Brazilian Society of Mechanical Sciences and Engineering*. 2004, 26(1): 1-10.

Ezugwu, E.O. Key improvements in the machining of difficult-to-cut aerospace superalloys. *International Journal of Machine Tools & Manufacture*. 2005, 45: 1353-1367.

Ezugwu, E.O., Bonney, J., Da Silva, R.B., Cakir, O. Surface integrity of finished turned Ti–6Al–4V alloy with PCD tools using conventional and high pressure coolant sulies. *International Journal of Machine Tools & Manufacture.* 2007, 47: 884-891.

Ezugwu, E.O., Da Silva, R.B., Bonney, J., Machado, A.R. Evaluation of the performance of CBN tools when turning Ti–6Al–4V alloy with high pressure coolant sulies. *International Journal of Machine Tools & Manufacture*. 2005, 45: 1009-1014.

Ezugwu, E.O., Wang, Z.M. Titanium alloys and their machinability - a review. *Journal of Materials Processing Technology*. 1997, 68: 262-274.

Fadare, D.A., Sales, W.F., Ezugwu, E.O., Bonney, J., Oni, A.O. Effects of Cutting Parameters on Surface Roughness During High-speed Turning of Ti-6Al-4V Alloy. *Journal of Applied Sciences Research*. 2009, 5(7): 757-764.

Fang, N., Wu, Q. A comparative study of the cutting forces in high speed machining of Ti–6Al–4V and Inconel 718 with a round cutting edge tool. *Journal of Materials Processing Technology*. 2009, 209: 4385–4389.

Fanning, J.C. Properties of TIMETAL 555 (Ti–5.5Al–5Mo–5V–3Cr). *Journal of Materials Engineering and Performance*. 2005, 14: 788–791.

Froes, F.H., Yau, T.L., Weidinger, H. G. Structure and Properties of Nonferrous Alloys, Titanium, Zirconium, and Hafnium, A Comprehensive Treatment, VCH Verlagsge-sellschaft mbH and VCH Publishers Inc. *Materials Science and Technology*. 1996, 8: 399-468.

Gente, A., Hoffmeister, H.W. Chip formation in machining Ti–6Al–4V at extremely high cutting speeds. *CIRP Annals - Manufacturing Technology*. 2001, 50(1): 49–52.

Germain, G., Morel, F., Lebrun, J.L., Morel, A. Machinability and surface integrity for a bearing steel and a titanium alloy in laser assisted machining (optimization on LAM on two materials). *Lasers in Engineering*. 2007, 17: 329–344.

Ginting, A., Nouari, M. Experimental and numerical studies on the performance of alloyed carbide tool in dry milling of aerospace material. *International Journal of Machine Tools and Manufacture*. 2006, 46: 758–768.

Grzesik, W. Experimental investigation of the cutting temperature when turning with coated indexable inserts. *International Journal of Machine Tools and Manufacture*. 1999, 39 (3): 355–369.

Guo, Y.B. An integral method to determine the mechanical behaviors of materials in cutting. *Journal of Materials Processing Technology*. 2003, 142 (1): 72–81.

Guo, Y.B., Chou, Y.K. The determination of ploughing force and its influence on material properties in metal cutting. *Journal of Materials Processing Technology*. 2004, 148: 368–375.

Hartung, P.D., Kramer, B.M. Tool Wear in Titanium Machining. *CIRP Annals - Manufacturing Technology*. 1982, 31: 75-80.

Hoffmeister, H.W., Gente A., Weber T.H., Schulz, H., Molinari, A., Dudzinski, D. Chip formation at titanium alloys under cutting speed of up to 100m/s. (Eds.). *2nd International Conference on High Speed Machining. PTW Darmstadt University*. 1999, 21–28.

Hong, S.Y., Ding, Y. Cooling approaches and cutting temperatures in cryogenic machining of Ti–6Al–4V. *Journal of Machine Tools and Manufactur*e. 2001a, 41: 1417–1437.

Hong, S.Y., Ding, Y., Jeong, W.-C. Friction and cutting forces in cryogenic machining of Ti–6Al–4V. *International Journal of Machine Tools and Manufacture*. 2001b, 41: 2271–2285.

Hong, S.Y., Markus, I., Jeong, W. New cooling approach and tool life improvement in cryogenic machining of titanium alloy Ti–6Al–4V. *International Journal of Machine Tools and Manufacture*. 2001c, 41: 2245–2260.

Hua, J., Shivpuri, R.Influence of crack mechanics on the chip segmentation in the machining of titanium alloys. *Proceedings of the Ninth ISPE International Conference on Concurrent Engineering, Cranfield, UK*. 27–31 July 2002.

Huang, J., Aifantis, E.C. A note on the problem of shear localization during chip formation in orthogonal machining. *Journal of Materials Engineering and Performance*. 1997, 6: 25.

Hughes, J.I., Sharman, A.R.C., Ridgway, K. The effect of cutting tool material and edge geometry on tool life and workpiece surface integrity. *Proceedings of the Institution of Mechanical Engineers: Journal of Engineering Manufacture*. 2001, 220(2): 93-107.

Imam, M.A. The 12th World Conference on Titanium Presents Research and Applications of "Wonder Metal". *JOM*. 2011, 63(10):16-23.

IMI Titanium. *Commercially Pure Titanium*. Kynoch Press. Birmingham, 1978.

Iqbal, S.A., Mativenga, P.T., Sheikh, M. A. A comparative study of the tool–chip contact length in turning of two engineering alloys for a wide range of cutting speeds. *International Journal of Advanced Manufacturing Technology*. 2009, 42: 30–40.

ISO 3685. Tool life testing with single-point turning tools. 1993.

Ivester, R.W., Whitenton, E., Deshayes, L. Comparison of Measurements and Simulations for Machining of Aluminum. *Transactions of the North American Manufacturing Research Institution of SME*. 2005, 33: 429-436.

Jawaid, A., Che-Haron, C.H., Abdullah, A. Tool wear characteristics in turning of titanium alloy Ti-6246. *Journal of Materials Processing Technology*. 1999, 92(93): 329-334.

Jawaid, A., Sharif, S., Koksal, S. Evaluation of wear mechanisms of coated carbide tools when face milling titanium alloy. *Journal of Materials Processing Technology*. 2000, 99: 266-274.

Jindal, P.C., Santhanam, A.T., Schleinkofer, U., Shuster, A. F. Performance of PVD TiN, TiCN, and TiAlN Coated Cemented Carbide Tools in Turning. *International Journal of Refractory Metals and Hard Materials*. May 1999, 17(1-3):163-170.

Kahles, J.F., Field, M., Eylon, D., Fores, F.H. Machining of titanium alloys. *Journal of Metals*. 1985, 7–35.

Kaminski, J., Alvelid, B. Temperature reduction in the cutting zone in water jet assisted turning. *Journal of Materials Processing Technology*. 2000, 106: 68-73.

Kitagawa, T., Kubo, A., Maekawa, K. Temperature and wear of cutting tools in high-speed machining of Inconel 718 and Ti6Al6V2Sn. *Wear*. 1997, 202(2): 142-148.

Klocke, F. Coated Tools for Metal Cutting - Features and Alications, Keynote paper. *CIRP Annals - Manufacturing Technology*. 1999, 48: 515-525.

Klocke, F., Eisenbl¨atter, G. Dry cutting. *CIRP Annals - Manufacturing Technology*. 1997, 46: 519–526.

Komanduri, R. Some clarifications on the mechanism of chip formation when machining titanium alloys. *Journal of Wear*. 1982, 76: 15.

Komanduri, R., Hou, Z.B. A review of the experimental techniques for the measurement of heat and temperatures generated in some manufacturing processes and tribology. *Tribology International*. 2001, 34: 653-682.

Komanduri, R., Von Turkovich, B.F. New observations on the mechanism of chip formation when machining titanium alloys. *Wear*. 1981, 69: 179.

Kopac, Achievements of sustainable manufacturing by machining. *Journal of Achievements in Materials and Manufacturing Engineering*. 2009, 34(2):180-187.

Korkut, I., Boy, M., Karacan, I., Seker, U. Investigation of chip-back temperature during machining depending on cutting parameters. *Material Design*. 2007, 28: 2329–2335.

Kosaka, Y., Fanning, J.C., Fox, S.P. Development of low cost high strength alpha/beta alloy with superior machinability. *Proceedings of the 10th World Conference on Titanium*. 2004, 3028-3034.

Kosaka, Y., Fox, S.P. Influences of Alloy Chemistry and Microstructure on the Machinability of Titanium Alloys. *Cost Affordable Titanium, TMS Conference*. 2004, 169-176.

Kovacevic, R., Cherukuthota, C., Mazurkiewicz, M. High pressure water jet cooling=lubrication to improve machining efficiency in milling. *International Journal of Machine Tool and Manufacture*. 1995, 35(10): 1459–1473.

Lantrip, Jeff. The Boeing Co., New Tools Needed. *Cutting Tool Engineering Magazine*. 2008, 60(8).

Larbi, S. Contribution a` l'E´tude de l'Usinage a` Grandes Vitesses de Mate´riaux Me´talliques par Simulation sur un Banc d'Essai a` Base de Barres de Hopkinson. Th. Doctorat, Universite´ de Nantes. 1990.

Lazoglu, I., Altintas, Y. Prediction of Tool and Chip Temperature in Continuous and Interrupted Machining. *International Journal of Tools and Manufacture*. 2002, 42(9): 1011-1022.

Lazoglu, I., Buyukhatipoglu, K., Kratz, H., Klocke, F. Forces and temperatures in hard turning. Mach. Sci. Technol. 2006, 10: 157–179.

Leyens, C., Peters, M. *Titanium and Titanium Alloys. Fundamentals and Applications.* Wiley-VCH, Koln, Germany. 2003, 1–497.

Loapez de lacalle, L.N., PeÂrez, J., Llorente, J.I., SaÂnchez, J.A. Advanced cutting conditions for the milling of aeronautical alloys. *Journal of Materials Processing Technology*. 2000, 100: 1-11.

Lütjering, G., Williams, J.C. *Titanium*. Springer. 2007.

Machado, A.R., Wallbank, J. Machining of titanium and it's alloys. *Proceedings of the Institution of Mechanical Engineers, Part B. Journal of Engineering Manufacture*. 1990, 204: 53.

Machai, C., Biermann, D. Machining of a Hollow Shaft Made of β- Titanium Ti-10V-2Fe-3Al. *IEEE International Symposium on assembly and Manufacturing*. 2011b, 1-6.

Machai, C., Biermann, D. Machining of β-titanium-alloy Ti-10V-2Fe-3Al under cryogenic conditions, Cooling with carbon dioxide snow. *Journal of Materials Processing Technology*. 2011a, 211: 1175–1183.

Mazurkiewicz, M., Kabula, Z., Chow, J. Metal machining with high pressure water jet cooling assistance—a new possibility. *Journal of Engineering for Industry, Transactions of ASME*. Feb 1989, 111: 7–12.

Ming, C., Fanghong, S., Haili, W., Renwei, Y., Zhenghong, Q., Shuqiao, Z., 2003. Experimental research on the dynamic characteristics of the cutting temperature in the process of high-speed milling. J. Mater. Process. Technol. 138, 468–471.

Molinari, A. Collective behavior and spacing of adiabatic shear bands. *Journal of the Mechanics and Physics of Solids*. 1997, 45: 1551.

Muller, B., Renz, U. Time resolved temperature measurements in manufacturing. *Measuremet*. 2003, 34: 363–370.

Nabhani, F. Machining of aerospace titanium alloys. *Robotics and Computer-Integrated Manufacturing*. 2001, 17: 99–106.

Nabhani, F. Wear mechanism of ultra-hard cutting tool materials. *Journal of Materials Processing Technology*. 2001, 115(3): 402–412.

Nagpal, B.K., Sharma, C.S. Cutting fluids performance, Part-1-Optimisation of pressure for Hi-Jet method of cutting fluid application. *Journal of Engineering for Industry - Transactions of ASME*. Aug 1973, 95: 881–889.

Nandy, A.K., Gowrishankar, M.C., Paul, S. Some studies on high-pressure cooling in turning of Ti–6Al–4V. *International Journal of Machine Tools & Manufacture*. 2009, 49: 182-198.

Nandy, A.K., Paul, S. Effect of Coolant Pressure, Nozzle Diameter, Impingement Angle and Spot Distance in High Pressure cooling with Neat Oil in Turning Ti-6AL-4V. *Machining Science and Technology*. 2008, 12: 445-473.

Narutaki, N., Murakoshi, A. Study on machining of titanium alloys. *CIRP Annals - Manufacturing Technology*. 1983, 32: 65.

Neugebauer, K., Bouzakis, D., Denkena, B., Klocke, F., Sterzing, A., Tekkaya, A.E., Wertheim R. Velocity effects in metal forming and machining processes. *CIRP Annals - Manufacturing Technology*. 2011, 60(2): 627–650.

Niu, Q.L., Cai, X.J., Liu, Z.Q., Chen, M., An Q.L. Wear behavior of carbide inserts in face milling TA19 alloy. *Advanced Materials Research*. 2012, 426: 339–343.

Niu, Q., Chen, M., Ming, W., An, Q. Evaluation of the performance of coated carbide tools in face milling TC6 alloy under dry condition. *Int J Adv Manuf Technol*. 2013, 64: 623 – 631.

Nouari, M., List, G., Girot, F., Coupard, D. Experimental Analysis and Optimization of Tool Wear in Dry Machining of Aluminum Alloys. *Wear*. Aug-Sept 2003, 255(7-12): 1359-1368.

Nurul Amin, A.K.M., Ahmad, F., Ismail, M.K., Khairusshima, N. Effectiveness of uncoated WC–Co and PCD inserts in end milling of titanium alloy—Ti–6Al–4V. *Journal of Materials Processing Technology*. 2007, 192(193): 147–158.

O'Sullivan, D., Cotterell, M. Temperature measurement in single point turning. *Journal of Materials Processing Technology*. 2001, 118: 301–308.

Ozel., T., Sima., M. Finite Element Simulation of High Speed Machining Ti-6Al-4V Alloy Using Modified Material Models. *Transactions of NAMRI/SME*. 2010, 38: 49-57.

Palanisamy, S., McDonald, S.D., Dargusch, M.S. Effects of coolant pressure on chip formation while turning Ti6Al4V alloy. *International Journal of Machine Tools & Manufacture*. 2009, 49: 739-743.

Philippon, S., Sutter, G., Molinari, A. An Experimental Study of Friction at High Sliding Velocities. *Wear – An International Journal on the Science and Technology of Friction Lubrication and Wear*. 2004, 257: 777-784.

Pigott, R.J.S., Colwell, A.T. Hi-jet system for increasing tool life. *Society of American Engineers, Quarterly Transactions*. 1952, 6(3): 547–566.

Quinto, D.T. Challenging Applications. *Cutting Tool Engineering Magazine*. October 2007, 59(10).

Rahim, E.A., Sharif, S. Investigation on Tool Life and Surface Integrity When Drilling Ti-6Al-4V and Ti-5Al-4V-Mo/Fe. *JSME International Journal*. 2006, 49: 340-345.

Rahman, M., Wang, Z.G., Wong, Y.S. A Review on High-Speed Machining of Titanium Alloys. *JSME International Journal*. 2006, 49: 11-20.

Rahman, M., Wong, Y.S., Zareena, A.R. Machinability of titanium alloys. *JSME International Journal Series*. 2003, 46(C): 107-115.

Rahman, Rashid, R.A., Sun, S., Wang, G., Dargusch, M.S. Machinability of a near beta titanium alloy. *Proceedings of the Institution of Mechanical Engineers Part B. Journal of Engineering Manufacture*. 2011, 225(12): 2151–2162.

Rajagopal, S., Plankenhorn, D.J., Hill, V.L. Machining aerospace alloys with the aid of a 15 kW laser. *Journal of Applied Metalworking*. 1982, 2: 170–184.

Rivero, A., Aramendi, G., Herranz, S. L., Lo´ pez de Lacalle. An experimental investigation of the effect of coatings and cutting parameters on the dry drilling performance of aluminium alloys. *The International Journal of Advanced Manufacturing Technology*. 2006, 28: 1–11.

Robert, W.I. Tool Temperatures in Orthogonal Cutting of Alloyed Titanium. *Proceedings of NAMRI/SME*. 2011, 39.

Saglam, H., Yaldiz, S., Unsacar, F. The effect of tool geometry and cutting speed on main cutting force and tool tip temperature. *Materials and Design*. 2007, 28: 101–111.

Sandvik - Titanium alloys (Available at http://www2.coromant.sandvik.com/coromant/pdf/aerospace/gas_turbines/C_2920_18_ENG_043_074.pdf).

Saoubi, R.M., Chandrasekaran, H. Investigation of the effects of tool-microgeometry and coating on tool temperature during orthogonal turning of quenched and tempered steel. *International Journal of Machine Tools and Manufacture.* 2004, 44: 213–224.

Sharma, C.S., Rice, W.B., Salmon, R. Some effects of injecting cutting fluids directly into the chip tool interface. *Journal of Engineering for Industry, Transactions of ASME*. May 1971, 93: 441–444.

Sharma, V.S., Dogra, M., Suri, N.M. Cooling techniques for improved productivity in turning. *International Journal of Machine Tools & Manufacture*. 2009, 49: 435–453.

Shokrani, A., Dhokia, V., Newman, S.T. Environmentally conscious machining of difficult-to-machine materials with regard to cutting fluids. *International Journal of Machine Tools & Manufacture*. 2012, 57: 83–101.

Siekmann, H.J. How to Machine Titanium. *The Tool Engineer*. 1955, 1: 78-82.

Siemers, C., Zahra, B., Leemet, T., Rosler, J. Development of advanced beta-titanium alloys. *Proceedings of the 8th AMMT Conference, St. Petersburg, Russia*. 2007.

Smith, G.T. *Cutting Tool Technology*. Springer-Verlag London Limited. 2008.

Sreejith, P., Ngoi, B. Dry machining: machining of the future. *Journal of Materials Processing Technology*. 2000, 101: 287–291.

Stephenson, D.A. Tool-Work Thermocouple Temperature Measurements – Theory and Implementation Issues. *ASME Journal of Engineering for Industry*. 1993, 115: 432-437.

Stephenson, D.A., Agapiou, J.S. *Metal Cutting Theory and Practice*. Marcel Dekker, New York, NY. 1997.

Stephenson, D.A., Ali, A. Tool Temperatures in Interrupted Metal cutting. *Transactions of the ASME - Journal of Engineering for Industry*. 1992, 114: 127–135.

Stevenson, R. The measurement of parasitic forces in orthogonal cutting. *International Journal of Machine Tools and Manufacture*. 1998, 38: 113–130.

Stevenson, R., Stephenson, D.A. The mechanical behavior of zinc during machining. *ASME Journal of Engineering for Industry*. 1995, 117: 173–178.

Sun, S., Brandt, M., Dargusch, M.S. Characteristics of cutting forces and chip formation in machining of titanium alloys. *International Journal of Machine Tools and Manufacture*. 2009, 49: 561–568.

Sun, S., Brandt, M., Dargusch, M.S. Thermally enhanced machining of hard-to-machine materials-a review. *International Journal of Machine Tools and Manufacture*. 2010a, 50: 663–680.

Sun, S., Brandt, M., Dargusch, M.S. Machining Ti-6Al-4V alloy with cryogenic compressed air cooling. *International Journal of Machine Tools and Manufacture*. 2010b, 50: 933–942.

Sun, S., Harris, J., Brandt, M. Parametric investigation of laser-assisted machining of commercially pure titanium. *Advanced Engineering Materials*. 2008, 10: 565–572.

Sutherland, J.W., DeVor, R.E. An improved method for cutting force and surface error prediction in flexible end milling systems. *ASME Journal of Engineering for Industry*. 1986, 108: 269–272.

Sutherland, J.W., Kulur, V.N., King, N.C., von Turkovich, B.F. An experimental investigation of air quality in wet and dry turning. *CIRP Annals—Manufacturing Technology*. 2000, 49: 61–64.

Sutter, G., Molinari, A. Analysis of cutting force components and friction in high speed machining. *Journal of Manufacturing Science and Engineering—Transactions of the ASME*. 2005, 127: 245–250.

Syed, Kareem. Finite Element Simulation of Chip Segmentation In Machining A Ti-6al-4v Alloy. *Faculty of the Graduate College of the Oklahoma State University. Degree of Master of Science*. December, 2004.

Taylor, F.W. On the art of cutting metals. *Transactions of the ASME*. 1906, 28: 31-350.

Terlinde, G.T., Duerig, T.W., Williams, J.C. The Effect of Heat Treatment on Microstructure and Tensile Properties of Ti-10V-2Fe-3Al. *Titanium 80 Science and Technology – Proceedings of the 4th International Conference on Titanium*. 1980, 2: 1571-1581.

Toenshoff, H.K., Wobker, H.G., Brandt, D. Hard turning—influences on the workpiece properties. *Transactions of NAMRI/SME*. 1995, 23: 215–220.

Trent, E.M. *Metal Cutting*. 3rd ed. Butterworth–Heineman Ltd., Oxford, UK. 1991.

Trucks, H.E. *Machining Titanium Alloys*. Machine and Tool Blue Book. 1987, 82(1): 39-41.

Ueda, T., Hosokawa, A., Oda, K., Yamada, K. Temperature on Flank Face of Cutting Tool in High Speed Milling. *CIRP Annals – Manufacturing Technology*. 2001, 50(1): 37–40.

Ugartea, A., M'Saoubia, R., Garay, A., Arrazola, P.J. Machining behaviour of Ti-6Al-4V and Ti-5553 alloys in interrupted cutting with PVD coated cemented carbide. *Procedia CIRP*. 2012, 1: 208 – 213.

Vargas Pérez, R.G. Wear mechanisms of WC inserts in face milling of gamma titanium aluminides. *Wear*. 2005, 259: 1160–1167.

Venkatesh, V., Kosaka, Y., Fanning, J., Nyakana, S. Processing and properties of Timetal 54M. *11th World Conference on Titanium, Kyoto, Japan*. 2007, 713–716.

Venugopal, K.A., Paul, S., Chattopadhyay, A.B. Growth of tool wear in turning of Ti-6Al-4V alloy under cryogenic cooling. *Wear*. 2007, 262: 1071-1078.

Wagner, V., Baili, M., Dessein, G., Lallement, D. Experimental study of coated carbide tools behaviour: application for Ti-5-5-5-3 turning. *International Journal of* Machining and *Machinability* of Materials. 2011, 9(3–4): 233– 248.

Wang, Z. G., Rahman, M., Wong, Y. S., Neo, K. S., Sun, J., Tan, C. H., Onozuka, H. Study on orthogonal turning of titanium alloys with different coolant suly strategies. *International Journal of Advanced Manufacturing Technology*. 2009, 42: 621–632.

Wang, Z.M. *Machining of aerospace superalloys with coated (PVD and CVD) carbides and self- propelled rotary tools*. Ph.D. Thesis, South Bank University. 1997.

Wang, Z.Y. and Rajurkar, K.P. Cryogenic machining of hard-to-cut materials. *International Journal of Wear*. 2000, 239: 168-175.

Wanigarathne, P.C., Kardekar, A.S., Dillon, O.W., Poulachon, G. and Jawahir, I.S. Progressive tool-wear in machining with coated grooved tools and its correlation with cutting temperature. *International Journal of Wear*. 2005, 259:1215–1224.

Weinert, K., Inasaki, I., Sutherland, J.W., Wakabayashi, T. Dry machining and minimum quantity lubrication. *CIRP Annals—Manufacturing Technology*. 2004, 53: 511–537.

Weiss, I., Semeatin, S.L. Thermomechanical processing of beta titanium alloys-an overview. *Journal of Materials Science and Engineering*. 1998, 243(A): 46-65.

Wertheim, R. Development and Alications of Coated Cutting Tool Carbides. *Rewrite of an Oral Presentation held at CIRP General Assembly in Athens*. 1998.

Whitenton, E. High-Speed Dual-Spectrum Imaging for the Measurement of Metal Cutting Temperatures. National *Institute of Standards and Technology Interagency Report (NISTIR)*. 2010, 7650.

Whitenton, E., Ivester, R., Yoon, H. Simultaneous Visible and Thermal Imaging of Metals During Machining. *Proceedings of Thermosense, Orlando, Florida*. 2005.

Wyen, C.F., Wegener, K. Influence of cutting edge radius on cutting forces in machining titanium. *CIRP Annals – Manufacturing Technology*. 2010, 59: 93-96.

Yang, X., Liu, C.R. Machining Titanium and Its Alloys. *Journal of Machining Science and Technology*. 1999, 3(1): 107–139.

Yen, Y.C., Jain, A., Altan, T. A finite element analysis of orthogonal machining using different tool edge geometries. *Journal of Materials Processing Technology*. 2004, 146: 72–81.

Yildiz, Y., Nalbant, M. A review of cryogenic cooling in machining processes. *International Journal of Machine Tools and Manufacture*. 2008, 48: 947-964.

Zemzemi, F., Rech, J., Ben Salem, W., Dogui, A., Kapsa, P. Identification of a Friction Model at Tool/Chip/Workpiece Interfaces in Dry Machining of AISI4142 Treated Steels. *Journal of Materials Processing Technology*. 2009, 209: 3978-3990.

Zhang, H.Z., Ming, W.W., Chen, M., Han, B., Rong, B., Liu, G., Zhang, Y.S. An investigation of the wear mechanism for carbide tools in face milling the Ti-5Al-4.75Mo-4.75 V-1Cr-1Fe alloy. *Key Engineering Materials*. 2010, 431–432: 547–550.

List of Publications

International Journals (SCI)

1. **Khanna, N.,** and Sangwan, K.S. Comparative machinability study on Ti54M titanium alloy in different heat treatment conditions. *Proceedings of the Institution of Mechanical Engineers, Part B: Journal of Engineering Manufacture*, 2013, 227(1), 96-101. (2011 I**mpact Factor**: **0.725**)
2. **Khanna, N.,** and Sangwan, K.S. Machinability study of α/β and β titanium alloy in different heat treatment conditions. *Proceedings of the Institution of Mechanical Engineers, Part B: Journal of Engineering Manufacture*, 2013, 227(3), 357-361. (2011 I**mpact Factor: 0.725**)
3. **Khanna, N.,** and Sangwan, K.S. Interrupted machining analysis for Ti6Al4V and Ti5553 titanium alloys using physical vapor deposition (PVD)–coated carbide inserts. *Proceedings of the Institution of Mechanical Engineers, Part B: Journal of Engineering Manufacture*, 2013, 227(3), 465-470. (2011 I**mpact Factor: 0.725)**
4. **Khanna, N.,** and Sangwan, K.S. Machinability Analysis of Heat Treated Ti64, Ti54M and Ti10.2.3 Titanium Alloys. *International Journal of Precision Engineering and Manufacturing*, 2013, **Springer** (**Accepted**) (2011 I**mpact Factor**: **1.141**)

International Conference Proceedings (Abroad)

1. **Khanna, N**., Sangwan, K.S. Machinability Analysis of Ti10.2.3 Titanium Alloy Using ANOVA, ***Proceedings of NAMRI/SME***, 2013, 41, Madison, Wisconsin, USA. (**Accepted**)
2. **Khanna, N**., Garay, A., Luis M. Iriarte, Daniel Soler, Sangwan, K.S., and Arrazola, P.J. Effect of heat Treatment Conditions on the Machinability of Ti64 and Ti54M Alloys, ***Procedia CIRP***, 2012, 1: 477–482, ETH Zurich, Switzerland.
3. **Khanna, N**., and Sangwan, K.S. Comparison of Cutting Tool Performance in Machining of Titanium Alloys and Inconel 718 Super Alloy, Paper: C11, *Proceedings of **4th CIRP** International Conference on High Performance Cutting*, 2010, Gifu, Japan.
4. **Khanna, N**., and Sangwan, K.S. Cutting Tool Performance in Machining of Ti555.3, Timetal®54M, Ti 6-2-4-6 and Ti 6-4 Alloys: A Review and Analysis, Paper: C22, *Proceedings of the **CIRP 2nd** Process Machine Interactions Conference*, 2010, UBC, Vancouver, Canada.

International Conference Proceedings (India)

1. **Khanna, N**., Sangwan, K.S. Machinability analysis of Ti6Al4V titanium alloy. *3rd International Conference on Production and Industrial Engineering*, NIT Jalandhar, 2013, India. (**Accepted**)

Biographies

Biography of the Candidate

Mr Navneet Khanna is a Lecturer in Mechanical Engineering Department at Birla Institute of Technology and Science Pilani (BITS - Pilani, Pilani campus), and currently pursuing his PhD under the supervision of Dr Kuldip Singh Sangwan. He has completed his B.Tech in Production Engineering from Shaheed Bhagat Singh College of Engineering and Technology, Ferozepur in the year 2004. He obtained his M.E degree in Mechanical Engineering from BITS Pilani in 2009. He earlier worked with Guru Jambheshwar University of Science and Technolgy, Hissar, Haryana and JMIT, Raduar, Haryana. He joined BITS Pilani in Mechanical Engineering Department as a Teaching Assistant in January 2007 and as a Lecturer in August 2009. He has more than 7 years of teaching experience. He is a member of ASME, USA and guest member of National Centre for Aerospace Innovation and Research (NCAIR), India. He has acted as a reviewer for many CIRP conferences and an ASME conference.

Biography of the Supervisor

Dr Kuldip Singh Sangwan did his B.E. and M.E. from Punjab Engineering College, Chandigarh, and PhD from BITS, Pilani. He has also obtained PG Diploma in Operations Management. He is presently working as Head of the Mechanical Engineering Department at BITS, Pilani and has over 20 years teaching experience at under graduate and graduate levels. He has published a monogram on concurrent engineering and many research papers

in national and international journals. His areas of research interest are CMS, Green Manufacturing, World-class Manufacturing, TPM, Concurrent Engineering, Operations Management, and application of Fuzzy Mathematics, Genetic Algorithms, Simulated Annealing, and Neural Networks in design of manufacturing system. Prof. Sangwan is life member of Institution of Engineers (India), Society of Operations Management and Indian Society of Technical Education. Prof. Sangwan has developed research collaborations with German and Spanish universities in the area of Titanium alloy machining, automotive life cycle engineering, and lean and green manufacturing. He has also developed many courses related to the manufacturing management, engineering design and design engineering for the working professionals.